B O L T   B E R A N E K   A N D   N E W M A N   I N C

C O N S U L T I N G · D E V E L O P M E N T · R E S E A R C H

CR 114352

AVAILABLE TO THE PUBLIC

INVESTIGATION OF THE FEASIBILITY OF MAKING MODEL ACOUSTIC MEASUREMENTS IN THE NASA AMES 40-BY 80-FOOT WIND TUNNEL

by David Alan Bies

Prepared under Contract NAS2-6206 by
Bolt Beranek and Newman Inc.
Canoga Park, California

for

NATIONAL AERONAUTICS AND SPACE ADMINISTRATION
AMES RESEARCH CENTER

INVESTIGATION OF THE FEASIBILITY OF MAKING
MODEL ACOUSTIC MEASUREMENTS IN THE NASA AMES
40-BY 80-FOOT WIND TUNNEL

by David Alan Bies

Prepared under Contract NAS2-6206 by
Bolt Beranek and Newman Inc.
Canoga Park, California

for

NATIONAL AERONAUTICS AND SPACE ADMINISTRATION
AMES RESEARCH CENTER

TABLE OF CONTENTS

TABLE OF CONTENTS (cont)

SUMMARY

Sound propagation in the Ames 40-by 80-foot wind tunnel has been investigated. The general results appear to be applicable to any closed test section, air return wind tunnel. It is shown that two simultaneous measurements of sound pressure levels upstream and downstream of the test section may be used to estimate forward, backward and total radiated sound power from a model provided that the sound pressure levels due to the model exceed those due to the operation of the tunnel. Measurements at the edge of the test section, in the inlet and diffuser, and in the area of the fans have been investigated. Measurements in the area of the fans give the most accurate estimate of total radiated sound power but require the greatest model sound power for measurement and are able only to give qualitative estimates of forward and backward radiation. Measurements closer to the test section require progressively less model sound power and give better estimates of forward and backward radiation but give less precise estimates of total radiated sound power.

Experiments in the test section have shown that reverberation limits measurements of the direct field of a monopole source with an omnidirectional midrophone to distances less than ten feet at all frequencies. Limited experiments with a directional porous pipe microphone have demonstrated that the distance over which direct field measurements may be made can be increased up to 30 ft. Although the experiments were limited to frequencies including and above 500 Hz, theoretical considerations suggest that improved microphone directivity would allow direct field measurements at even greater distances and lower frequencies.

I. INTRODUCTION

The National Aeronautics and Space Administration Ames Research Center at Moffett Field, California, is interested in making acoustic measurements of various V/STOL aircraft and models in their 40-by 80-ft wind tunnel. However, the wind tunnel which was constructed some thirty years ago was not designed for the purpose of making acoustic measurements and as a consequence it is quite noisy and quite reverberant. Thus to make acoustic measurements the model must generate more noise than is produced by the tunnel fans.

In addition, the reverberant buildup of sound in the wind tunnel is so high that it is difficult to distinguish the direct field of the source even if the source is noisier than the fans. It will be shown that the reverberant property can be used to advantage, however, to enable measurements of total radiated power.

A brief description of the wind tunnel is given in Section II. Section III describes the tunnel noise and provides a means for estimating the minimum sound power that a source must exceed in order that measurements of acoustic power are feasible. Section IV describes acoustic power measurements conducted with various sources in the test section. Section V describes measurements in the test section to investigate the possibility of distinguishing the direct field of a source from the reverberant background field with a directional microphone. Section VI briefly describes possible focusing problmes in the test section, inlet and diffuser. Section VII presents conclusions and recommendations drawn from the body of the report. The appendices provide information about the sources and measurement systems as well as an analysis of the acoustic properties of the tunnel.

II. DESCRIPTION OF THE WIND TUNNEL

Plan and elevation views of the National Aeronautics and Space Administration Ames Research Center 40-by 80-ft wind tunnel are shown in Fig. 1. The center line distance around the wind tunnel is 2000 ft. The tunnel test section is 40 ft high, 80 ft wide, and 80 ft long. The tunnel is driven by six 40-ft diameter fans which are capable of developing a maximum dynamic pressure in the test section of 130 lbs/ft^2 at a speed of 230 mph. The relations between fan speed and test section dynamic pressure and speed are shown in Fig. 2.[1/]

The walls of the tunnel are constructed of steel plate and corrugated asbestos cement sheet. The floor is concrete in the portion of the tunnel between the fans and the test section inlet. Because of the hard wall construction, the tunnel is quite reverberant.

Reference will be made to various measurement locations in the tunnel indicated in Fig. 1 by the letters A through G, b and c. Other measurement locations in the test section will be described as needed. All of the measurement locations outside of the test section were relatively close to the floor generally at an elevation of 5 or 6 ft. Measurement locations in the test section were both well above the floor at heights up to 20 ft and close to the floor at 5 or 6 ft. Measurements were made both with and without the tunnel in operation.

III. TUNNEL BACKGROUND NOISE

A series of measurements of sound pressure levels were made at position E (see Fig. 1) with the tunnel in operation at various dynamic pressures in the test section. The results of these measurements are shown in Fig. 3. The data have been scaled according to the well-known fan law[2]

$$PWL_B = PWL_A + 50 \log_{10}(N_B/N_A) + 70 \log_{10}(D_B/D_A) \qquad (1)$$

and frequency shifted in proportion to N_B/N_A where

PWL = sound power level in dB re 10^{-12} watt,

N = fan speed,

D = fan diameter,

and the subscripts refer to conditions A and B. The figure shows that the collapse of the data is satisfactory.

For convenience, the data have been scaled arbitrarily to 100 rpm although the operating range of the tunnel fans is generally above this speed as shown by reference to Fig. 2. Review of Fig. 3 shows that while the collapse of data is quite good in the frequency range below 500 Hz in the frequency range above 500 Hz a general tendency for the data to drop to lower levels at higher fan speeds is observed. It is suggested that at low fan speeds the sound pressure levels in the frequency range above 500 Hz may be controlled by wind noise which does not scale according to the fan laws. Thus, at high fan speeds one may expect sound pressure levels in the high frequency range that are somewhat lower than would be indicated by the general trend of data shown in Fig. 3.

With the possible exception of wind noise at high frequencies, noise from the fans controls the background levels at all places in the tunnel during operation. Figures 2 and 3 provide a means for estimating the upper bound of the tunnel background noise at any dynamic pressure. When an estimate of model sound power is available, Appendix A provides a criterion for determining the feasibility of making acoustic power measurements in the wind tunnel.

Additional measurements of tunnel background noise taken at various stations in the tunnel at dynamic pressures of 30 lbs/ft^2 and 50 lbs/ft^2 are shown in Figs. 4, 5, and 6. These figures contain several sets of data which will now be discussed. In the discussion of the data that follows it will also be useful to make reference to Fig. 1.

Measurements were made with a hand-held sound level meter octave band analyzer at position E. These measurements have been corrected to estimated third octave levels and are shown in Figs. 4 and 6 as solid lines. They represent levels due to the fans in operation at position E at the dynamic pressures shown.

In Figs. 4 and 5 measurements are shown which were made at five locations distributed between positions E and G.[3/] The measured levels indicated by the shaded area ranged from the upper bound to the lower bound as one proceeded from position E to position G. The general decrease in levels toward the test section is due to propagation losses. The comparison between these measurements and the measurements made at position E as shown in Fig. 4 are considered satisfactory. The shaded area in the figure may thus be taken as a measure of the sound pressure levels that exist in the portion of the tunnel upstream of the test section.

In Fig. 4 the results are shown of measurements made with a porous pipe microphone pointing upstream and across stream. The porous pipe microphone which is discussed in Appendix B was used in several experiments to be discussed in this report. The measurements taken with the porous pipe pointing upstream generally lie below the shaded area and can be regarded as in reasonable agreement with the latter data since further propagation loss on advancing into the test section is to be expected. On the other hand, the porous pipe pointing across stream gives levels which are very much higher than observed anywhere in the tunnel. In this case the porous pipe apparently hears wind noise generated at the microphone itself. Thus while the porous pipe is quite satisfactory when oriented parallel to the flow, it is unsatisfactory for the present purpose when oriented across the flow.

In Fig 5 measurements made with the porous pipe microphone pointing downstream are shown. The data taken with the porous pipe pointing downstream are in general agreement with the data taken in the upstream area. In addition measurements are shown in the figure which were made with a 1/2-in. condenser microphone with a wind screen nose cone. The nose cone measurements are in fair agreement at low frequencies below 500 Hz but at high frequencies the nose cone measurements exceed the general background noise. It is concluded that in the high frequency range the nose cone microphone hears locally generated aerodynamic noise.

In Fig. 6 measurements are shown which were made at a dynamic pressure of 50 lbs/ft^2 in the test section . Besides measurements made at position E as described earlier, measurements are shown in the figure which were made with the porous pipe pointing upstream and pointing downstream. For comparison, measurements are shown which were made with a 1/2-in. condenser microphone with nose cone in the diffuser.

With the porous pipe pointing upstream the measured levels are generally below those levels measured close to the fan at position E except perhaps at frequencies above 4000 Hz. As mentioned earlier this kind of behavior is expected since the sound should attenuate as it propagates from position E toward the test section. The behavior of the porous pipe measurements at frequencies above 4000 Hz suggests that the levels are controlled by wind noise.

With the porous pipe pointing downstream the measurements of background noise made with the porous pipe are in excellent agreement with the measurements made in the diffuser. On the other hand with the porous pipe pointing upstream the measurements of background noise made with the porous pipe are in general agreement with measurements made at position E when propagation losses are taken into account. The two measurements of background noise made with the porous pipe are in good agreement in the frequency range below the 500 Hz one-third octave band but above this band the upstream background noise is very much less than the downstream background noise. Whether the higher levels downstream are due to turbulence generated noise or smaller propagation losses is not known.*

IV. ACOUSTIC POWER LEVEL MEASUREMENTS

Introduction

In this section a series of experiments will be described which were designed to investigate two questions.

1. Do areas of reverberant buildup exist in the wind tunnel which can be used for power measurements?

   The power radiated from an acoustic source in a reverberant room may be measured by measuring the resulting sound pressure levels having previously calibrated the room either with a reference source or by reverberation measurements. As pointed out earlier, the 40-by 80-ft wind tunnel is quite reverberant but its "tunnel" shape makes it unlike the usual reverberant enclosure used for making acoustic power measurements.5/ It will be shown

---

*In the frequency range above 500 Hz atmospheric propagation loss becomes important. It is a function of humidity4/ and is subject to the weather. It is proportional to the volume in the reverberant space. The very large size of the upstream portion of the wind tunnel suggests that atmospheric losses may be dominant in determining the response of the wind tunnel to any sound source at 8000 Hz and perhaps at 4000 Hz.5/

that the portions of the wind tunnel upstream and downstream of the fans are characterized by reverberant buildup and that measurements in these areas can be used to measure the acoustic power radiated from a source in the test section.

2. Can upstream and downstream acoustic power propagation be differentiated?

   It will be shown that the acoustic coupling through the fans is sufficient to make the reverberant levels in the areas of the tunnel upstream and downstream of the fans relatively insensitive to the direction in which the sound is propagated. Although such measurements can give a qualitative estimate of energy propagation, they cannot give a quantitative measure of upstream and downstream propagation.

   As a possible alternative procedure, it will be shown that measurements in the diffuser and the test section inlet can be used: (a) to give rough estimates of the total acoustic power radiated, and (b) estimates of the acoustic power radiated upstream and downstream by a source in the test section.

Description of Experiments

A series of tests were run without the tunnel in operation using two acoustic sources. One source was a dodecahedron; the other source was a horn. These sources are described in Appendices C and D.

The dodecahedron was mounted in the tunnel test section 22 ft above the floor midway between the two walls and 12 ft downstream from the front lift wire. The latter is 25 ft downstream from the beginning of the test section. When all 12 speakers of the dodecahedron were driven with equal phase and equal input voltage, the source was essentially omnidirectional for the purpose of the tests. Indeed the dodecahedron behaved like a monopole over most of its frequency range up to and including the 1000 Hz one-third octave band and again in the 8000 Hz one-third octave band. In the intermediate range, the radiation field of the source was somewhat inhomogeneous due primarily to noncoalescence of the radiated fields of the twelve speakers. When a single speaker in one face of the dodecahedron was driven, the source was directional in the frequency range above 250 Hz.

In a separate series of tests, a high power horn was mounted at the center of the test section 20 ft above the floor and 15 ft downstream from the front lift wire. The horn was pointed upstream, downstream, and across the tunnel in several tests with and without the tunnel in operation.

During all tests the sources were driven with one-third octave bands of noise centered at the preferred octave band center frequencies. The resulting sound pressure levels at various locations around the tunnel (see Fig. 1) were measured with a portable sound level meter and octave band analyzer. These measurements were taken relatively close to the floor at an elevation of about 5 ft. Additional measurements were made in some cases within the test section with a microphone held well above the floor on a pole.

All measurements described in the following sections were made with omnidirectional microphones unless explicitly stated in the text that the porous pipe directional microphone was used. The various measurement systems are described in Appendix E.

Experimental Results

The results of measurements using the dodecahedron as an omnidirectional source are shown in Figs. 7 through 13. For comparison with the tunnel measurements, the free field response of the source is shown in Figs. 7 through 10 and in 13. An equivalent free field response curve is shown in Figs. 11 and 12 which is the response of a monopole of the same acoustic power. The data in Figs. 7 through 12 show that the sound pressure levels depart from free field at distances from the source of the order of 10 ft. From 10 ft onward, the sound pressure levels decrease at the approximate rate of 3 dB per doubling of distance in contrast to the free field response rate of 6 dB per doubling of distance. At 8000 Hz, Fig. 13 shows that the sound pressure levels decrease approximately at the rate of 6 dB per doubling of distance.

As mentioned earlier in the frequency range between 1000 Hz and 8000 Hz, the output from the various speakers did not sufficiently well coalesce to form a true monopole although for the purposes described here the source was essentially omnidirectional. The low sound pressure levels observed at close range to the source in Figs. 11 and 12 were taken at positions between speaker axes and they reflect the inhomogeneity in the radiation field of the source in this frequency range.

Review of the data shows that sound pressure levels measured at positions G, F, and E are always lower than sound pressure levels measured at positions B, C, and D. Reference to Fig. 1 shows that positions G, F, and E are in parts of the tunnel which are very much larger in cross section than are the parts of the tunnel in which measurements B, C, and D were made. Thus, it is of interest to investigate the possible effect of the wind tunnel cross section on the several measurements.

A correction is proposed based upon the following assumption: relative to an advance away from a sound source in a tunnel of varying cross section sound energy predominantly propagates in the direction of increasing cross section and propagates about equally in both directions in the direction of decreasing cross section. The test data reviewed here and the fan noise data reviewed earlier is consistent with this assumption to the extent that propagation losses may be ignored as is implicitly assumed here. The following correction is proposed

$$10 \log_{10} \frac{\text{cross sectional area at measurement location}}{\text{cross sectional area at source location}} \; . \quad (2)$$

Note that the assumption implies that the correction for measurements at position E should be the same as the correction for measurements at position G and F (see Fig. 1) since the cross section decreases toward the fans. Thus the field at E and at F is reverberant according to the assumption and the sound pressure levels should be the same. The corrected data are shown in the figures. The area correction seems to decrease the data scatter and the corrected levels upstream and downstream of the fans are nearly equal in all cases.

Reference to Fig. 1 shows that the turning vanes lie between positions G and F upstream of the test section and between positions C and D downstream of the test section. Reference to the corrected levels shown in Figs. 7 through 13 show rather abrupt drops in levels between positions C and D and G and F which is fairly significant at low and at high frequencies and less significant in the midfrequency range. The abrupt drop in sound pressure levels may be attributed to propagation loss through the turning vanes.

It may be postulated that at low frequencies, where the acoustic wavelength is quite large, the turning vanes present a partial obstruction to sound propagation and are reflective. In this range only the chord length and percentage open area are important. At high frequencies the sound waves are scattered by the turning vanes. In the midfrequency range where the wavelengths are small compared to the chord but not too small compared to the spacing between turning vanes, the sound is guided through the vanes with minimum loss.

The experimental results obtained with the directional sources in the test section are shown in Figs. 14 through 23. Inspection of the data shows that the measured sound pressure level at any particular location increases if the source is directed toward that location and decreases if the source is directed away. For example, note the behavior observed at position B downstream in the diffuser or at position G upstream in the inlet. Further inspection shows that the sound pressure levels measured at position D upstream of the fans are always higher than the sound pressure levels measured downstream of the fans at position E if the source is pointing downstream while the opposite is true if the source is pointing upstream. These observations will be investigated in detail in the following sections.

Analysis of Measurements in the Area of the Fans

Experimental results reviewed earlier indicated that sound pressure levels in the area of the fans could be associated with total acoustic power radiated by an omnidirectional sound source in the test section. The results of the experiments with the omnidirectional source could be used to calibrate the tunnel. If the results of tests with a model in the test section indicated that the corrected sound pressure levels upstream and downstream of the fans were essentially equal, one might conclude that the source was effectively omnidirectional in acoustic radiation and one could estimate the acoustic power radiated. However, the possibility of acoustic coupling through the fans would seem to obscure the experimental results and might make a slightly directional source seem omnidirectional. If, on the other hand, the corrected sound pressure levels upstream and downstream were appreciably different one could conclude that the source was directional but little else without further analysis.

The effect of acoustic coupling through the fans on the results of experiments using various sources will now be considered.* For the purpose of analysis the following assumptions will be made. It will be assumed that the section of tunnel between the fans and the end of the diffuser forms a reverberant enclosure which shall be characterized as volume one, V_1, and the section of tunnel downstream of the fans and upstream of the test section inlet forms a second reverberant enclosure characterized as volume two, V_2. It shall be assumed that the energy densities, that is, the acoustic pressures, are essentially constant throughout their respective volumes although the data shows that this is a very rough approximation. The energy density in volume one shall be E_1 while the energy density in volume two shall be E_2. Similarly, the acoustic power flow into either volumes one or two will be represented by P_1 or P_2.** The energy balance equations are then as follows[6/].

$$P_1(\omega) = \omega\eta_1E_1V_1 + \omega\eta_{12}E_1V_1 + \omega\eta_DE_1V_1 - \omega\eta_{21}E_2V_2 \qquad (3)$$

$$P_2(\omega) = \omega\eta_2E_2V_2 + \omega\eta_{21}E_2V_2 + \omega\eta_DE_2V_2 - \omega\eta_{12}E_1V_1 \qquad (4)$$

Equations 3 and 4 hold approximately for narrow bands of energy centered at the angular frequency ω. In the equations, the acoustic loss factors for the chambers are represented by η_1 and η_2, respectively. The coupling coefficient across the fans from volume one to volume two is given by η_{12} while the coupling coefficient in the reverse direction is given by η_{21}. η_D represents possible loss in the duct connecting the two volumes. In this case the duct would be the fan ports. The energy lost in propagation through the fans will be assumed to be zero and thus η_D shall be taken as zero.

The cross coupling coefficients are related to the modal densities n_1 and n_2 of the two reverberant encloures as follows:

$$n_1\eta_{12} = n_2\eta_{21} \qquad (5)$$

---

*See Appendix F for further discussion.

** See Glossary of Symbols for definitions and units.

The modal density in either volume is in turn proportional to the volume. Thus the relation between the volumes and the cross coupling coefficients is as follows:

$$V_1\eta_{12} = V_2\eta_{21} \tag{6}$$

An equation for the total radiated power is obtained by adding Eqs. 3 and 4.

$$P_{total}(\omega) = \omega\eta_1 E_1 V_1 + \omega\eta_2 E_2 V_2 \tag{7}$$

The loss factor η_1 or η_2 is the ratio of energy dissipated per cycle divided by energy stored. The energy dissipation largely takes place at the walls of the enclosure and thus is proportional to the total wall area while the energy stored is proportional to the volume. The tunnel shape of the enclosure, however, insures that the ratio of surface area to total volume is approximately the same for volumes one and two. Thus the loss factors η_1 and η_2 may be expected to be approximately equal.

$$\eta_1 \approx \eta_2 = \eta \tag{8}$$

Thus the expression for the total acoustic power radiated by a source in the test section may be written as follows:

$$P_{total}(\omega) = \frac{\omega\eta V_2}{\rho c^2}\left(p_2^2 + \frac{V_1}{V_2} p_1^2\right) \tag{9}$$

where the energy densities have been expressed in terms of sound pressures p_1 and p_2 using the expression for the acoustic energy density.

$$E = p^2/\rho c^2 \tag{10}$$

In Eqs. 9 and 10 ρ is the air density and c is the speed of sound. The ratio V_2/V_1 is approximately 4.6.

Equation 9 suggests the following rule for the interpretation of sound pressures upstream and downstream of the fans. Reduce the sound pressure as measured in the area of D (see Fig. 1) by 6-1/2 dB to account for the relatively small volume. Logarithmically add (see Appendix G) the reduced sound pressure level thus determined at D to the sound pressure level determined at E. The result is a weighted sound pressure level which is proportional to the total power according to Eq. 9.

Table I has been constructed according to the rule just suggested using the data contained in Figs. 7 through 13 for the omnidirectional source. The table gives the relation between power level and sound pressure level as a function of frequency for the various third-octave bands shown which may be used to estimate the acoustic power from the other sources investigated. The rule applied to the data in Figs. 14 through 23 and the data in the last column of Table I have been used to construct Tables II and III. The power levels based on the tunnel measurements are in reasonably good agreement with the power levels determined independently for these sources. Therefore the procedure just described can be used to determine the sound power levels of any directional or omnidirectional source in the test section based on sound pressure levels measured at D and E (see Fig. 1). Although the procedure has only been verified when the tunnel was inoperative Appendix A provides criteria for determining the feasibility of measurements at any fan speed.

The question of whether measurements in the area of the fans can be used to determine directivity is considered in Appendix F. There it is shown that the sound pressure levels upstream and downstream of the fans are sufficiently coupled by transmission through the fans that the sound pressure levels are relatively insensitive to directivity of the source. Quantitative directivity information can not be determined from measurements made in the area of the fans.

In Appendix F an additional experiment is described which enabled the calculation of the various quantities shown in Eqs. 3 and 4. It is shown that the loss factors for chambers one and two are indeed approximately equal. The magnitudes of the cross coupling coefficients are estimated and it is shown that the results of measurements with the directional source are in reasonable agreement with the theory.

POWER LEVELS AND WEIGHTED SOUND
PRESSURE LEVELS MEASURED IN THE AREA OF THE TUNNEL FANS

(Model: dodecahedron sound source, no flow)

Center Band Frequency (Hz)	Weighted One-Third-Octave Band Sound Pressure Level (SPL) (dB re 2 x 10^{-5} N/m)	One-Third Octave Band Sound Power Level (PWL) (dB re 10^{-12} watt)	PWL - SPL (dB)
125	82.0	118.5	36.5
250	83.5	119.5	36.0
500	79.5	113.5	34.0
1000	75.0	109.5	34.5
2000	70.5	108.5	38.0
4000	60.0	105.5	45.5
8000	32.0	97.5	65.5

PRESSURE LEVELS MEASURED IN THE AREA OF THE TUNNEL FANS

(Model: single speaker in a dodecahedron sound source, no flow)

Center Band Frequency (Hz)	Source Direction	Weighted One-Third Octave Band Sound Pressure Level (SPL) (dB re 2 x 10^{-5} N/m^2)	One-Third Octave Band Sound Power Level (PWL) (dB re 10^{-12} watt)	
			Tunnel Measurement	Calibration From Appendix C
250	Upstream	63.5	99.5	101.5
	Downstream	63.0	99.0	101.5
500	Upstream	68.0	102.0	100.5
	Downstream	67.5	101.5	100.5
1000	Upstream	62.5	97.0	96.5
	Downstream	59.5	94.0	93.5
2000	Upstream	61.5	99.5	100.0
	Downstream	56.5	94.5	93.0
4000	Upstream	52.5	98.0	96.5
	Downstream	59.5	95.0	96.5
8000	Upstream	27.5	93.0	89.0
	Downstream	20.0	85.5	94.0

PRESSURE LEVELS MEASURED IN THE AREA OF THE TUNNEL FANS

(Model: horn sound source, no flow)

Center Band Frequency (Hz)	Source Direction	Weighted One-Third Octave Band Sound Pressure Level (SPL) (dB re 2 x 10^{-5} N/m^2)	One-Third Octave Band Sound Power Level (PWL) (dB re 10^{-12} watt)	
			Tunnel Measurement	Calibration From Appendix D
500	Upstream	88.0	122.0	119.0
	Downstream	86.5	120.5	119.0
	Across stream	86.5	120.5	119.0
1000	Upstream	87.0	121.5	119.5
	Downstream	85.0	119.5	119.5
	Across stream	85.0	119.5	119.5
2000	Upstream	82.0	120.0	117.5
	Downstream	80.0	118.0	117.5
	Across stream	79.0	117.0	117.5
4000	Upstream	68.0	113.5	113.0
	Downstream	64.5	110.0	113.0
	Across stream	63.0	108.5	113.0

Analysis of Measurements in the Diffuser and Inlet

Review of the background noise data associated with the operation of the fans in Section III showed that the sound pressure levels did not increase on advancing into the test section in spite of the decreasing cross section of the tunnel. On the other hand, review of the test section data associated with a source in the test section indicated that part of the observed sound pressure level decrease as one moves away from the test section could be associated with the increasing cross section of the tunnel. This suggests that sound power travels from a smaller cross section to a larger cross section, but not in the opposite direction. This in turn suggests that sound power might be measured by measuring sound pressure levels in an expanding part of the tunnel such as in the diffuser at location B or in the inlet at location G. For such power measurements sound pressure levels should be measured at approximately equal distance upstream and downstream from the source.

The data for positions B and G shown in Figs. 14 through 23 have been used to construct Tables IV, V and VI. In the tables, sound pressure level measurements at position B have been corrected for propagation losses by interpolation of the measurements at B and C to give values at a distance equal to the distance of position G from the source. This procedure has resulted in small corrections at 4000 and 8000 Hz as noted in the tables. Measurements at position G have been increased by 5 dB to correct them for the cross sectional area difference between measurement positions G and B.

The corrected sound pressure levels measured at positions B and G have been used to determine an average sound pressure level at the distance of G which is 210 ft from the source. The relation between the acoustic power radiated in one direction and the average sound pressure level measured at 210 ft is shown in the last column of Table IV. This relation between power level and sound pressure level has been used in Tables V and VI to determine the forward and backward radiated energy from the various sources. Logarithmic addition (see Appendix G) of the energy radiated forward and backward has provided an estimate of the total radiated sound power.

Review of Table V shows that the estimated sound power radiated forward is generally lower than expected while the sound power radiated backward is generally in fairly good agreement with the expected level. The estimate of

EQUAL DISTANCES FROM THE MODEL

(Model: dodecahedron sound source, no flow)

Center Band Frequency (Hz)	Sound Pressure Level (SPL) at Position B Corrected for Propagation Loss*	Sound Pressure Level (SPL) at Position G Corrected for Cross-Section Change**	Average Sound Pressure Level (SPL)	One-Third Octave Band Sound Power Level (PWL) (dB re 10^{-12} watt)	PWL-SPL (dB)
	One-Third Octave Band Sound Pressure Level (dB re 2×10^{-5} N/m^2)				
125	91.0, 92.0	93.0	92.0	115.5	23.5
250	94.0, 93.0	93.0	93.5	116.5	23.0
500	86.5, 88.0	87.0	87.0	110.5	23.5
1000	82.0, 84.0	82.0	82.5	106.5	24.0
2000	79.0, 79.0	78.0	78.5	105.5	27.0
4000	74.0, 74.0	73.0	73.5	102.5	29.0
8000	58.0, 57.0	54.0	56.5	94.5	38.0

*The measured levels at 4000 Hz and 8000 Hz were reduced respectively by 1 dB and 3 dB to account for apparent propagation losses. These corrections were determined from inspection of Figures 12 and 13 and would not be necessary if the measurement positions B and G were equally distant from the source.

**The sound pressure levels at G have been increased by 5 dB to account for the greater cross section of the tunnel at G than at B.

(Model: single speaker in dodecahedron sound source, no flow)

One-third octave band sound power level in dB re 10^{-12} watt

Radiation	Forward			Backward			Total	
Source Direction Measurement Location	Upstream G	Downstream B		Upstream B	Downstream G			
Center Band Frequency (Hz)			Calib.**			Calib.**	Sum*	Calib.**
250	96.0		100.0	93.0		95.0	98.0	101.5
		95.0	100.0		94.0	95.0	97.5	101.5
500	96.5		99.5	93.5		94.5	98.5	100.5
		97.5	102.5		94.5	97.5	100.0	103.5
1000	95.0		9[illegible].0	88.0		86.5	96.0	96.5
		91.0	93.0		83.0	83.5	91.5	93.5
2000	95.0		100.0	86.0		84.5	95.5	100.0
		92.0	93.0		82.0	76.5	92.5	93.0
4000	91.0		96.5	78.0		79.5	91.0	96.5
		93.0	96.5		79.0	79.5	93.0	96.5
8000	87.0		89.0	65.0		67.0	87.5	89.0
		88.0	94.0		75.0	72.0		94.0

* See Appendix G.
** See Appendix C.

One-third octave band sound power level in dB re 10^{-12} watt

adiation	Forward			Backward			Sideward			Total	
urce rection asurement cation	Up-stream G	Down-stream B		Up-stream B	Down-stream G		Across stream B	Across stream G			
nter Band requency (Hz)			Calib.**			Calib.**			Calib.**	Sum*	Calib.**
500	117.5		118.0	113.5		112.0				119.0	119.0
		117.5	118.0		113.5	112.0				119.0	119.0
							114.5	115.5	116.0	118.0	119.0
1000	118.5		119.0	110.0		108.0				119.0	119.5
		120.5	119.0		112.0	108.0				121.0	119.5
							115.0	115.0	116.5	118.0	119.5
2000	118.5		117.5	111.0		<103.0				119.0	117.5
		120.0	117.5		108.0	<103.0				120.0	117.5
							113.0	113.0	114.5	116.0	117.5
4000	107.0		113.0	95.0		<93.0					113.0
		111.0	113.0		94.0	<93.0					113.0
							104.5	103.0	110.0	106.5	113.0

See Appendix G.
See Appendix D.

the total radiated power is thus lower than expected. The results with the horn given in Table VI give generally better agreement than the results with the dodecahedron. In both cases, the results tend to deteriorate at high frequencies.

Analysis of Measurements at the Edge of the Test Section

The relative success of the previous section suggests the possibility that measurements at the edge of the test section might be used to infer total radiated acoustic power. Such measurement locations would have the advantage over those measurement locations already considered, of being much closer to the control room; microphone calibration procedures, for example, would be much simplified. Reference to Fig. 1 shows that measurement position A was located at the edge of the test section. Measurements taken at the latter position will now be considered.*

Following procedures used previously in constructing Tables IV, V, and VI, Tables VII and VIII have been prepared. Table VII gives the relation between sound pressure levels measured at position A and acoustic energy radiated upstream by an omnidirectional source in the test section. Table VIII makes use of this relation to provide estimates of sound power radiated by a directional sound source. The comparison between estimated levels based on sound pressure levels measured at position A and estimates of radiated sound power based on calibration of the source is only moderately fair.

It is of interest to consider further the data contained in the last column of Table VII. It has been assumed that the sound energy propagates out of the test section and that very little of it propagates back. This is equivalent to the assumption that the duct is infinitely long. This in turn implies a definite relation between sound power and sound pressure which may be compared with the experimental relation given in the last column of Table VII.

---

*Additional measurements at the downstream edge of the test section would enable determination of the acoustic power flow downstream and would be required for a determination of the total radiated acoustic power.

... MEASURED AT THE INLET EDGE OF THE TEST SECTION

(Model: dodecahedron sound source; no flow)

Center band frequency (Hz)	One-third octave band sound pressure level (SPL) at position A (dB re 2×10^{-5} N/m^2)	One-third octave band sound power level (PWL)* (dB re 10^{-12} watt)	PWL-SPL** (dB)
125	95	115.5	20.5
250	96	116.5	20.5
500	91.5	110.5	19.0
1000	86	106.5	20.5
2000	85	105.5	20.5
4000	79	102.5	23.5
8000	67	94.5	27.5

* See Appendix C.

** See Appendix H.

LEVELS MEASURED AT THE INLET EDGE OF THE TEST SECTION

(Model: horn source, no flow)

One-third Octave Band Sound Power Level dB re 10^{-12} watt

Radiation	FORWARD		BACKWARD		SIDEWARD	
ource Direction	Upstream		Downstream		Across Stream	
leasurement Location	A		A		A	
nter Band equency (hz)		calibration*		calibration*		calibraticn*
500	119	118	116	112	119.5	116
000	120	119	110	108	120	116.5
000	116.5	117.5	105.5	< 103	115.5	114.5
000	108.5	113	95.5	< 93	109	110

* See Appendix D.

It is shown in Appendix H that the average intensity over the cross section of the duct is

$$I_{av} = 0.67 \frac{p_{rms}^2}{\rho c} \tag{11}$$

Multiplication of this expression by the cross section A of the test section gives for the relation between sound power level (PWL in dB re 10^{-12} watt) and sound pressure level (SPL in dB re 2×10^{-5} N/m^2) the following expression

$$PWL - SPL = 10 \log A - 12.3 \text{ dB} \tag{12}$$

The cross section A is 1914 ft^2, therefore, according to Eq. 12 the relation between sound power level and sound pressure level is

$$PWL - SPL = 20.5 \text{ dB} \tag{13}$$

The agreement with the data at low frequencies given in the last column of Table VII is excellent.

At high frequencies attenuation associated with propagation and reflection must be considered. At the edge of the test section, the sound field is dominated by reverberant sound. The reverberant sound has propagated back and forth between the walls of the duct and has suffered loss propagating through the air and additional loss on reflecting from the duct walls. This makes the measured sound pressure level less than that assumed in the expression for the average intensity. If attenuation is taken into account, the relationship between sound power level and sound pressure level at high frequencies is

$$PWL - SPL = 20.5 + \text{attenuation} \tag{14}$$

The attenuation is a positive number as written in Eq. 14.

Comparison of the expected relation given by Eq. 14 and the measured relation shown at 8000 Hz in the last column of Table VII shows a net attenuation of 7.0 dB. The indicated attenuation seems reasonable as it includes the cumulative effect of propagation back and forth across the duct and many reflections and not just the propagation loss along the straight line between the source and the microphone. As mentioned previously, air propagation loss depends upon the relative humidity and is thus subject to weather conditions. An alternative explanation, however, is that the acoustic energy is not distributed among all possible modes at high frequencies and the value of the constant is thus too small. The resolution of this matter must await further investigation.

V. TEST SECTION MEASUREMENTS

Investigation Without Flow

As shown in the previous section, sound pressure level measurements taken in the test section depart from free field measurements at distances greater than 10 ft. Thus, free field measurements in the test section with an omnidirectional microphone would be limited to less than 10 ft. The experiments described in this section were designed to test the feasibility of increasing the distance over which free field measurements could be made in the test section by use of a directional microphone. A porous pipe, as described in Appendix B, attached to a 1/2-in. condenser microphone provided a directional microphone for the purpose of these tests. In this section, measurements with the porous pipe are compared with measurements made with an omnidirectional 1/2-in. condenser microphone. The measurement systems are described in Appendix E.

Tests were conducted in the test section with and without flow. For the tests conducted without flow, a horn driver without the horn was mounted at the center of the tunnel 20 ft above the floor. The horn driver was coupled into the surrounding space through a short neck of the order of 2-in. in length and 2-in. in diameter. In this configuration, the horn driver behaved effectively like a point source. Measurements were taken with the two microphones at various radial positions about the source in its plane 20 ft above the floor. The source was driven with one-third octave bands of noise centered at the preferred octave band frequencies. The distances were measured from the center of the source support system as shown in Fig. 24. The slight displacement of the source downstream from the center of the coordinate system resulted from the mechanical support system used.

It may be assumed that the sound produced by the horn driver without a horn radiates spherically; for the dimensions of the source and the wavelengths considered, this assumption is probably quite well satisfied. For ease in considering the data the sound pressure levels have been reduced by 20 log of the distance from the source in feet. For spherical radiation the reduced sound pressure levels should be constant independent of distance from the source. The slight displacement of the source from the coordinate center has been accounted for in the presentation of the data.

The data would all lie on a straight line if there were no reverberant field. The presence of the reverberant field tends to make the data rise above the straight line at some distance from the source. The distance from the source at which the data departs by 3 dB from the straight line is the hall radius. The hall radius is the distance at which the reverberant field and the direct field are equal. Thus the limit of effectiveness of the microphone in discriminating against the reverberant field is shown by a departure of the data from a horizontal line with increasing distance from the source.

The results of the measurements are shown in Figs. 25 through 28. Review of the figures shows that the normalized sound pressure levels are fairly uniform or constant up to the distance of 10 ft and that beyond 10 ft the sound pressure levels as measured tend to rise. However, in every case the sound pressure levels measured with the omnidirectional microphone lie appreciably above the levels measured with the porous pipe. The porous pipe has been effective in discriminating against the reverberant field.

As shown in Appendix B the porous pipe is not strongly directive at 500 Hz. Thus in Fig. 25 the difference between the porous pipe data (open data points) and the omnidirectional microphone data (filled data points) is not very great although even in this case the porous pipe has extended the hall radius to perhaps 15 ft. However as shown in the appendix the porous pipe is quite directional at 2000 Hz. At this frequency as shown in Fig. 27, the porous pipe has become quite effective in discriminating against the reverberant field and has extended the effective hall radius to about 35 ft.

Figure 28 shows quite a bit of data scatter in the range close to the source. It is postulated that this is due to the presence of the model support struts which are of the order of 1-1/2 ft in diameter and are especially large compared to the wavelength at 4000 Hz. At distances greater than 10 ft the data are satisfactory. At 4000 Hz the porous pipe has extended the hall radius to about 30 ft. It may be concluded that the porous pipe can provide a means for increasing the distance to which measurements of the free field sound pressure levels can be made in the reverberant field of the tunnel.

The porous pipe used in these experiments was of the order of 1/2 wavelength long at 500 Hz; that is, of the order of 1 ft in length. At 2000 Hz it is of the order of 2 wavelengths in length. Thus if one desired the same kind of directivity performance at 500 Hz as observed at 2000 Hz, it would be necessary to use a porous pipe which was 4 ft in length. With a longer porous pipe, directivity could be increased at lower frequencies. However, as shown in Sppendix B the sensitivity of the porous pipe microphone rolls off quite sharply at high frequencies. Thus the longer porous pipe would be restricted to use in the lower frequency range. The need for at least two porous pipes of different lengths seems indicated to adequately cover the audio frequency range in the test section.

Investigation With Flow

A horn sound source described earlier in Section IV and in Appendix D was mounted at the center of the tunnel test section. The source was mounted horizontally so that it could beam either upstream, downstream or across the tunnel. The source was driven with one-third octaves bands with noise at 500, 1000, 2000, and 4000 Hz.

The sound pressure levels were measured at position b (see Fig. 1) with two 1/2-in. condenser microphones equipped respectively with an omnidirectional wind screen nose cone and with a directional porous pipe. The porous pipe microphone was placed upstream pointing downstream toward the source. The omnidirectional microphone pointed upstream into the wind and was mounted beside the porous pipe. The porous pipe microphone was 15.2 ft above the floor and oriented so that it tipped upward slightly at a small angle of 13.7° with respect to the horizontal toward the source which was 20 ft above the floor and 20 ft downstream. For these measurements the source was oriented in various directions while the porous pipe and omnidirectional microphones remained fixed.

With the arrangement described the radiation of sound due to a directional source in the test section in the presence of flow was investigated. Figure 29 shows the results of measurements made with the porous pipe microphone of sound radiated by the directional source. Only data for which the sig was at least 5 dB above the background noise in the corresponding one-third octave band is reported. The solid lines in the figure show free field measurements (described in Appendix D) of the source while the data points show measurements taken at various dynamic pressures up to 50 lbs/ft^2 in the test section. When the source points upstream the agreement between the test section measurements and the free field measurements is quite satisfactory. When the source points downstream, away from the microphone, the agreement is less satisfactory. The porous pipe microphone detects sound pressure levels slightly higher than those which would be expected in the free field. When the source points across the stream the levels at 500 Hz and 1000 Hz are considerably above those which would be expected in a free field but the agreement at 2000 Hz and 4000 Hz is satisfactory.

For comparison with the porous pipe data just discussed data taken with the omnidirectional microphone is shown in Fig. 30. The solid lines again represent free field measurements and are the same as shown in Fig. 29 while the data points show measurements taken at the various dynamic pressures. For reasons which are not understood, the nose cone microphone seems to decrease in sensitivity especially at 4000 Hz with increasing flow as is shown by the data with the source pointing upstream. Note that the levels as measured with the nose cone microphone steadily decrease below those which were expected from free field measurements.

When the source points downstream the levels as measured with the omnidirectional microphone are much higher than those indicated by free field measurements, while with the source pointing across the stream there is very little correspondence between levels measured and those which are expected. By contrast, as is observed in Fig. 29, the porous pipe has quite successfully detected the free field levels at 2000 and 4000 Hz. At these frequencies the porous pipe microphone is quite directional. It may be concluded from the comparison that the porour pipe microphone does offer promise of improving the distance over which free field measurements may be made in the test section but with the limitations discussed in the previous section.

V. OPTICAL MODEL

An optical model of the section of the 40- by 80-ft wind tunnel including part of the inlet, the test section and the downstream diffuser was constructed. A scale of 10 ft to one inch was adopted. Difficulties encountered in construction limit the accuracy of dimensions obtained from the model to approximately plus or minus one foot.

The model walls were covered with a highly reflective surface. A source in the tunnel was simulated with a very small light. The field was explored in the tunnel by means of a piece of semi-transparent paper suspended on a stick and thrust into the model from one end. The resulting light pattern on the paper was then observed and recorded.

The model simulates specular reflection which would characterize sound of very short wavelengths or sound after several reflections. The model does not give information about interference effects which are to be expected for the first one or two reflections of sound over most of the audible frequency range in the Ames 40- by 80-ft tunnel. Thus, the model will point out areas of strong focusing but it must be understood that interference effects must be superimposed on the sound field observed in the tunnel. Areas of strong focusing should be avoided in making acoustic measurements in the wind tunnel.

Some sketches of the patterns observed with the model are shown in Figs. 31, 32, and 33. The dimensions are those predicted in the full scale tunnel. The regions of focusing (optically bright, acoustically loud) are indicated in the figures.

VII. CONCLUSIONS AND RECOMMENDATIONS

The work reviewed in this report leads to the following conclusions:

1. In a long duct of varying cross section and cross sectional dimensions very large compared to a wave length sound predominantly propagates away from a source where the cross section of the duct increases in the direction away from the source and reverberates (propagates equally in both directions) where the cross section of the duct decreases in the direction away from the source.

2. The measurement of sound power radiated forward or backward by a sound source in the 40- by 80-ft wind tunnel is possible by means of a single sound pressure measurement provided that sound power is uniformly distributed among all possible modes which are either propagating as in the inlet and diffuser or standing as in the areas of the tunnel upstream and downstream of the fans. The required distribution of acoustic energy among all possible modes is accomplished in all portions of the tunnel by an omnidirectional source in the test section. However, the distribution requires greater space for a directional source being only completely accomplished in the areas of the fans and partially completed in the inlet and diffuser.

3. Measurements of sound pressure levels in the areas of the tunnel upstream and downstream of the fans may be used to estimate total acoustic power with good precision. However, power radiation directivity information is only qualitative.

4. Measurements of sound pressure levels at equal distances from the source upstream in the inlet and downstream in the diffuser may be used to estimate forward, backward and total radiated acoustic power with fair precision.

5. Measurements of sound pressure levels at the edge of the test section may be used to estimate with fair to poor precision acoustic power radiated forward and backward from a source in the test section.

6. The tunnel fan noise obeys ordinary fan scaling laws over most of its frequency range.

7. The fan noise controls the tunnel background levels at all locations in the wind tunnel except possibly in the diffuser in the high frequency range. High frequency noise may possibly be generated by turbulence at the turning vanes or it may be due to the fans and to low propagation loss in this portion of the tunnel. Acoustic signals to be measurable by the techniques described in this report must exceed the tunnel background noise.

8. Sound propagates from the tunnel fans into the test section attenuating as it propagates. The contributions in the test section from upstream and downstream are essentially equal at low frequencies but at high frequencies upstream propagation seems to predominate.

9. The distance at which the direct field and the reverberant field of a source are equal, called the hall radius, is of the order of 10 ft in the test section, however, the effective hall radius may be increased by use of a directional microphone.

10. The general results of the sound propagation study in the Ames 40- by 80-ft wind tunnel appear to be applicable to any large closed test section, air return wind tunnel.

11. A directional porous pipe microphone has been shown capable of increasing the effective hall radius but its usefulness is limited to orientation parallel to the air stream because of excessive wind noise at other than parallel orientation. Thus the porous pipe can only be used upstream or downstream of a sound source.

12. The porous pipe has much better wind noise cancelling characteristics than has the Bruel and Kjaer 1/2-inch nose cone wind screen provided that the porous pipe is oriented parallel to the flow.

13. The porous pipe has been shown to perform quite adequately in the test section at dynamic pressures up to and including 50 lb/ft^2. Its performance has not, however, been explained theoretically. (See Appendix B).

14. Background noise in the frequency range above 50 Hz as measured by the Bruel and Kjaer 1/2-inch microphone equipped with nose cone wind screen in the test section is due to aerodynamically produced noise at the microphone and is not characteristic of the sound in the test section.

Based on the conclusions listed above the following recommendations are offered:

(1) During the course of flight model investigations, make simulaneous acoustic measurements at (a) locations upstream and downstream of the tunnel fans, (b) locations equally distant from the model in the inlet and diffuser and (c) at the edge of the test section both upstream and downstream. When some experience has been gained with several models it may be possible to determine beforehand when measurements at the edge of the test section etc. will suffice.

(2) Continue the investigation with directional microphones and arrays to find a system capable of good resolution over the entire frequency range and good wind noise rejection. Such a system should ultimately be able to give good source directivity information.

REFERENCES

1. Guide for Planning Investigations in the Ames 40-By 80-Foot Wind Tunnel, NASA Ames Research Center, Moffett Field, California, Oct. 1969.
2. Fan Engineering, Sixth ed., Buffalo Forge Company, Buffalo, New York, p. 226.
3. Investigation of the Feasibility of Making Model Acoustic Measurements in the NASA Ames 40 x 80 Ft Wind Tunnel, BBN Report 1870, Contract NAS 2-5742, April 1970.
4. Harris, Cyril M.: Absorption of Sound in Air versus Humidity and Temperature. J. Acoust. Soc. Am. vol. 40, July 1966, pp. 148-159.
5. Beranek, L. L., ed.: Noise Reduction. Chp. 11. McGraw-Hill Book Company, New York, 1960.
6. Lyon, R. H.: Lecture notes for course, Bolt Beranek and Newman Inc., Program for Advanced Study, "Aerospace Vehicle Noise and Vibration," Los Angeles 1966 (see also Preston W. Smith, Richard H. Lyon, "Sound and Structural Vibration," NASA CR-160, March 1965).

GLOSSARY OF SYMBOLS

A	Area, ft^2
c	Speed in air, m/sec
D	Fan Diameter, ft
E	Acoustic energy density, joules/m^3
f	Frequency, sec^{-1}
H	Duct height, m
I	Acoustic energy intensity, watts/m^2
k	Wave number vector, m^{-1}
k_i	ith component of wave number vector m^{-1}
n, m	Mode numbers, dimensionless
n_i	Number of acoustic modes characteristic of volume V_i, in a frequency bandwidth divided by that bandwidth, dimensionless
N	Fan speed, rpm; number of allowed values of wave number component k_i, dimensionless
p	Acoustic pressure, newtons/m^2
P	Acoustic power, watts
PWL	Sound power level in dB re 10^{-12} watt
SPL	Sound pressure level in dB re 2×10^{-5} N/m^2
t	Time, sec
T	Reverberation time, time required for reverberant field to decrease 60 dB, sec; length of time for one period, sec

v_i	ith component of particle velocity, m/sec
V	Volume of a space, m^3
W	Duct width, m
x, y, z	Cartesian coordinates, m
η_i	Energy dissipated per cycle divided by energy stored in Volume V_i, dimensionless
η_{ij}	Cross coupling coefficient, proportionality between energy stored in volume V_i and power flow into volume V_j, dimensionless
ρ	Density of air, kg/m^3
ϕ	Potential function, m^2/sec
ω	Angular frequency, radians/sec

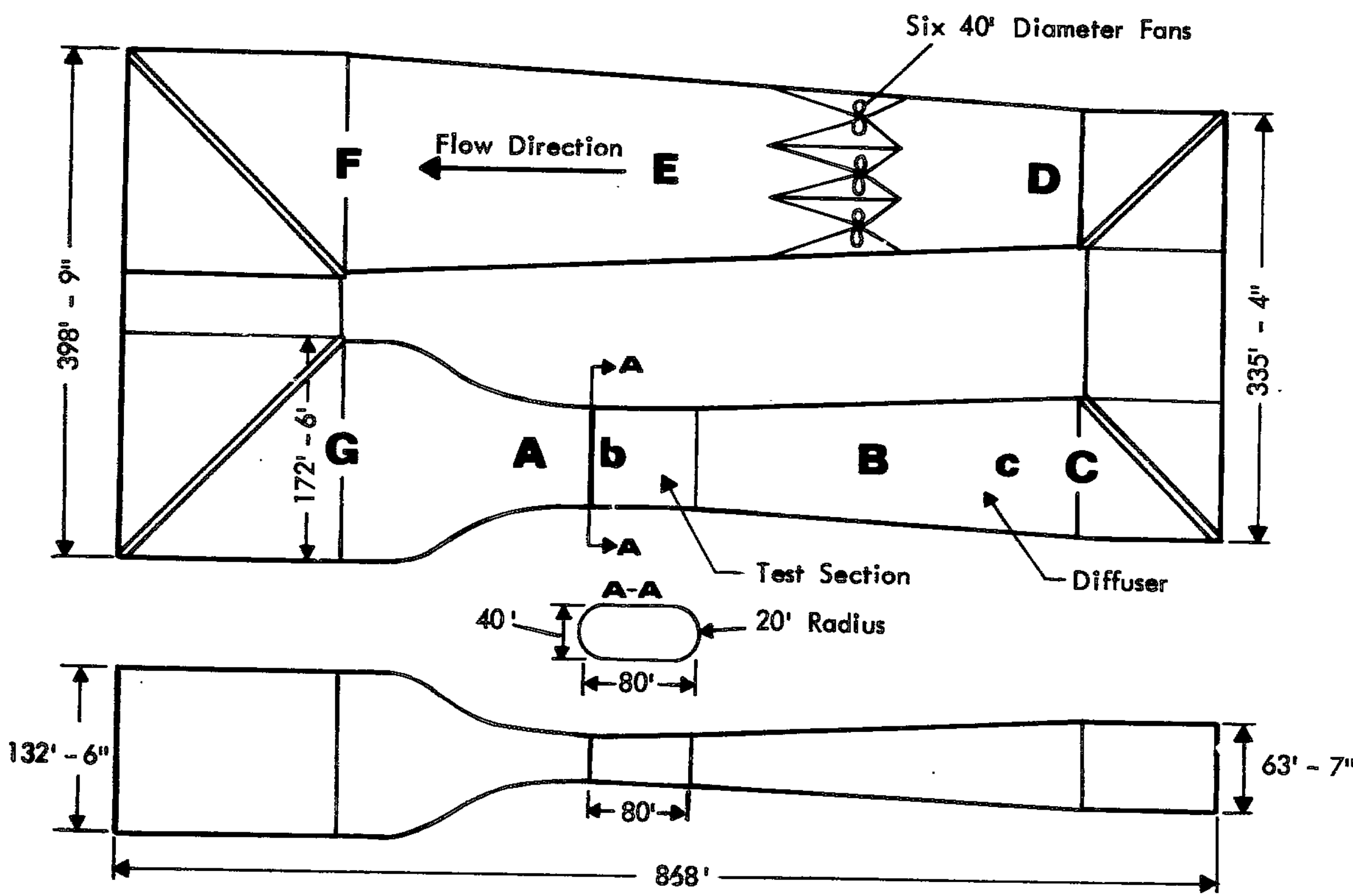

FIGURE 1. NASA AMES 40 FT x 80 FT WIND TUNNEL

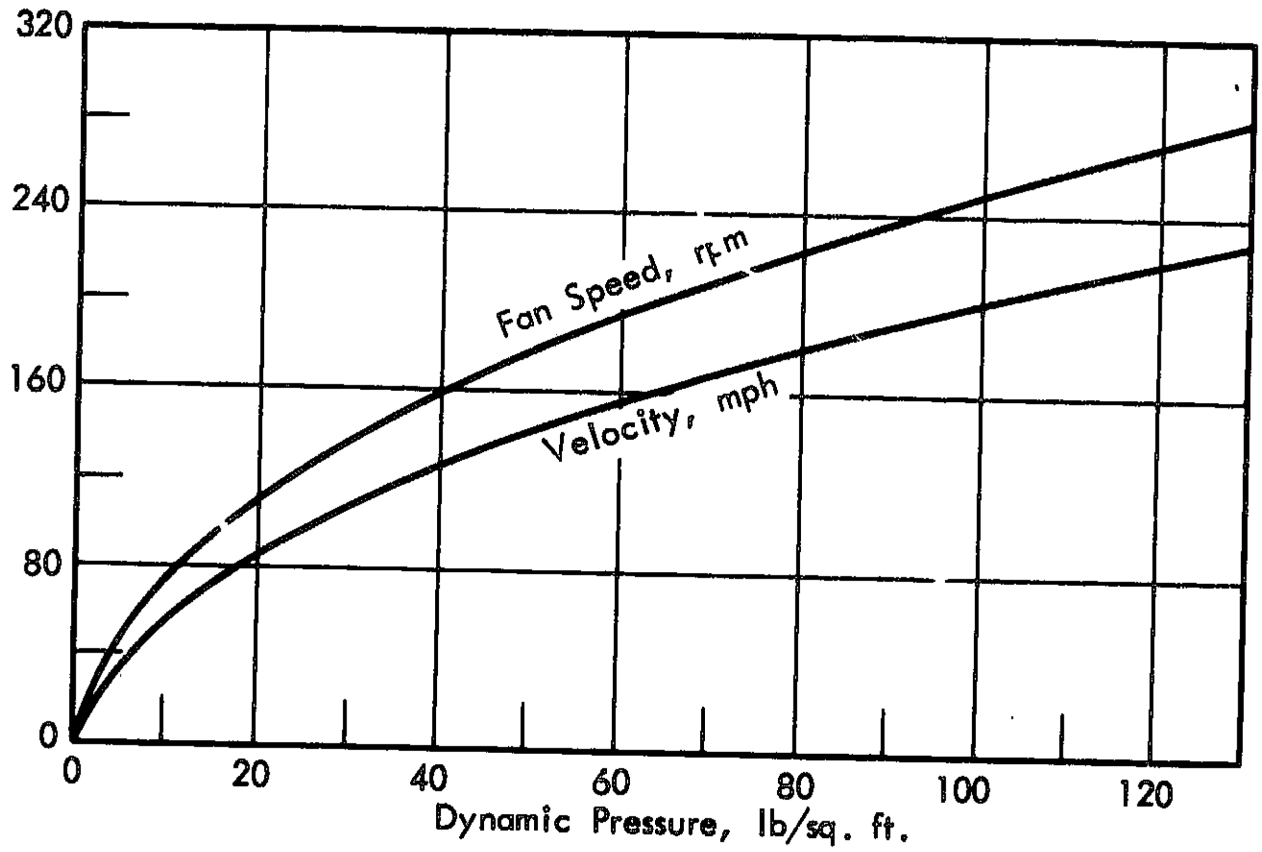

FIGURE 2. FAN SPEED AND TEST SECTION VELOCITY AS A FUNCTION OF TEST SECTION DYNAMIC PRESSURE

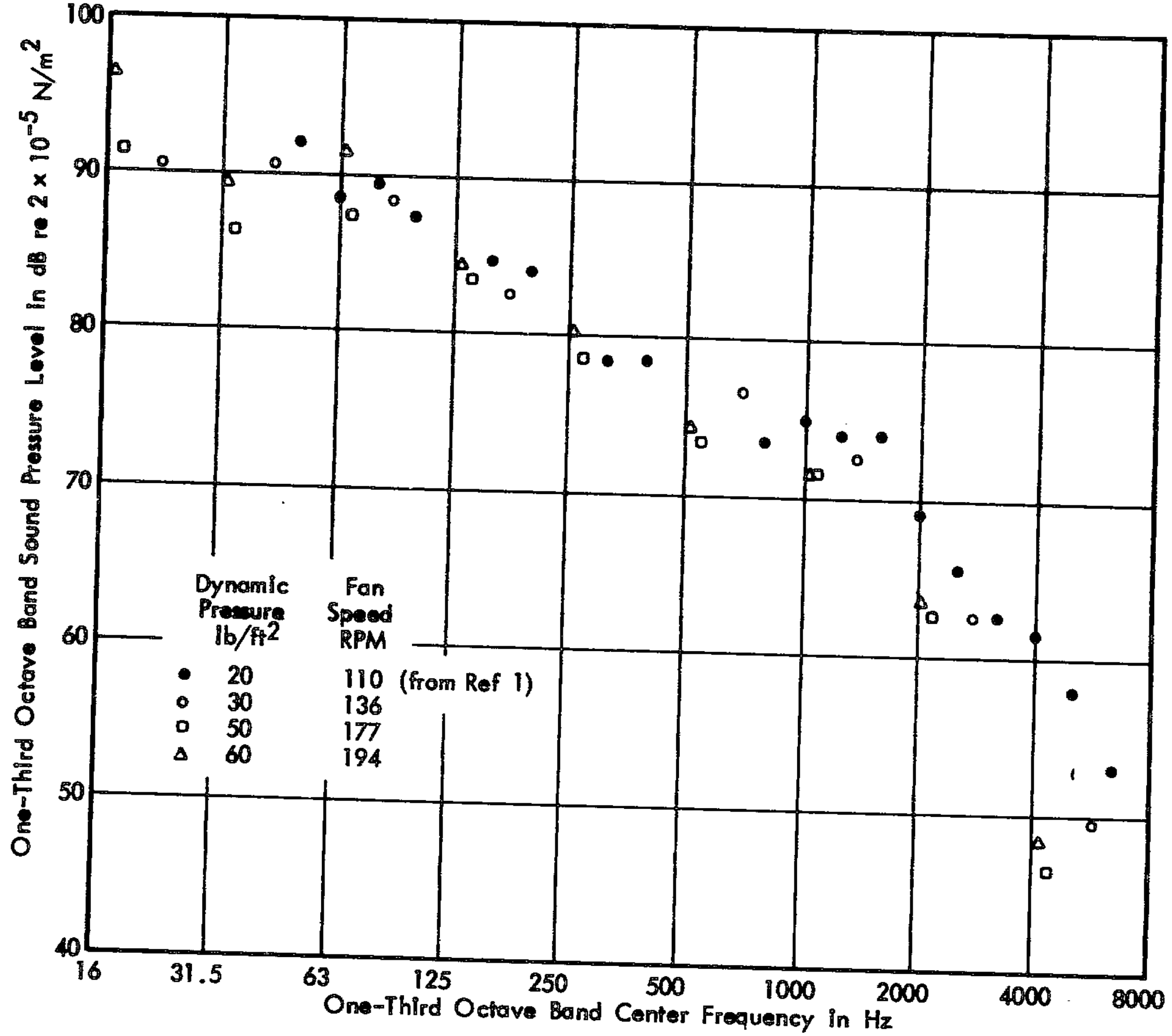

FIGURE 3. FAN SPECTRA NORMALIZED TO 100 RPM BASED ON MEASUREMENTS AT POSITION E (SEE FIG 1 AND TEXT)

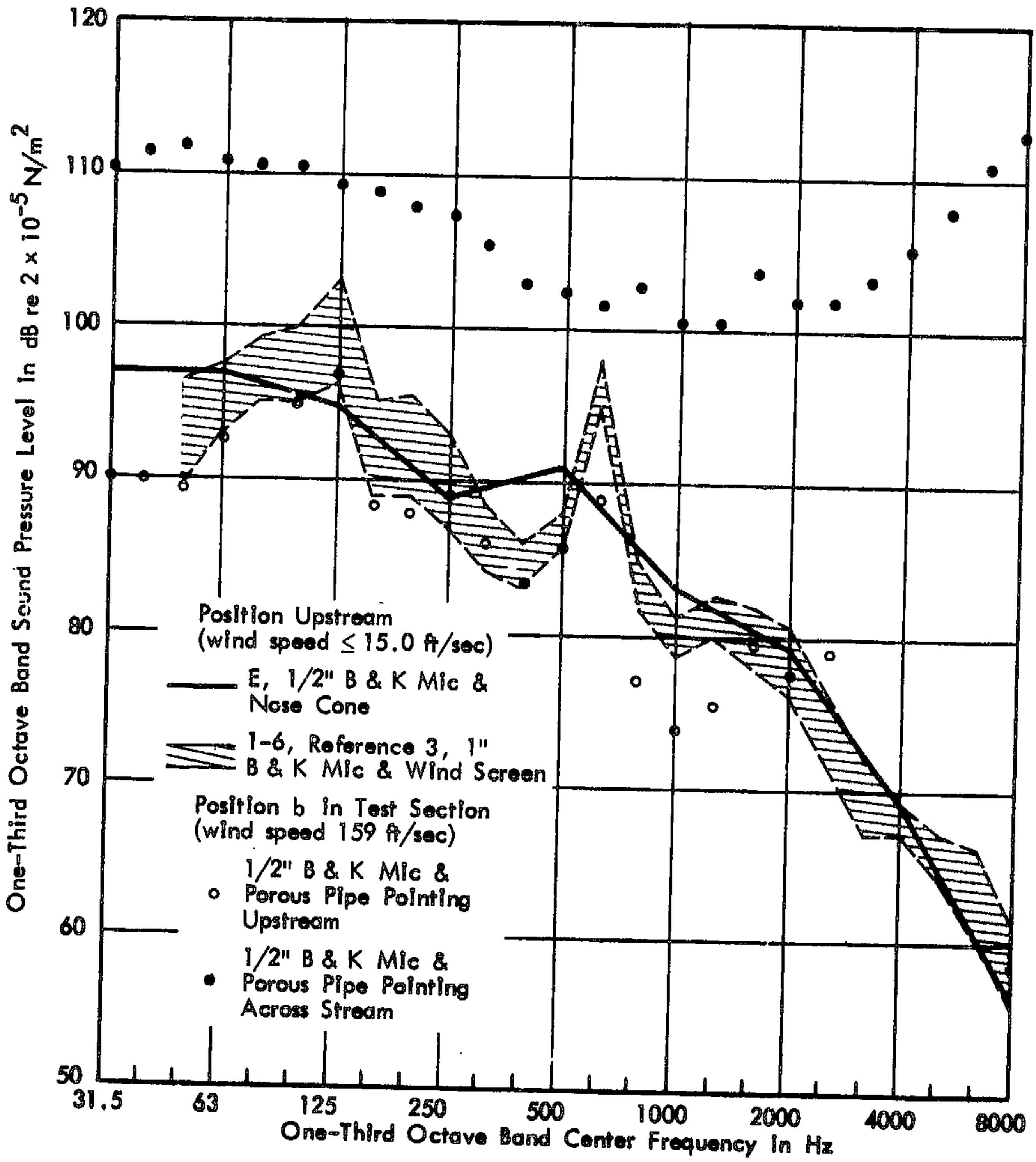

FIGURE 4. COMPARISON OF MEASUREMENTS OF TUNNEL BACKGROUND NOISE IN THE 40 FT x 80 FT WIND TUNNEL AT A TEST SECTION DYNAMIC PRESSURE, $q = 30 \text{ lb/ft}^2$

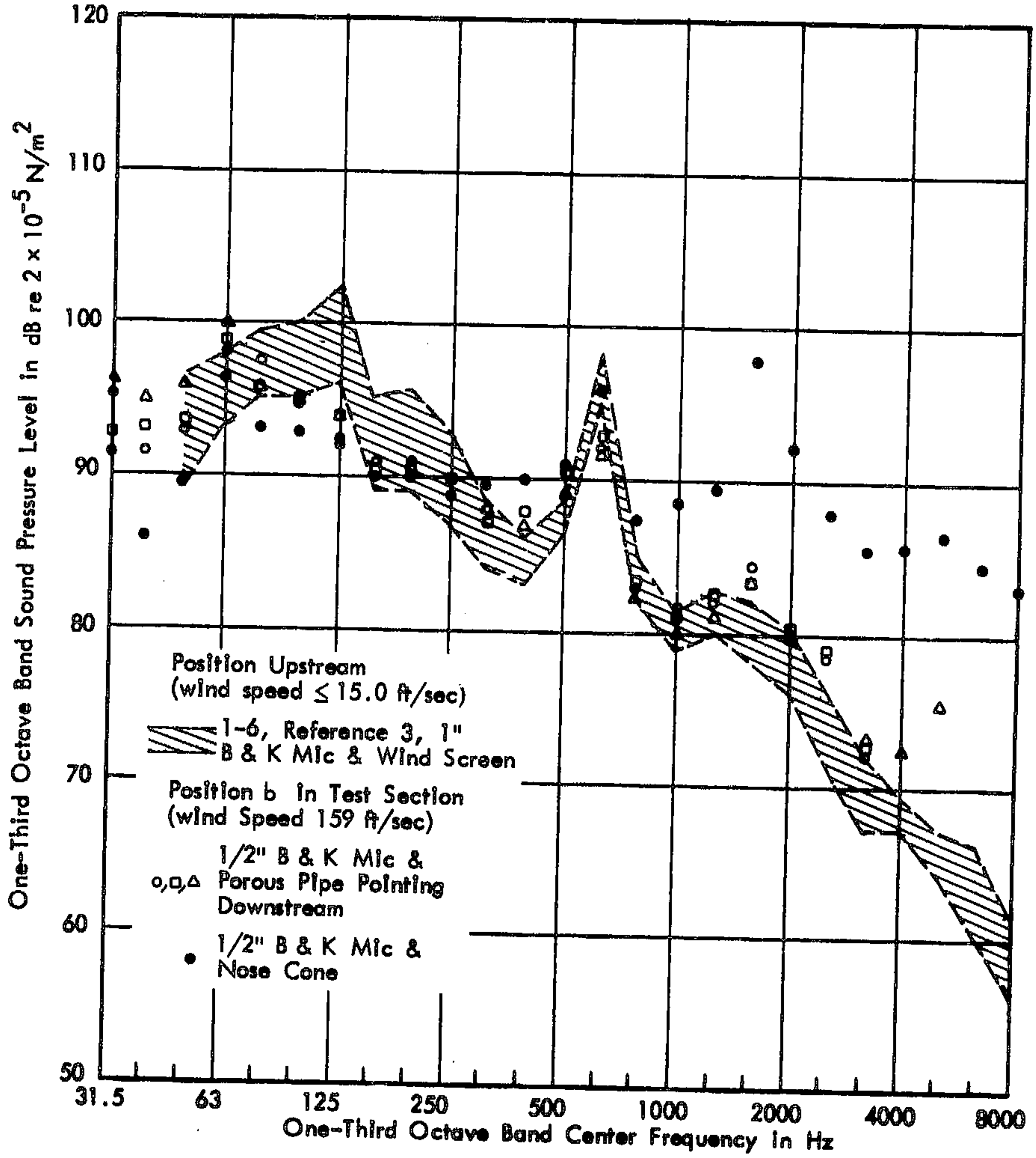

FIGURE 5. COMPARISON OF MEASUREMENTS OF TUNNEL BACKGROUND NOISE IN THE 40 FT x 80 FT WIND TUNNEL AT A TEST SECTION DYNAMIC PRESSURE, $q = 30\ lb/ft^2$

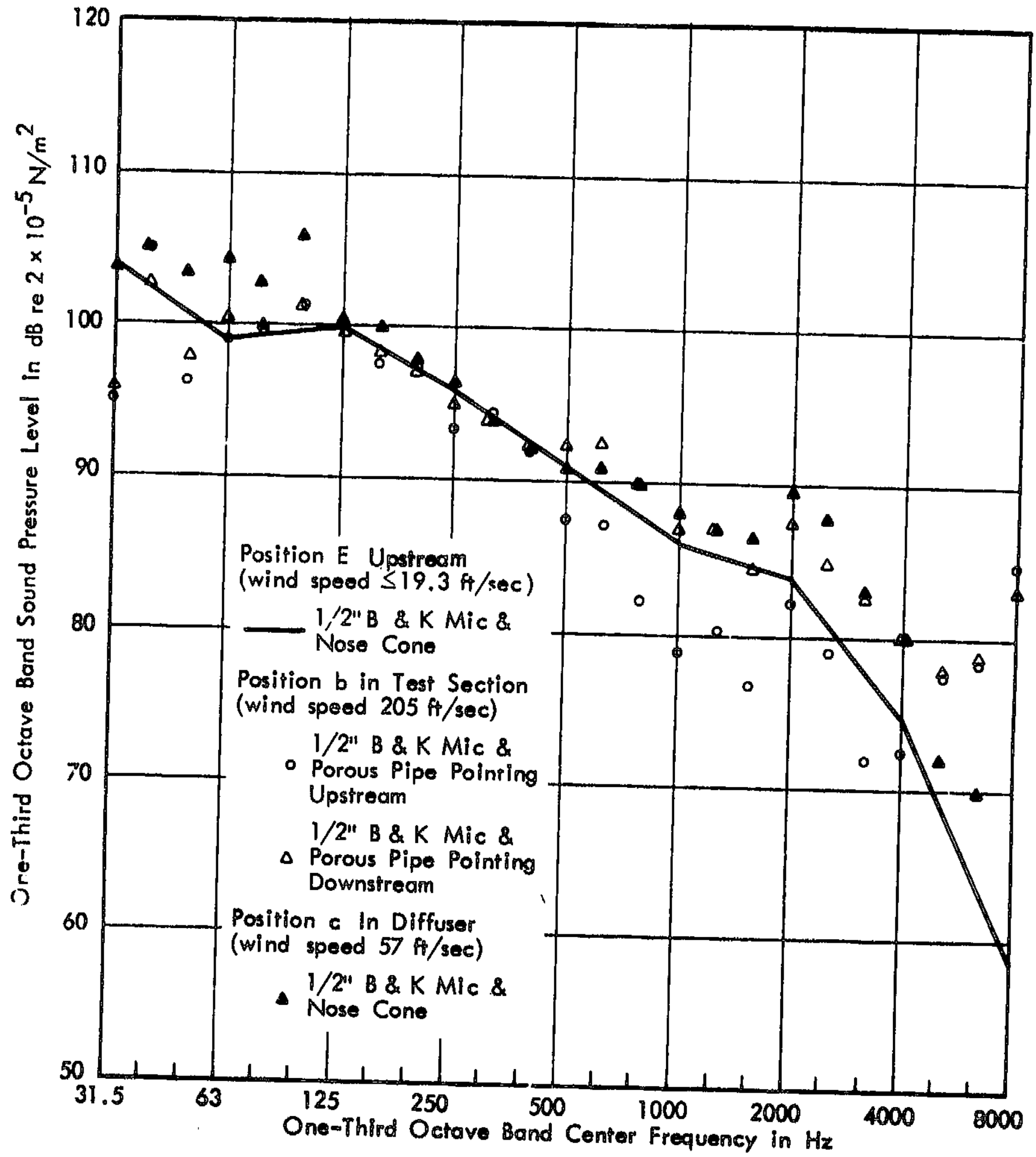

FIGURE 6. COMPARISON OF MEASUREMENTS OF TUNNEL BACKGROUND NOISE IN THE 40 FT × 80 FT WIND TUNNEL AT A TEST SECTION DYNAMIC PRESSURE, $q = 50\ lb/ft^2$

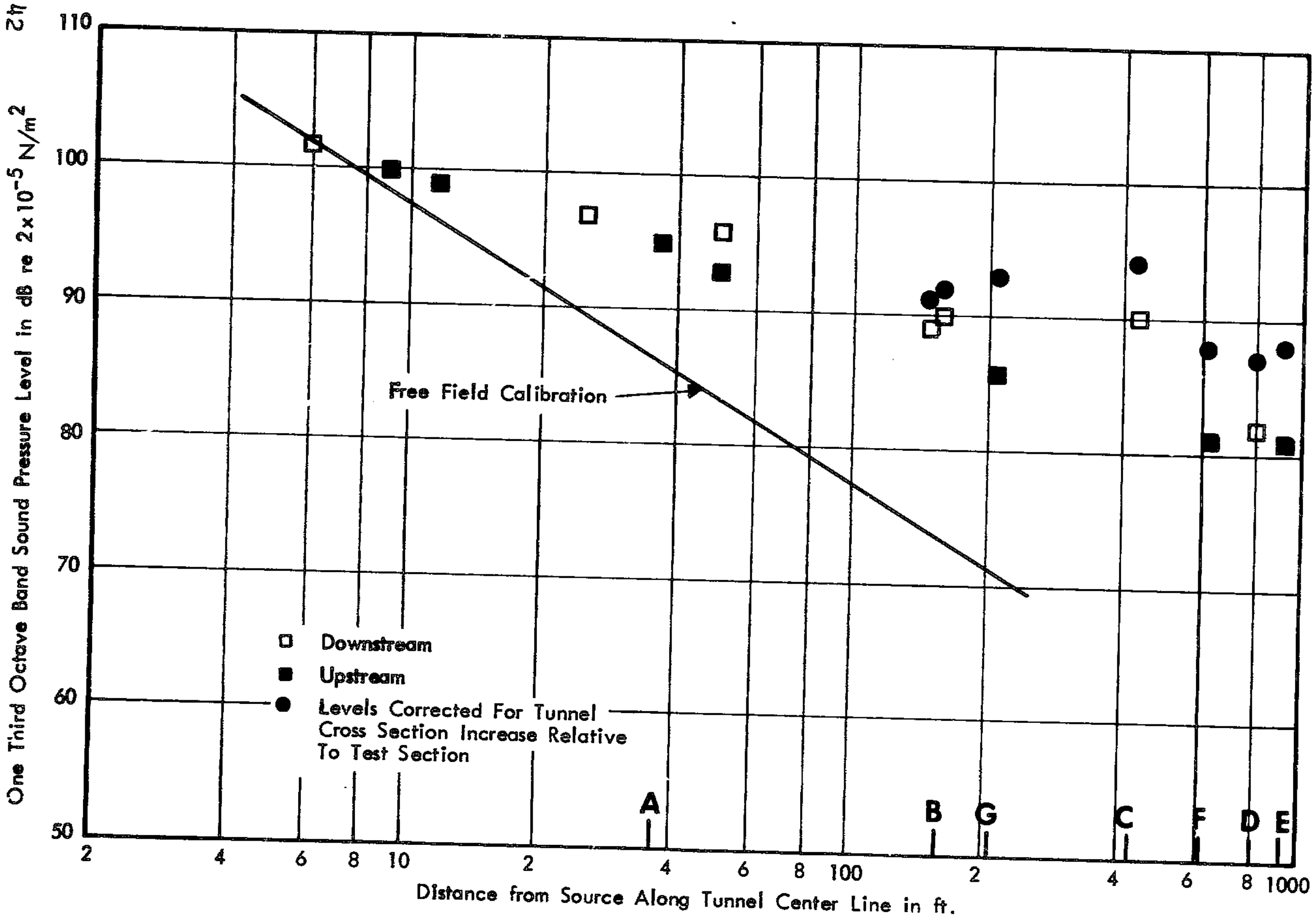

FIGURE 7. TUNNEL SOUND PRESSURE LEVELS DUE TO A DODECAHEDRON SOUND SOURCE IN THE TEST SECTION, 125 HZ 1/3 OCTAVE BAND, 12 VOLTS RMS INPUT, SOUND POWER LEVEL 118.5 dB RE 10-12 WATT

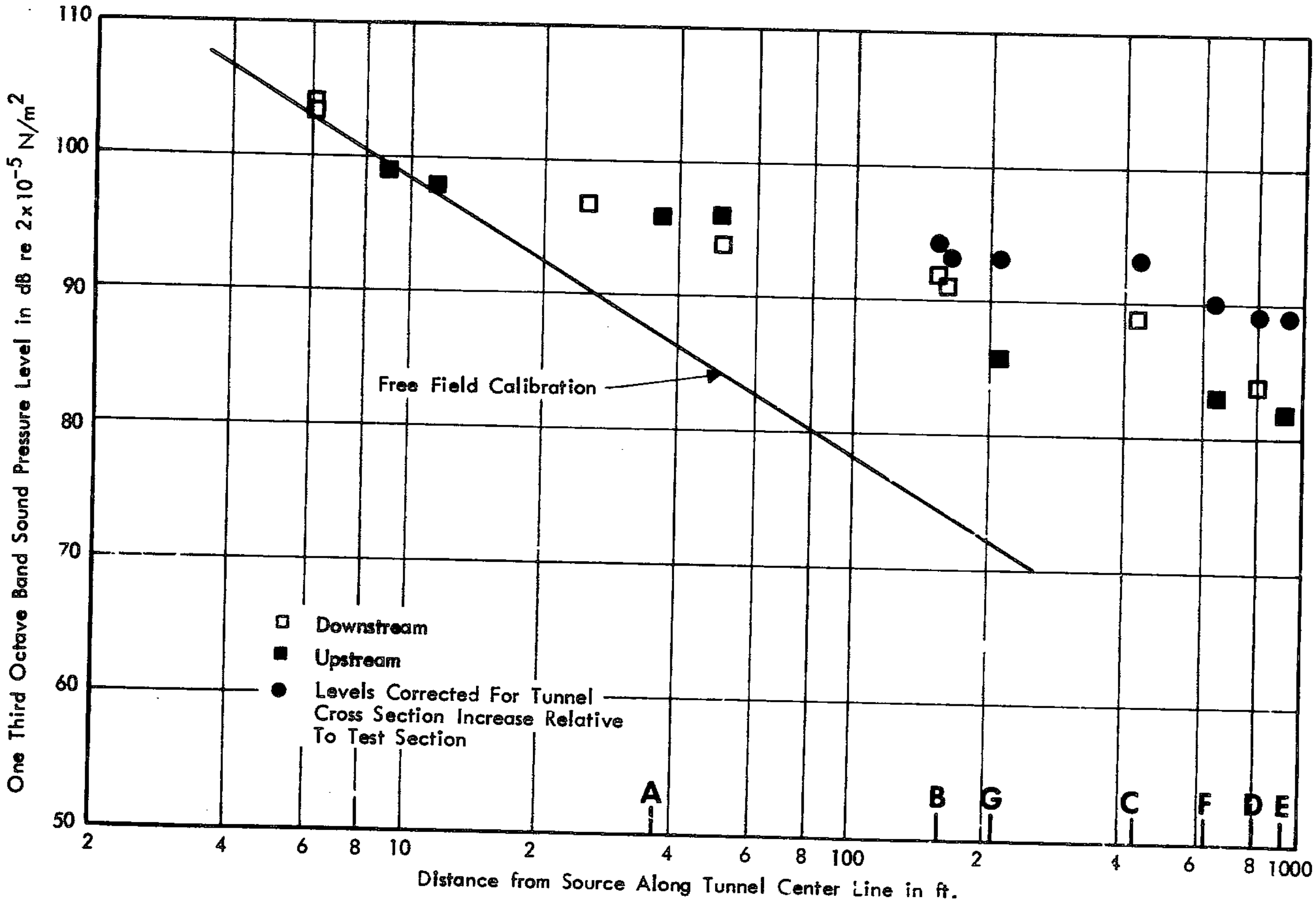

FIGURE 8. TUNNEL SOUND PRESSURE LEVELS DUE TO A DODECAHEDRON SOUND SOURCE IN THE TEST SECTION, 250 HZ 1/3 OCTAVE BAND, 12 VOLTS RMS INPUT, SOUND POWER LEVEL 119.5 dB RE 10-12 VOLT

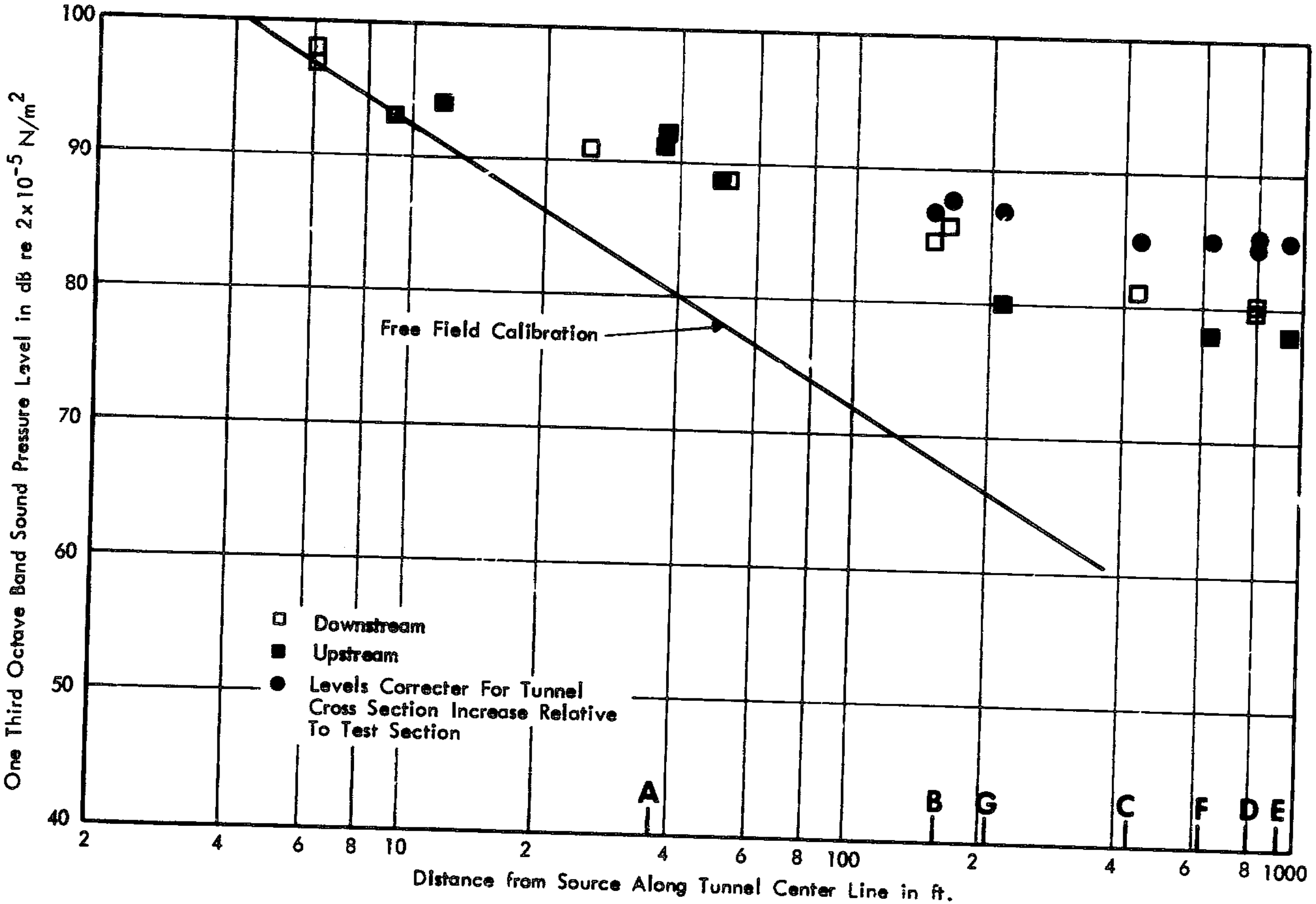

FIGURE 9. TUNNEL SOUND PRESSURE LEVELS DUE TO A DODECAHEDRON SOUND SOURCE IN THE TEST SECTION, 500 HZ 1/3 OCTAVE BAND, 12 VOLTS RMS INPUT, SOUND POWER LEVEL 113.5 dB RE 10^{-12} VOLT

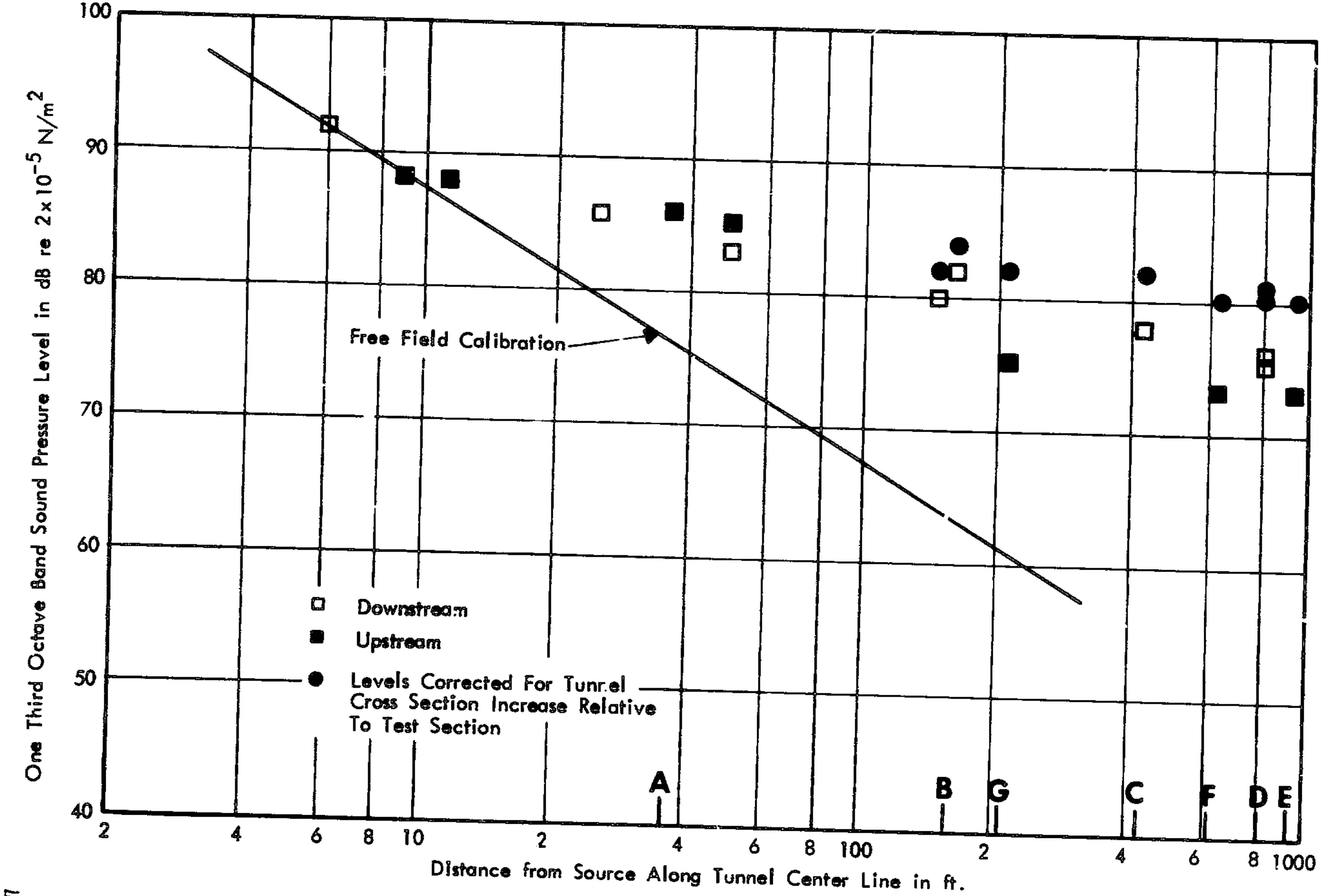

FIGURE 10. TUNNEL SOUND PRESSURE LEVELS DUE TO A DODECAHEDRON SOUND SOURCE IN THE TEST SECTION, 1000 HZ 1/3 OCTAVE BAND, 12 VOLTS RMS INPUT, SOUND POWER LEVEL 109.5 dB RE 10-12 VOLT

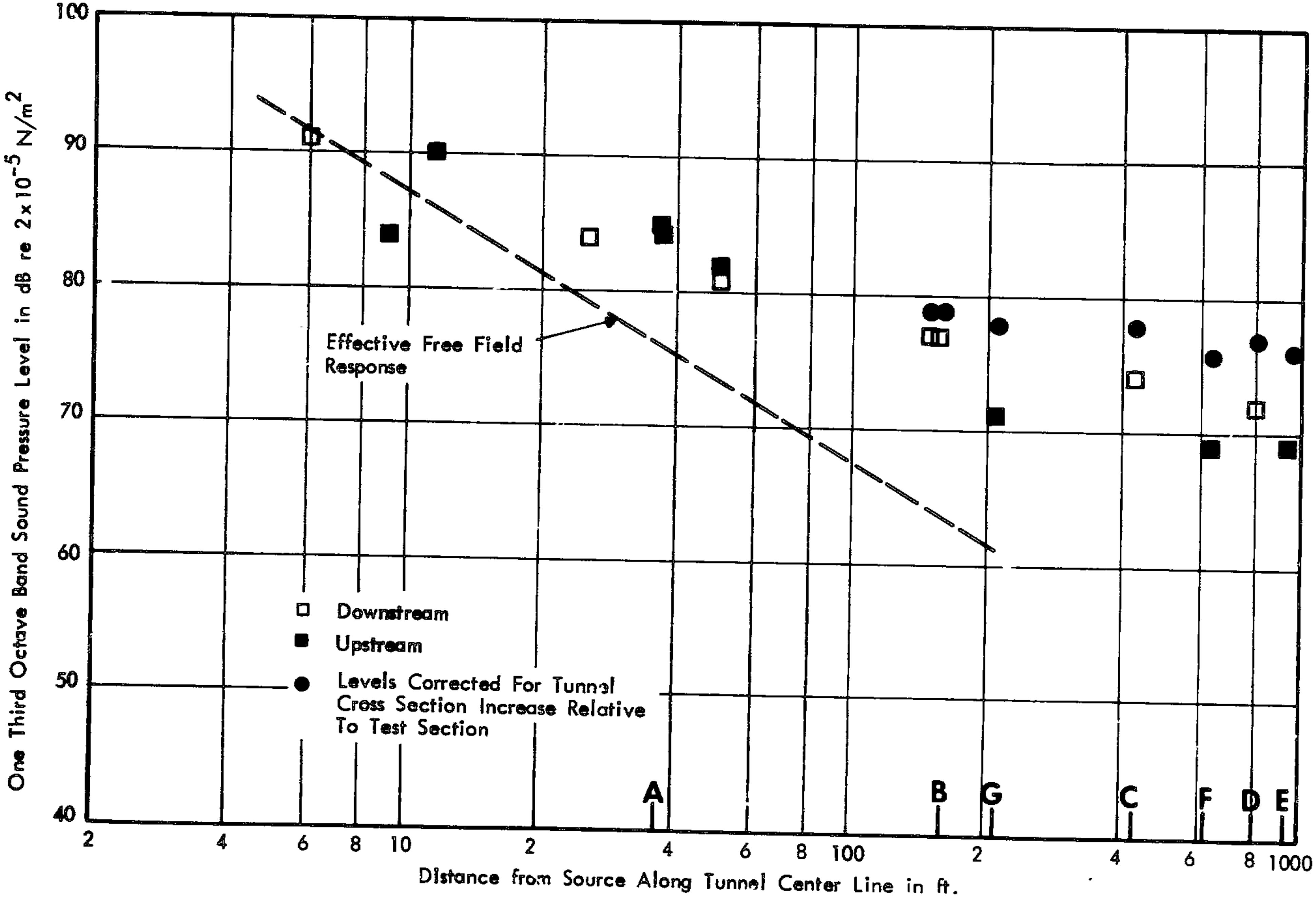

FIGURE 11. TUNNEL SOUND PRESSURE LEVELS DUE TO A DODECAHEDRON SOUND SOURCE IN THE TEST SECTION, 2000 HZ 1/3 OCTAVE BAND, 12 VOLTS RMS INPUT, SOUND POWER LEVEL 108.5 dB RE 10^{-12} WATT

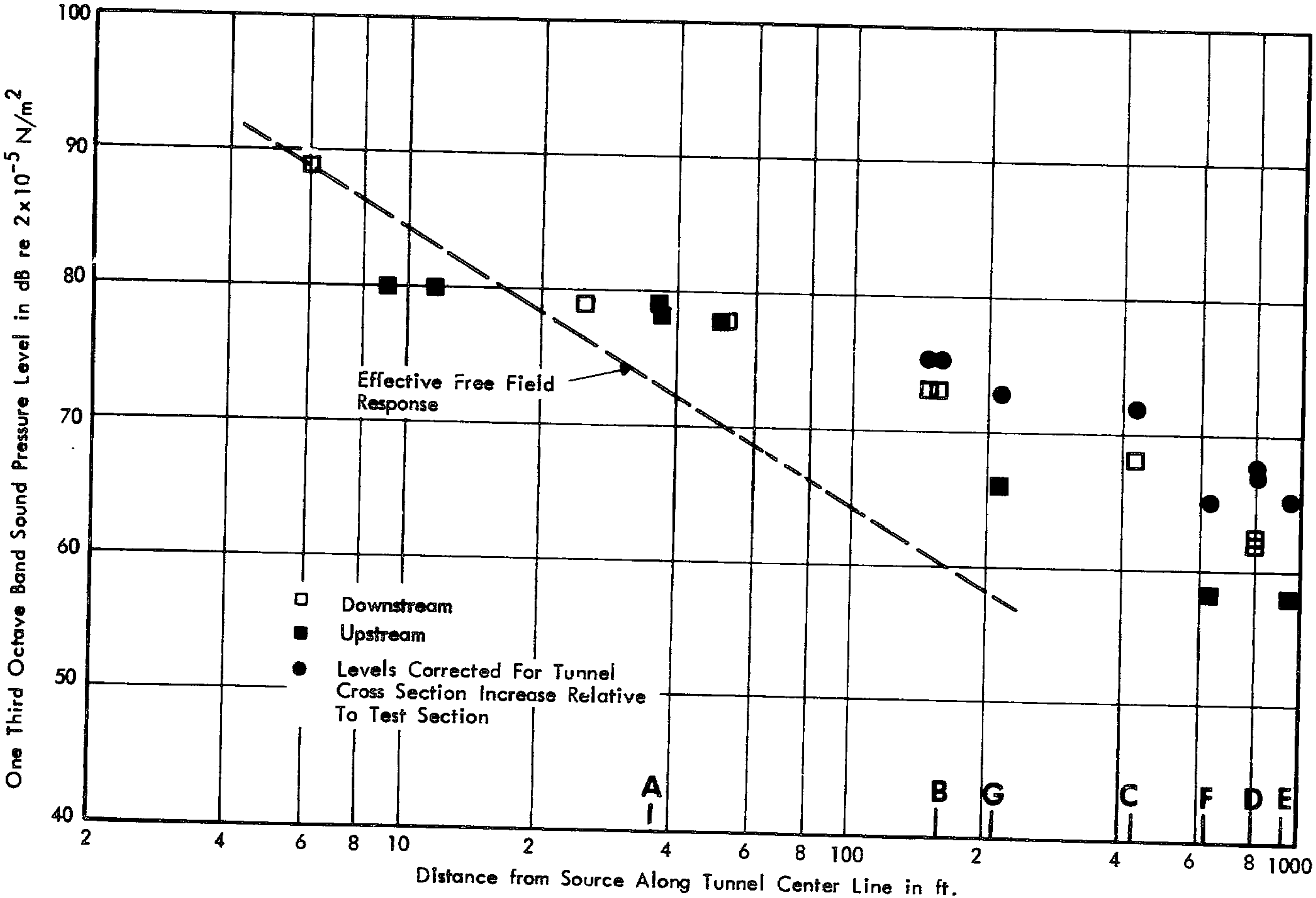

FIGURE 12. TUNNEL SOUND PRESSURE LEVELS DUE TO A DODECAHEDRON SOUND SOURCE IN THE TEST SECTION, 4000 HZ 1/3 OCTAVE BAND, 12 VOLTS RMS INPUT, SOUND POWER LEVEL 105.5 dB RE 10^{-12} WATT

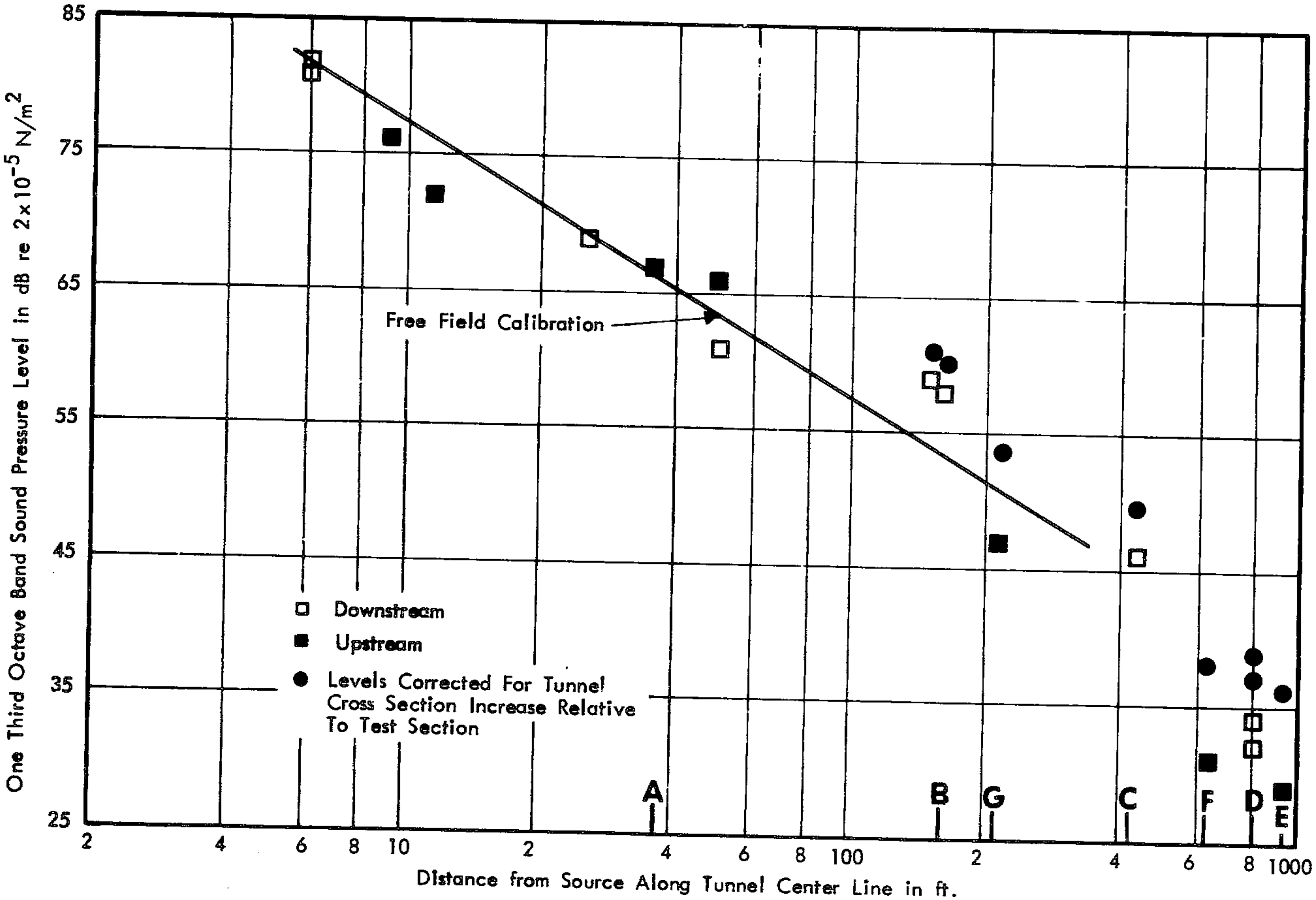

FIGURE 13. TUNNEL SOUND PRESSURE LEVELS DUE TO A DODECAHEDRON SOUND SOURCE IN THE TEST SECTION, 8000 HZ 1/3 OCTAVE BAND, 12 VOLTS RMS INPUT, SOUND POWER LEVEL 97.5 dB RE 10^{-12} WATT

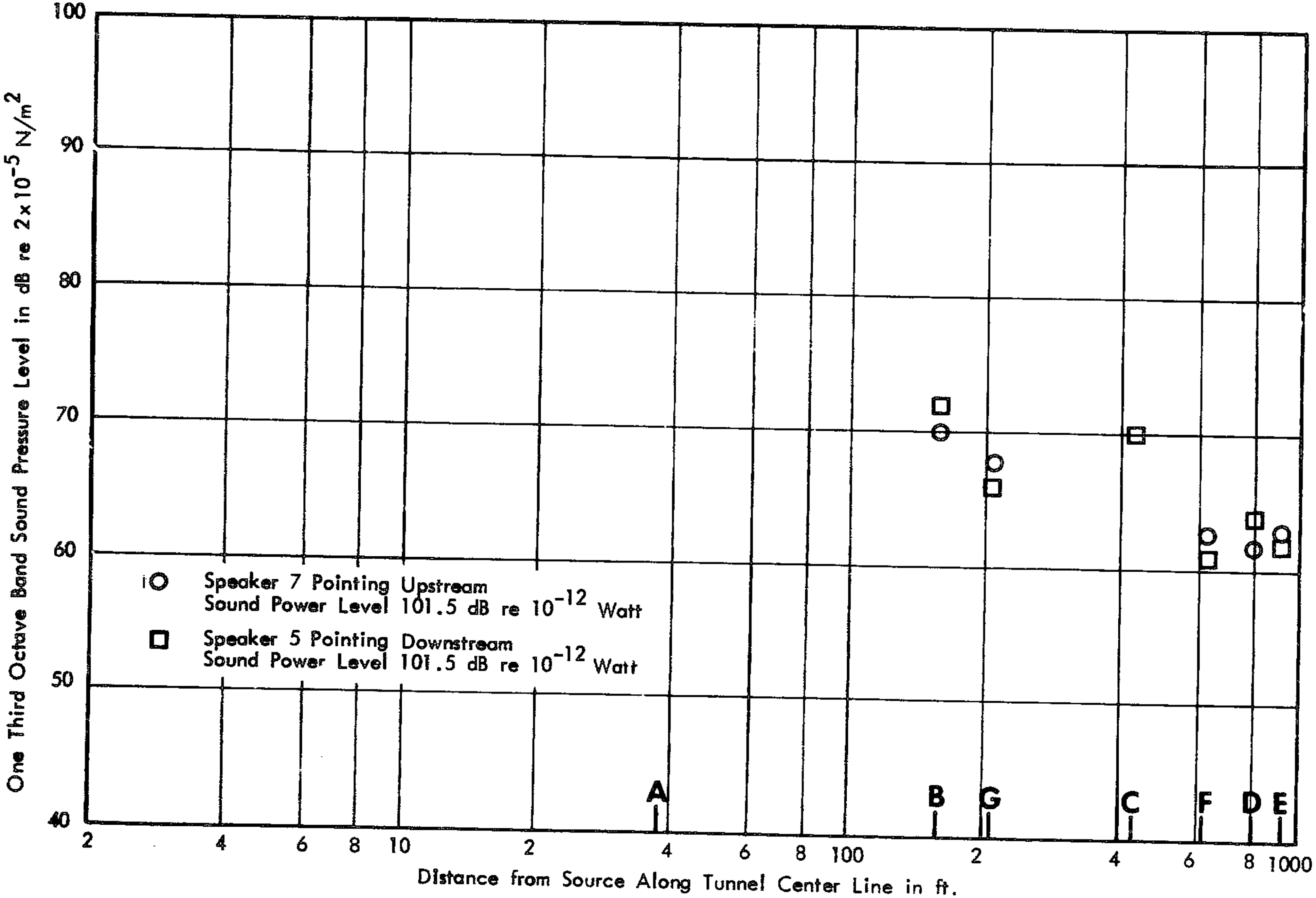

FIGURE 14. TUNNEL SOUND PRESSURE LEVELS DUE TO A DIRECTIONAL SOUND SOURCE IN THE TEST SECTION, 250 HZ 1/3 OCTAVE BAND, 4 VOLTS RMS INPUT

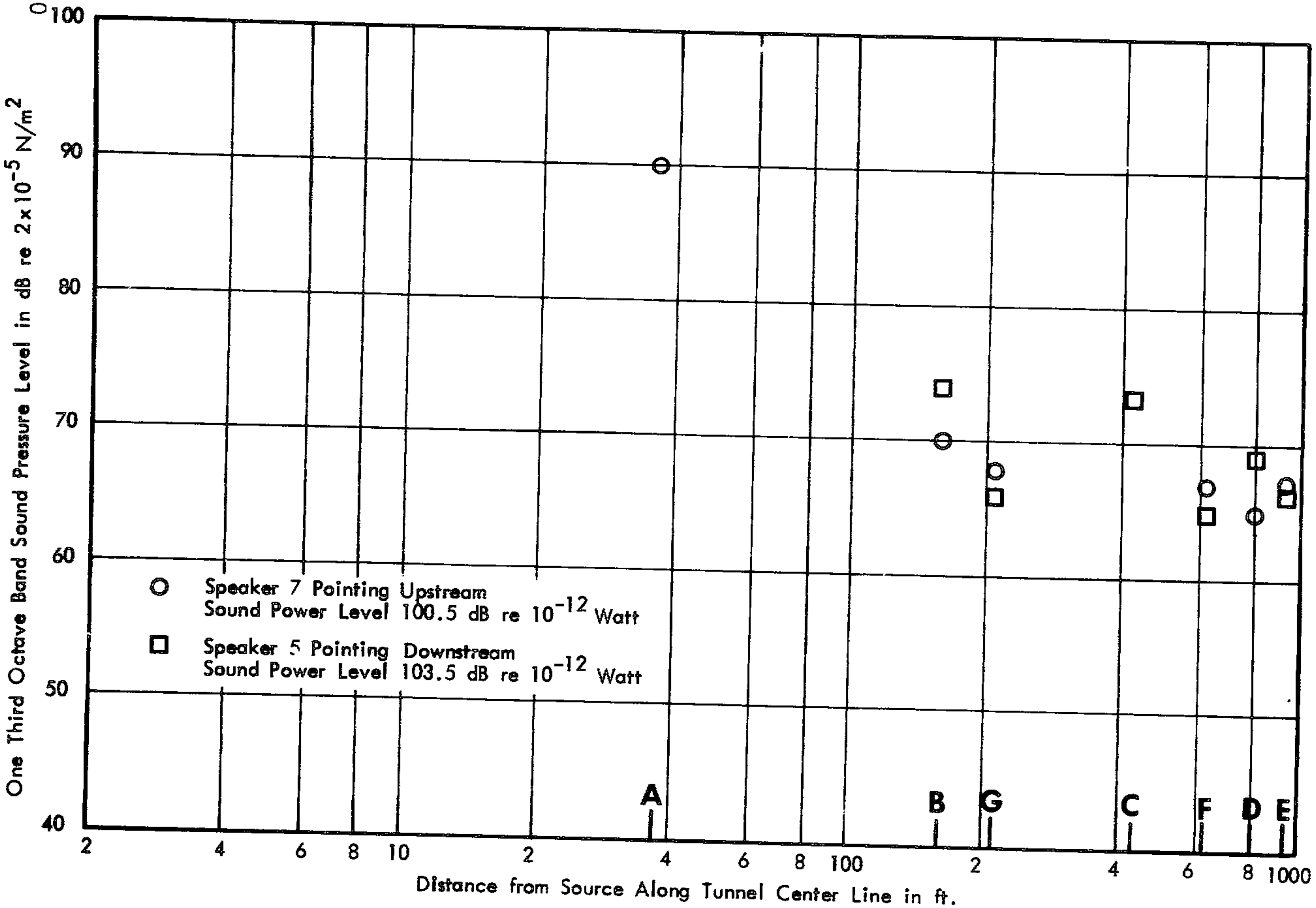

FIGURE 15. TUNNEL SOUND PRESSURE LEVELS DUE TO A DIRECTIONAL SOUND SOURCE IN THE TEST SECTION, 500 HZ 1/3 OCTAVE BAND, 4 VOLTS RMS INPUT

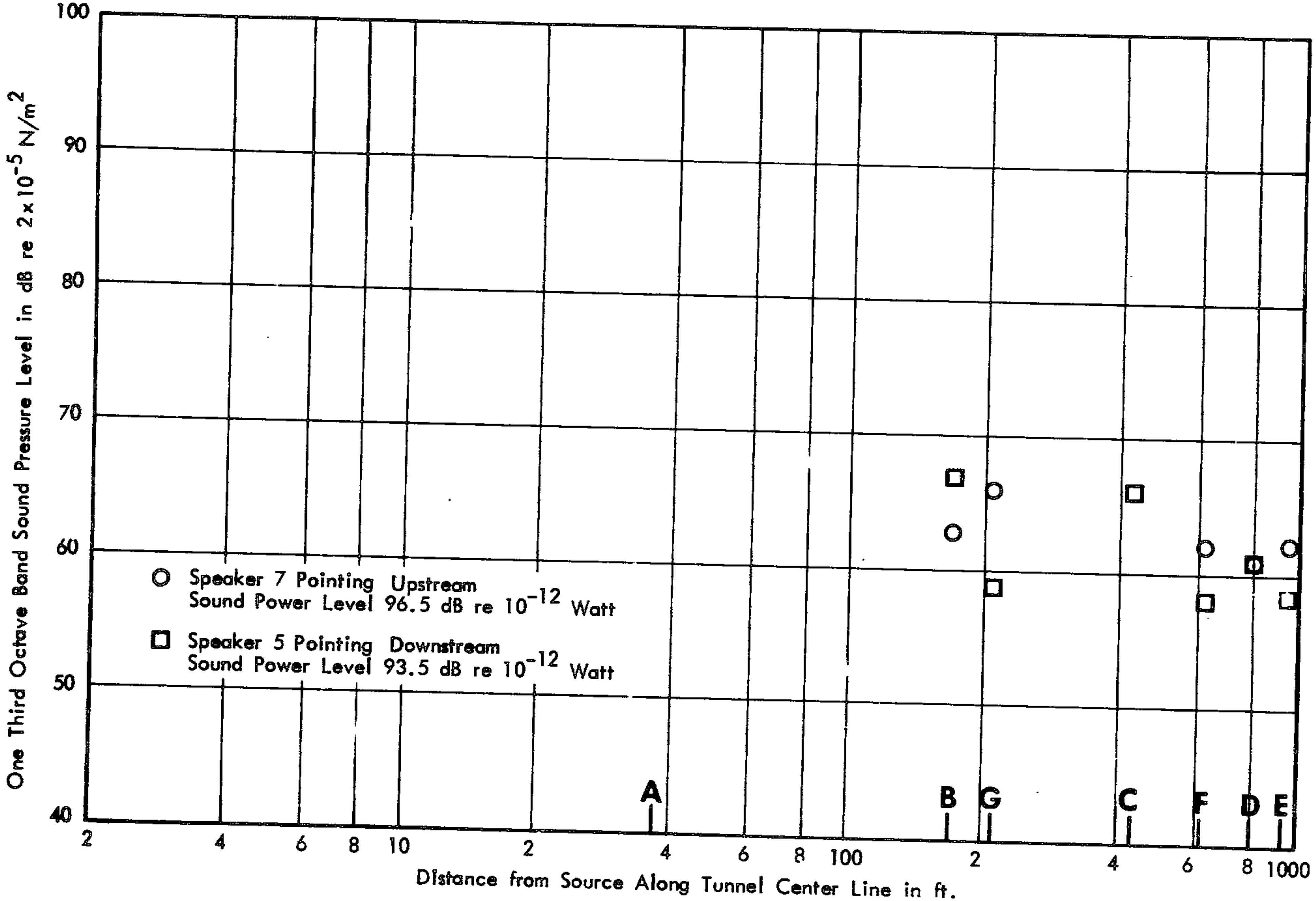

FIGURE 16. TUNNEL SOUND PRESSURE LEVELS DUE TO A DIRECTIONAL SOUND SOURCE IN THE TEST SECTION, 1000 HZ 1/3 OCTAVE BAND, 4 VOLTS RMS INPUT

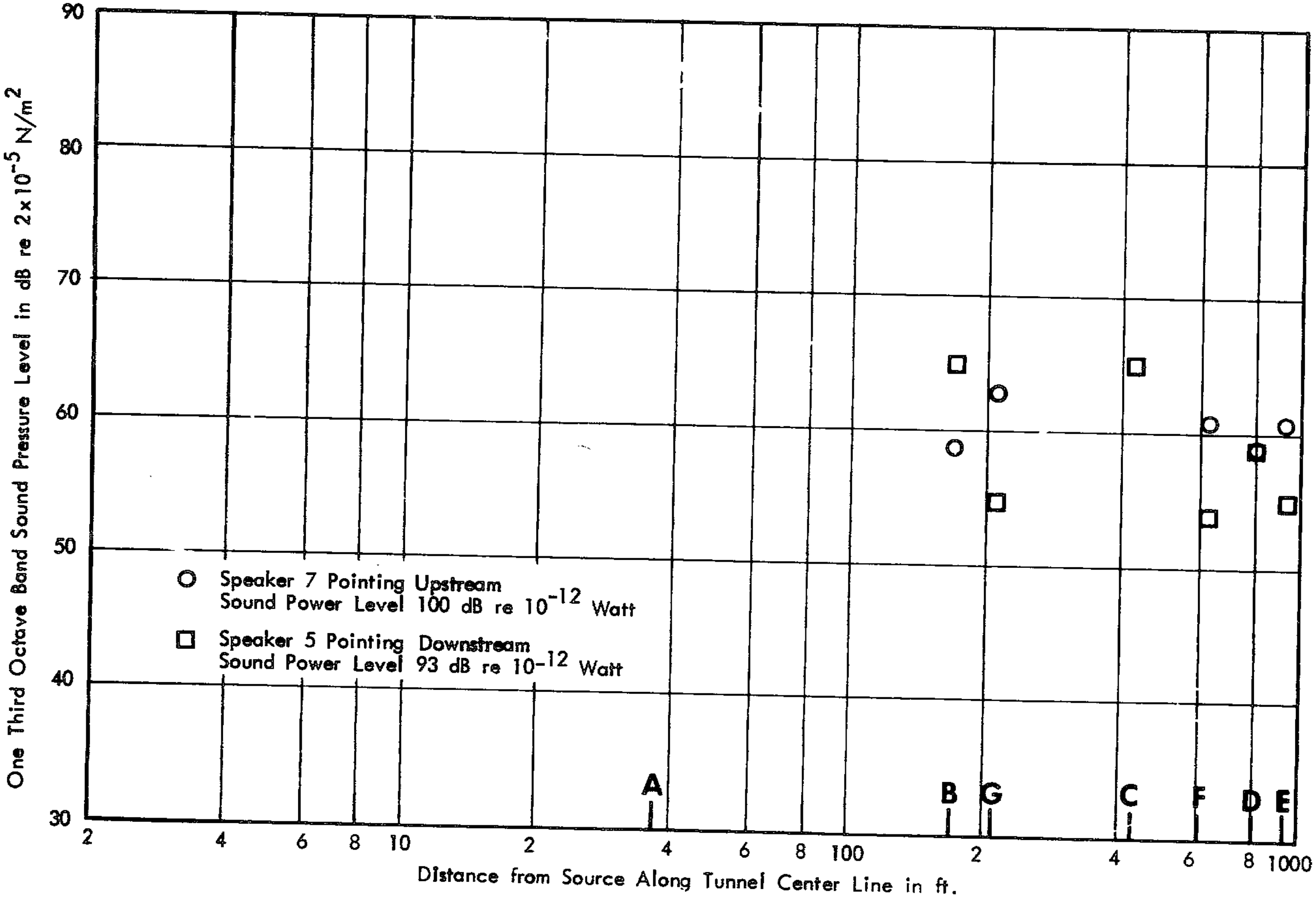

FIGURE 17. TUNNEL SOUND PRESSURE LEVELS DUE TO A DIRECTIONAL SOUND SOURCE IN THE TEST SECTION, 2000 HZ 1/3 OCTAVE BAND, 4 VOLTS RMS INPUT

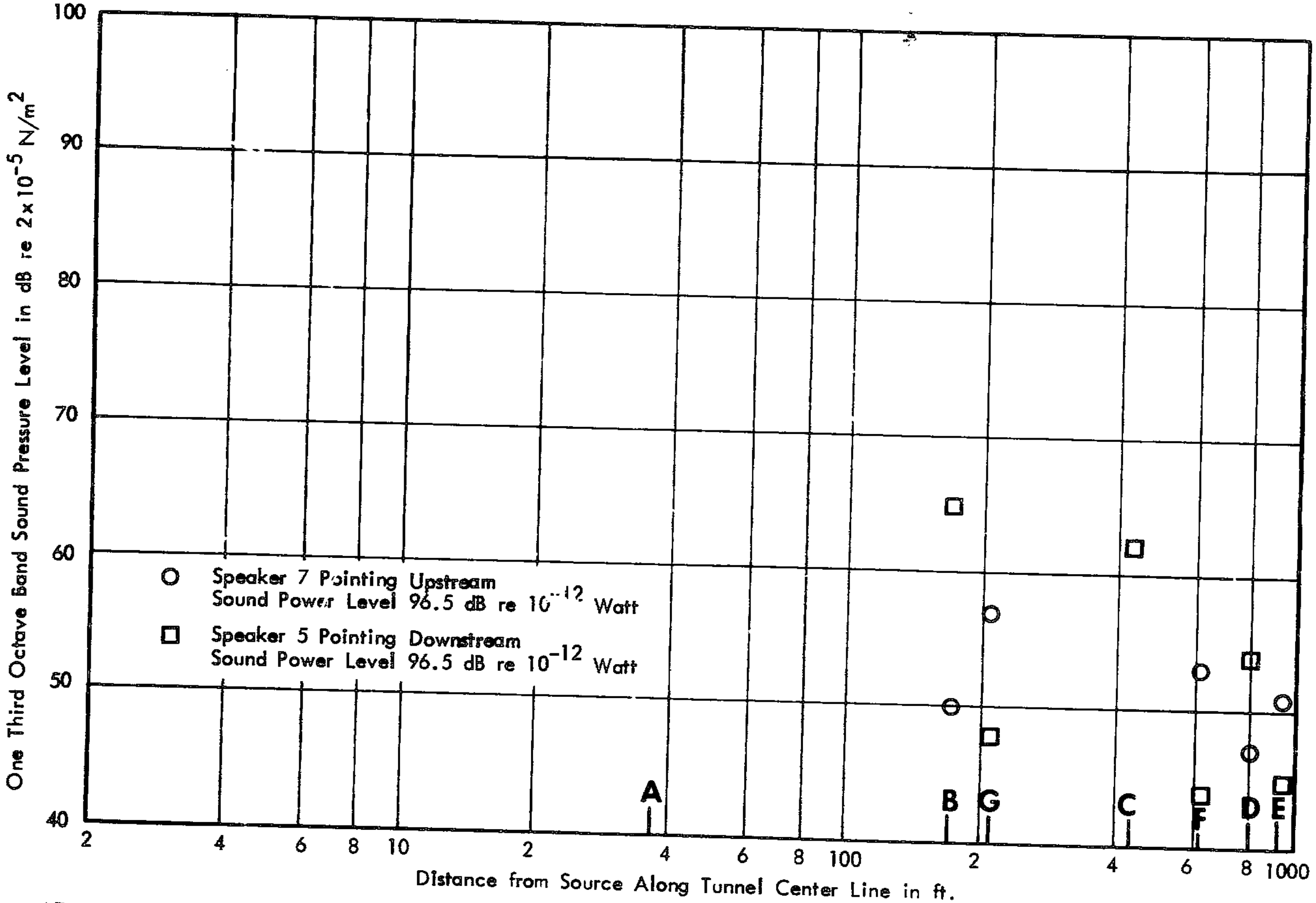

FIGURE 18. TUNNEL SOUND PRESSURE LEVELS DUE TO A DIRECTIONAL SOUND SOURCE IN THE TEST SECTION, 4000 HZ 1/3 OCTAVE BAND, 4 VOLTS RMS INPUT

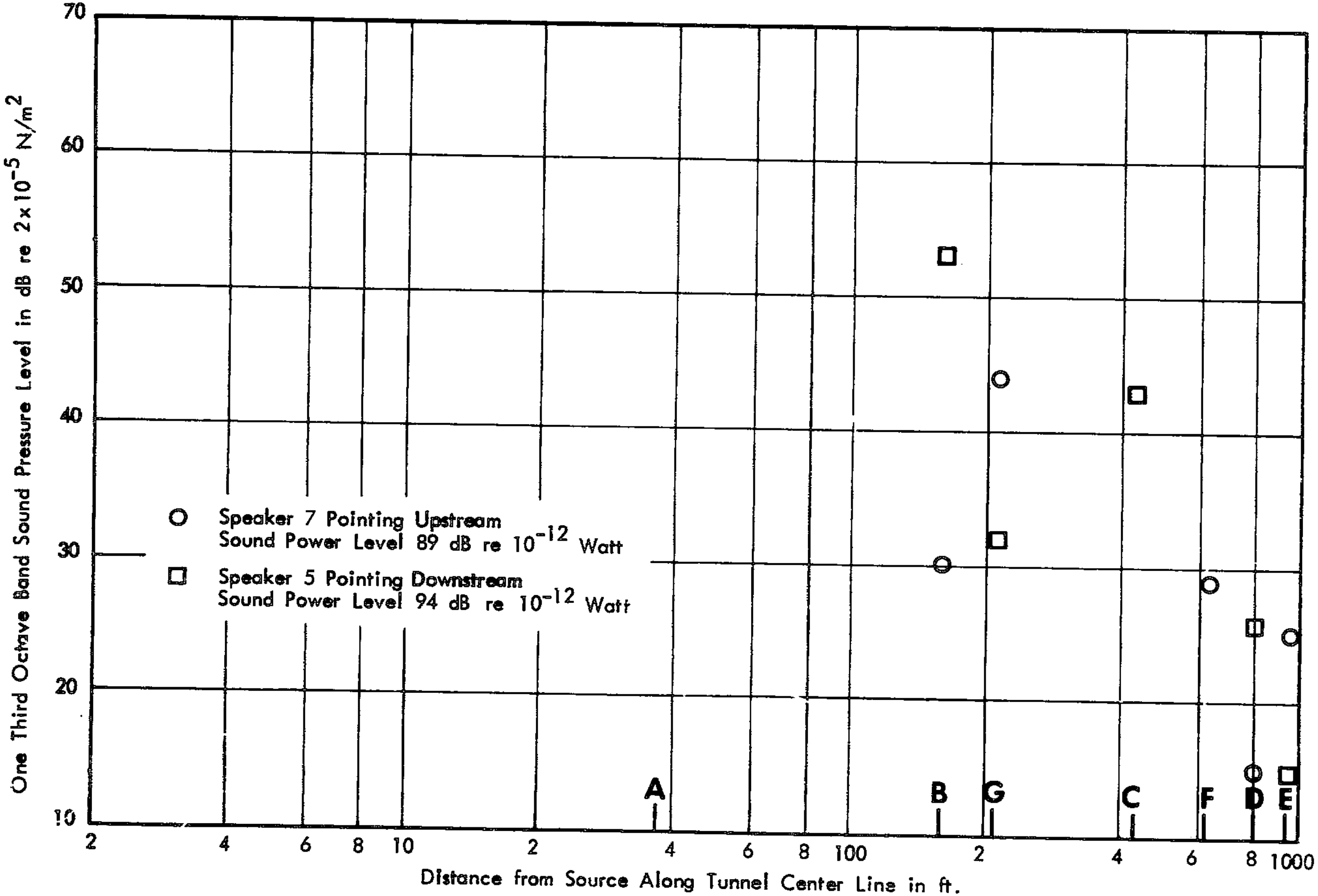

FIGURE 19. TUNNEL SOUND PRESSURE LEVELS DUE TO A DIRECTIONAL SOUND SOURCE IN THE TEST SECTION, 8000 HZ 1/3 OCTAVE BAND, 4 VOLTS RMS INPUT

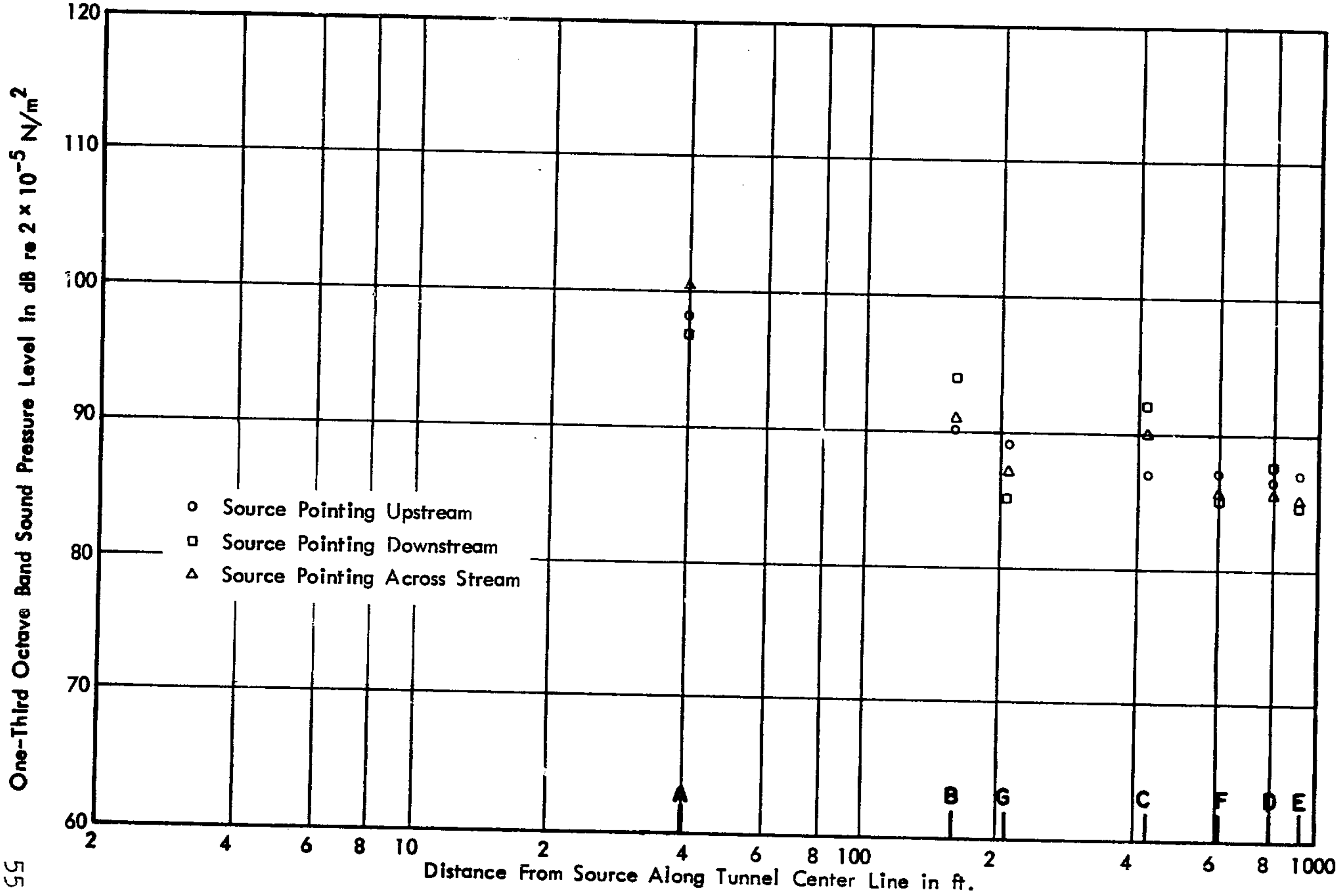

FIGURE 20. TUNNEL SOUND PRESSURE LEVELS DUE TO A DIRECTIONAL SOUND SOURCE IN THE TEST SECTION, 500 HZ 1/3 OCTAVE BAND, 10 VOLTS RMS INPUT INTO JBL 2480 DRIVER AND RCA Mi 9594A HORN SOUND POWER LEVEL 119 dB RE 10^{-12} WATT

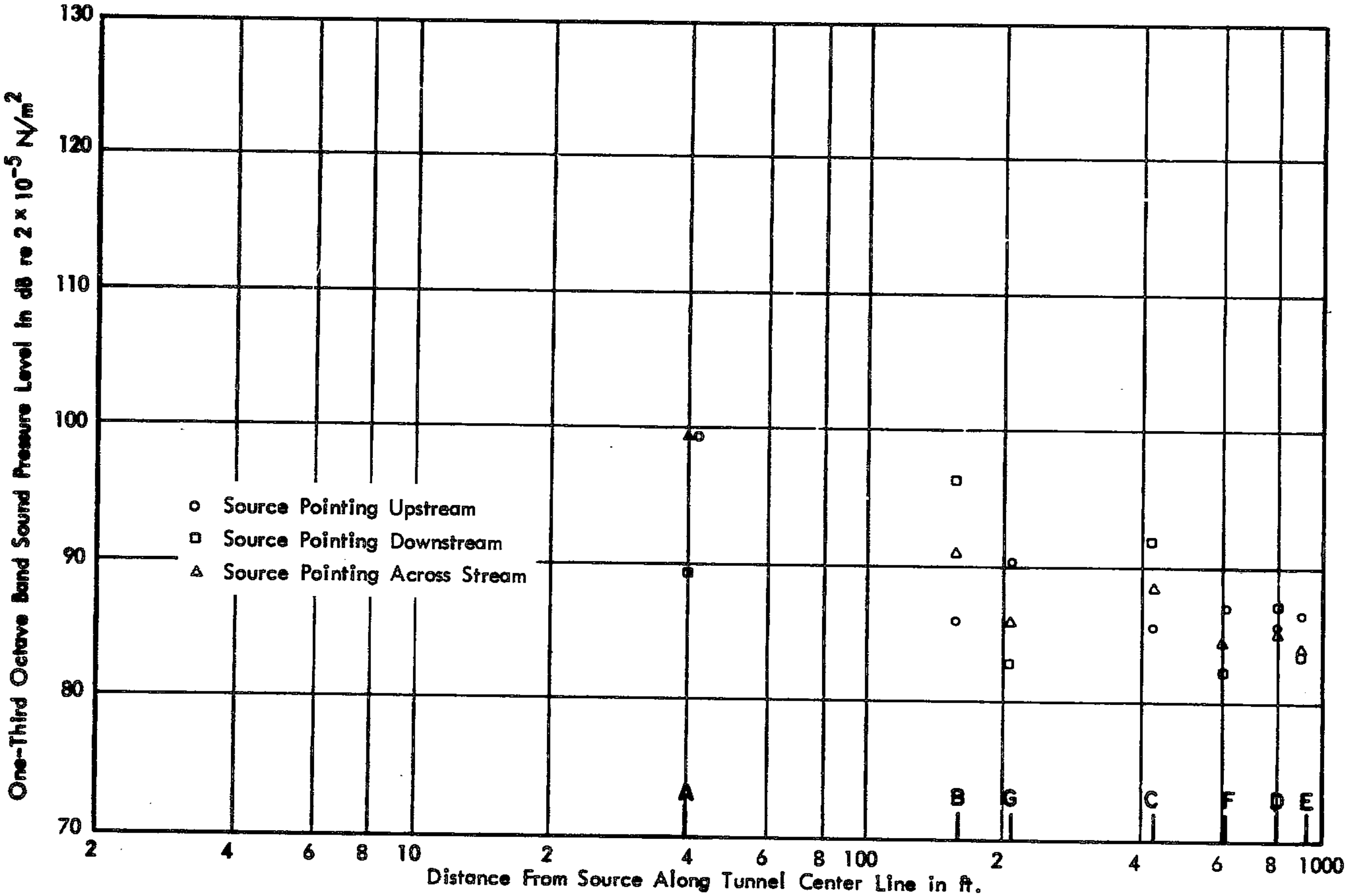

FIGURE 21. TUNNEL SOUND PRESSURE LEVELS DUE TO A DIRECTIONAL SOUND SOURCE IN THE TEST SECTION, 1000 HZ 1/3 OCTAVE BAND, 10 VOLTS RMS INPUT INTO JBL 2480 DRIVER AND RCA MI 9594A HORN SOUND POWER LEVEL 119.5dB RE 10^{-12} WATT

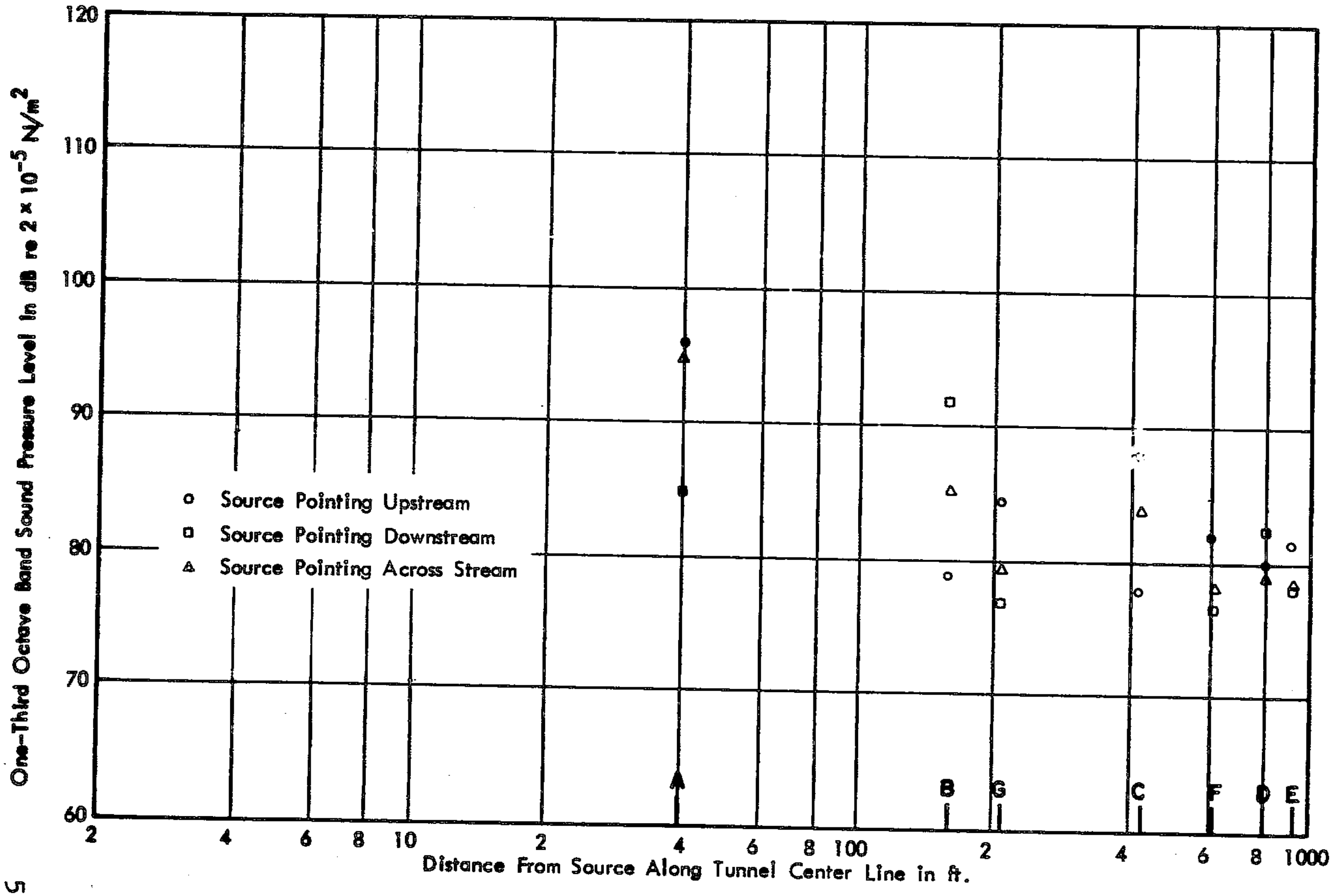

FIGURE 22. TUNNEL SOUND PRESSURE LEVELS DUE TO A DIRECTIONAL SOUND SOURCE IN THE TEST SECTION, 2000 HZ 1/3 OCTAVE BAND, 10 VOLTS RMS INPUT INTO JBL 2480 DRIVER AND RCA MI 9594A HORN SOUND POWER LEVEL 117.5dB RE 10^{-12} WATT

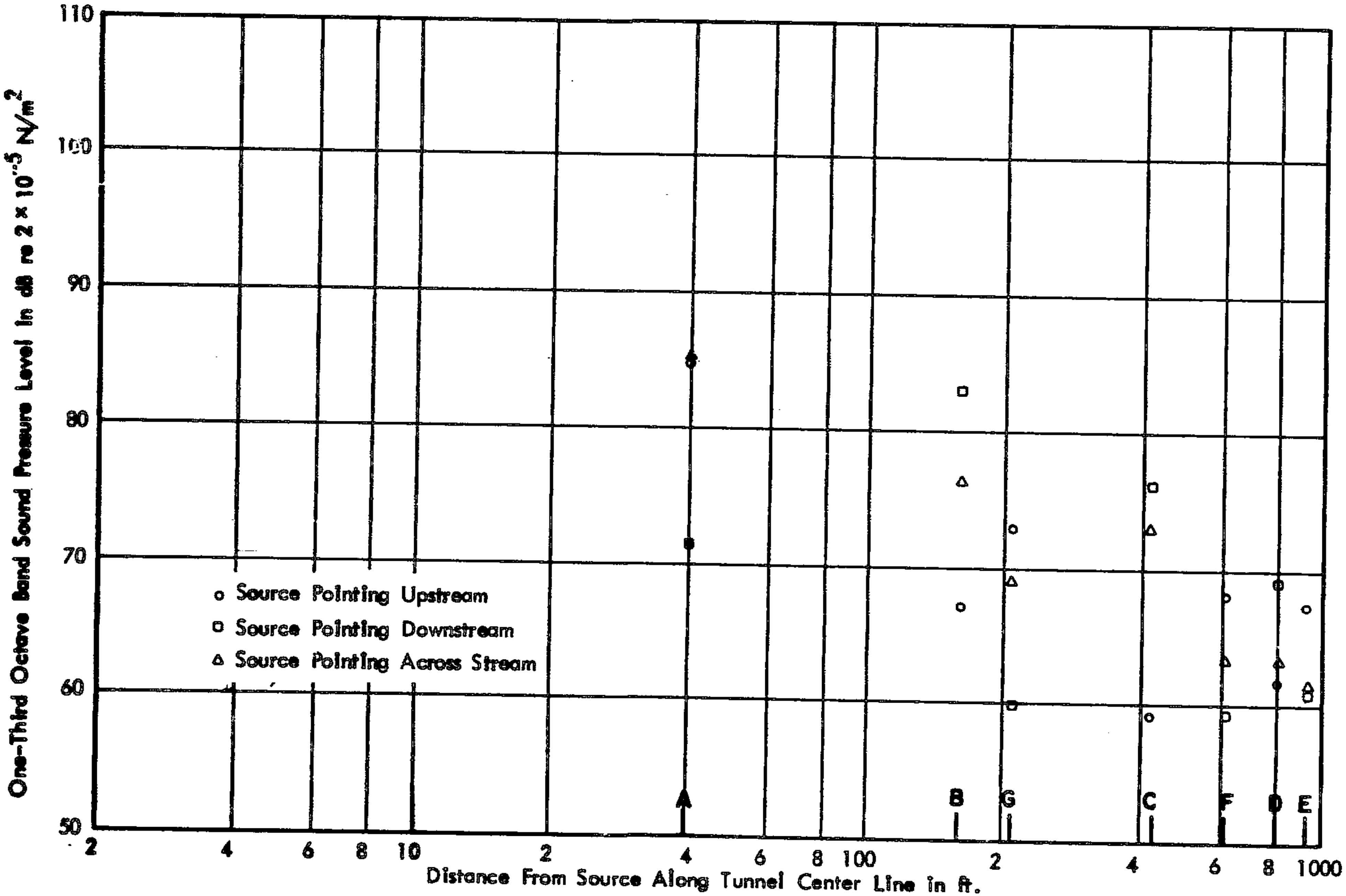

FIGURE 23. TUNNEL SOUND PRESSURE LEVELS DUE TO A DIRECTIONAL SOUND SOURCE IN THE TEST SECTION, 4000 HZ 1/3 OCTAVE BAND, 10 VOLTS RMS INPUT INTO JBL 2480 DRIVER AND RCA MI 9594A HORN SOUND POWER LEVEL 113 dB RE 10^{-12} WATT

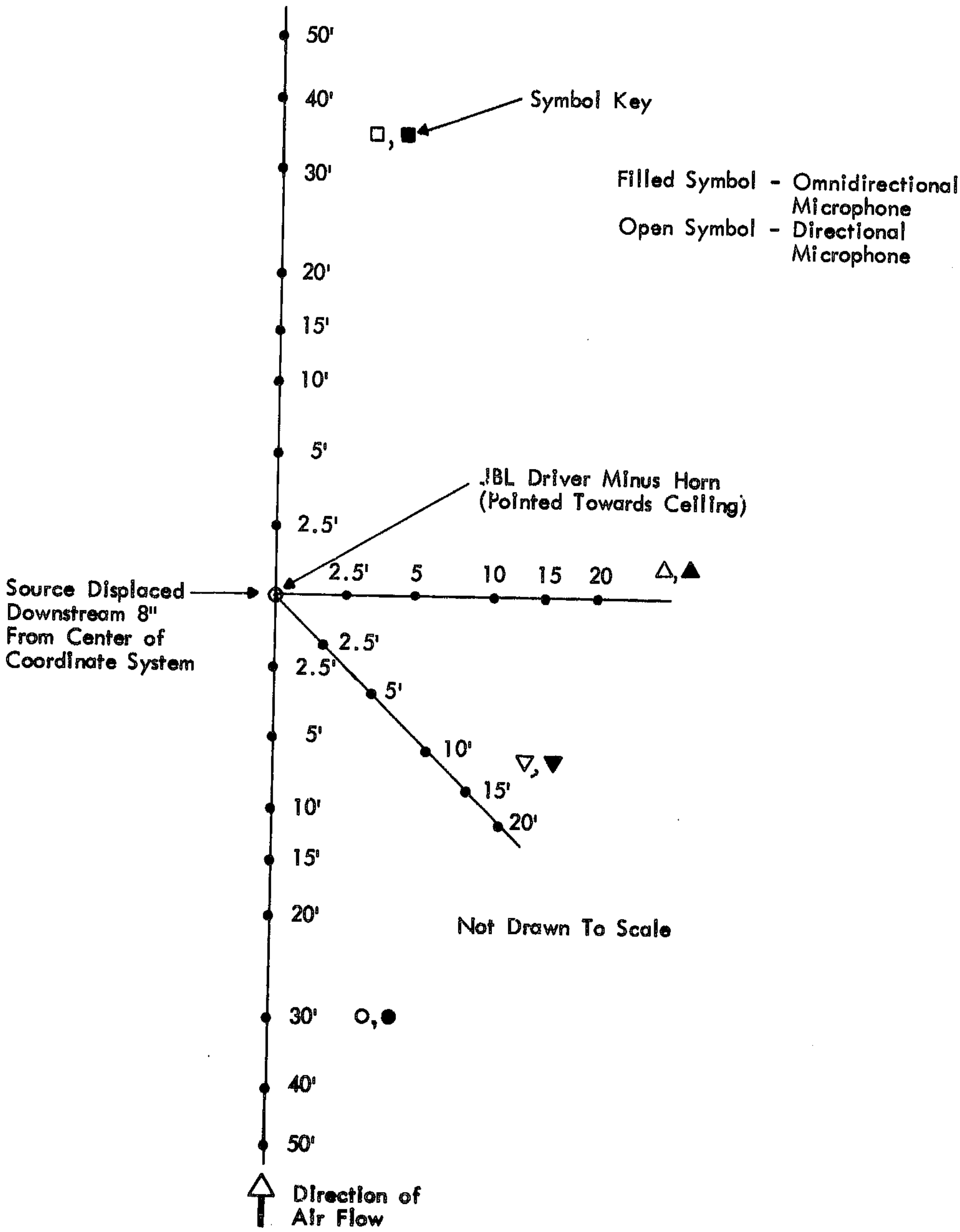

FIGURE 24. TEST SECTION MEASUREMENT LOCATIONS

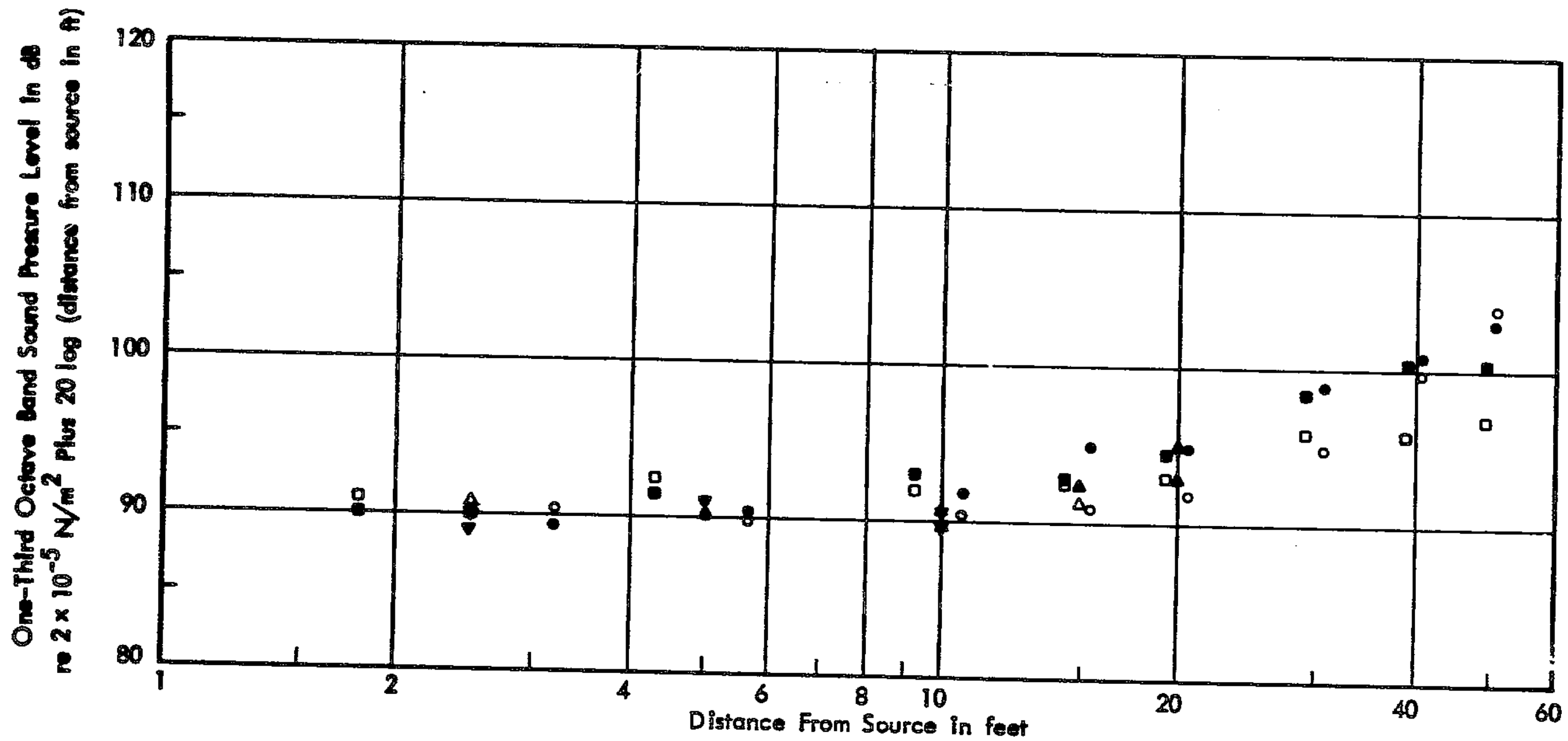

FIGURE 25. MEASURED 500 HZ ONE-THIRD OCTAVE BAND SOUND PRESSURE LEVELS CORRECTED FOR DISTANCE DUE TO A POINT SOURCE LOCATED AT THE CENTER OF THE 40 FT × 80 FT WIND TUNNEL TEST SECTION. The filled symbol data were measured with an omnidirectional microphone and the open symbol data were measured with a porous pipe directional microphone. All data were measured in the plane of the source 20 ft above the tunnel floor. See Fig. 24 for symbol key.

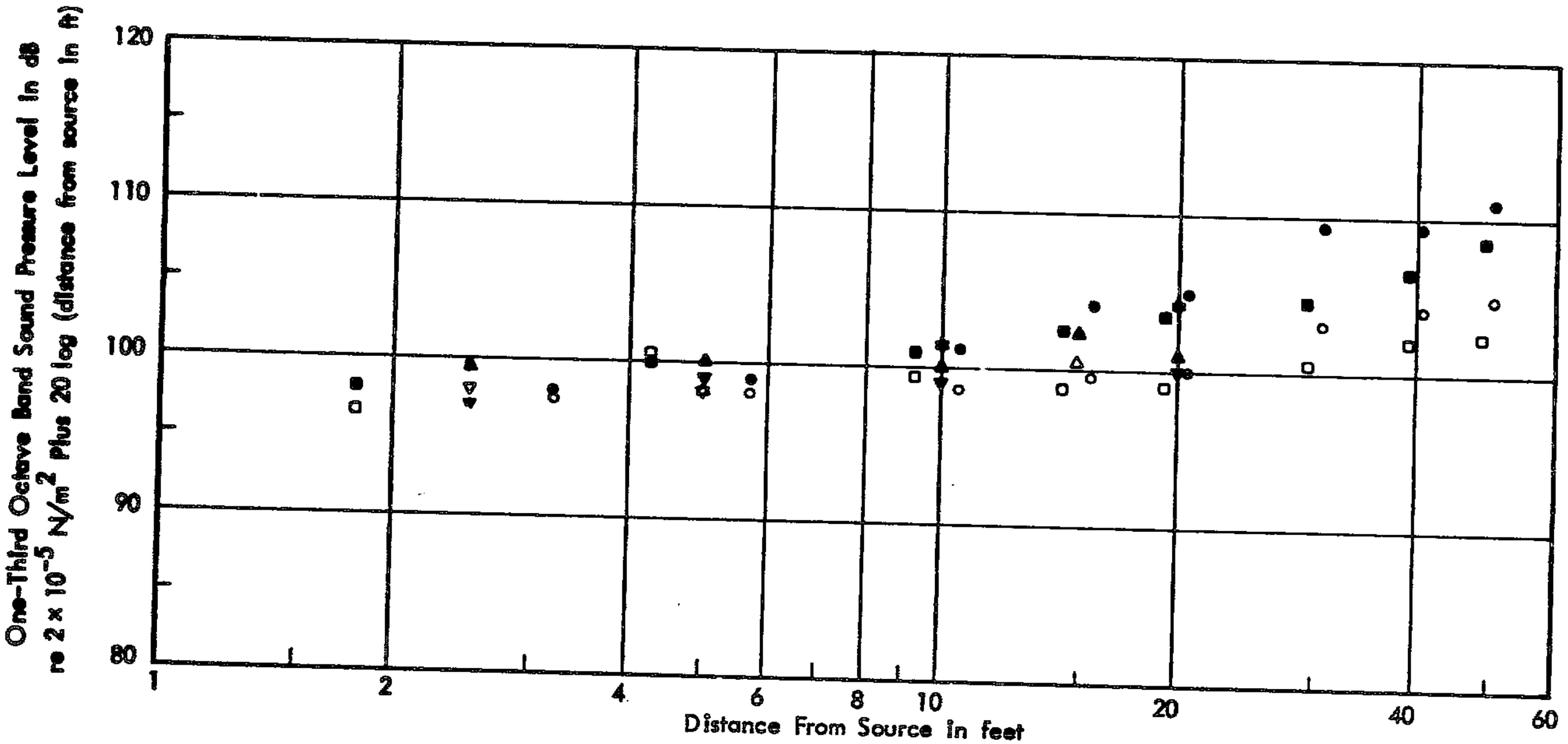

FIGURE 26. MEASURED 1000 HZ ONE-THIRD OCTAVE BAND SOUND PRESSURE LEVELS CORRECTED FOR DISTANCE DUE TO A POINT SOURCE LOCATED AT THE CENTER OF THE 40 FT × 80 FT WIND TUNNEL TEST SECTION. The filled symbol data were measured with an omnidirectional microphone and the open symbol data were measured with a porous pipe directional microphone. All data were measured in the plane of the source 20 ft above the tunnel floor. See Fig. 24 for symbol key.

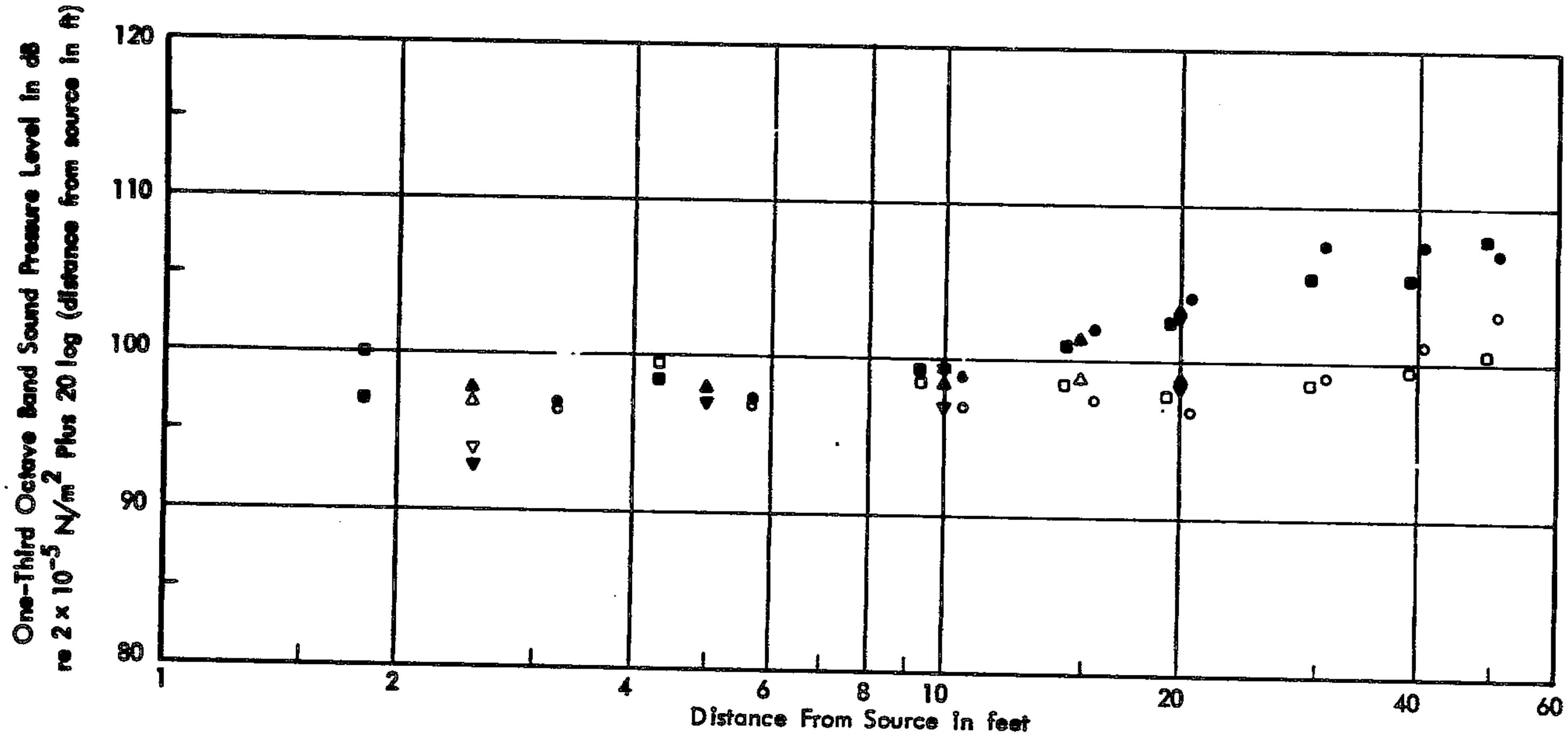

FIGURE 27. MEASURED 2000 HZ ONE-THIRD OCTAVE BAND SOUND PRESSURE LEVELS CORRECTED FOR DISTANCE DUE TO A POINT SOURCE LOCATED AT THE CENTER OF THE 40 FT × 80 FT WIND TUNNEL TEST SECTION.
The filled symbol data were measured with an omnidirectional microphone and the open symbol data were measured with a porous pipe directional microphone. All data were measured in the plane of the source 20 ft above the tunnel floor. See Fig. 24 for symbol key.

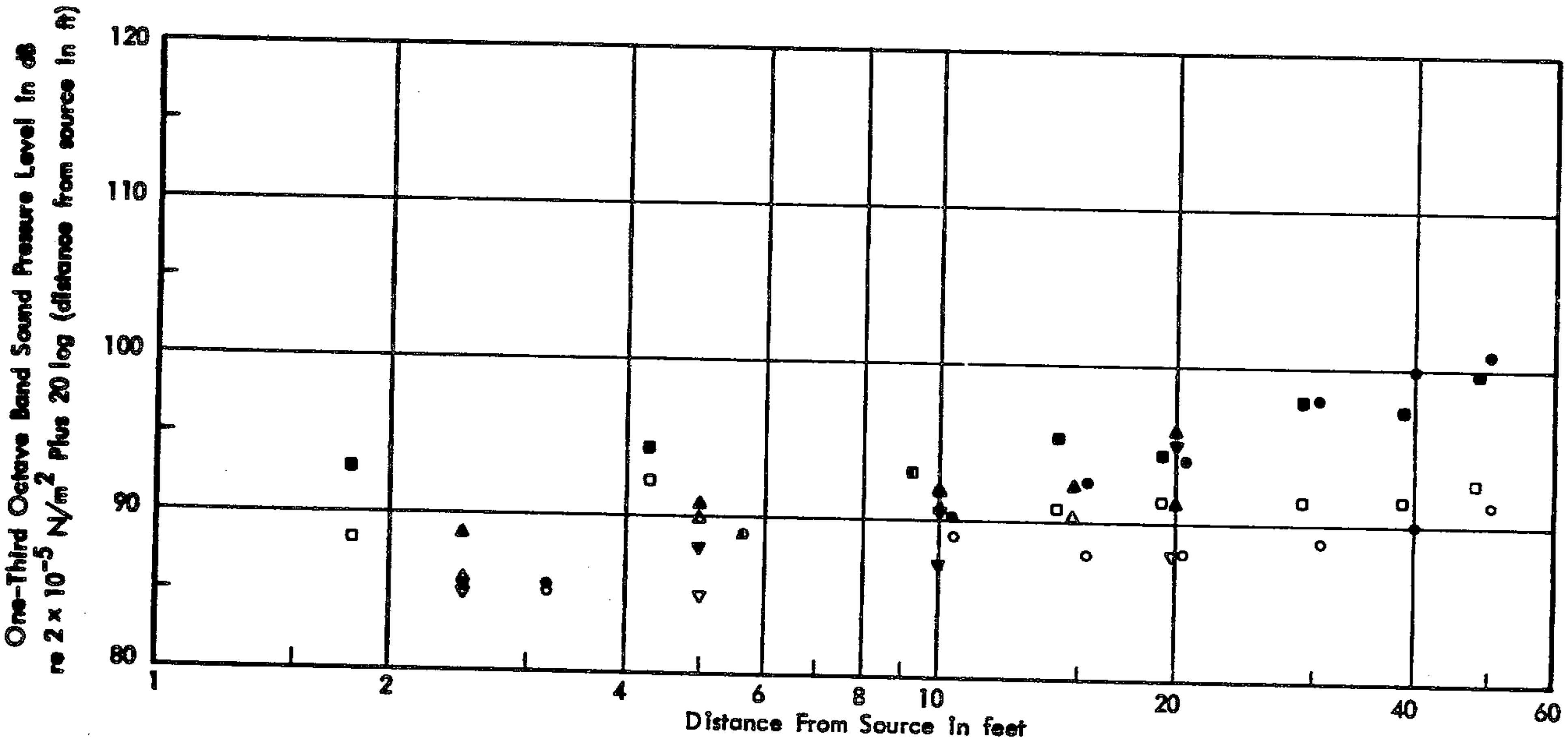

FIGURE 28. MEASURED 4000 HZ ONE-THIRD OCTAVE BAND SOUND PRESSURE LEVELS CORRECTED FOR DISTANCE DUE TO A POINT SOURCE LOCATED AT THE CENTER OF THE 40 FT × 80 FT WIND TUNNEL TEST SECTION. The filled symbol data were measured with an omnidirectional microphone and the open symbol data were measured with a porous pipe directional microphone. All data were measured in the plane of the source 20 ft above the tunnel floor. See Fig. 24 for symbol key.

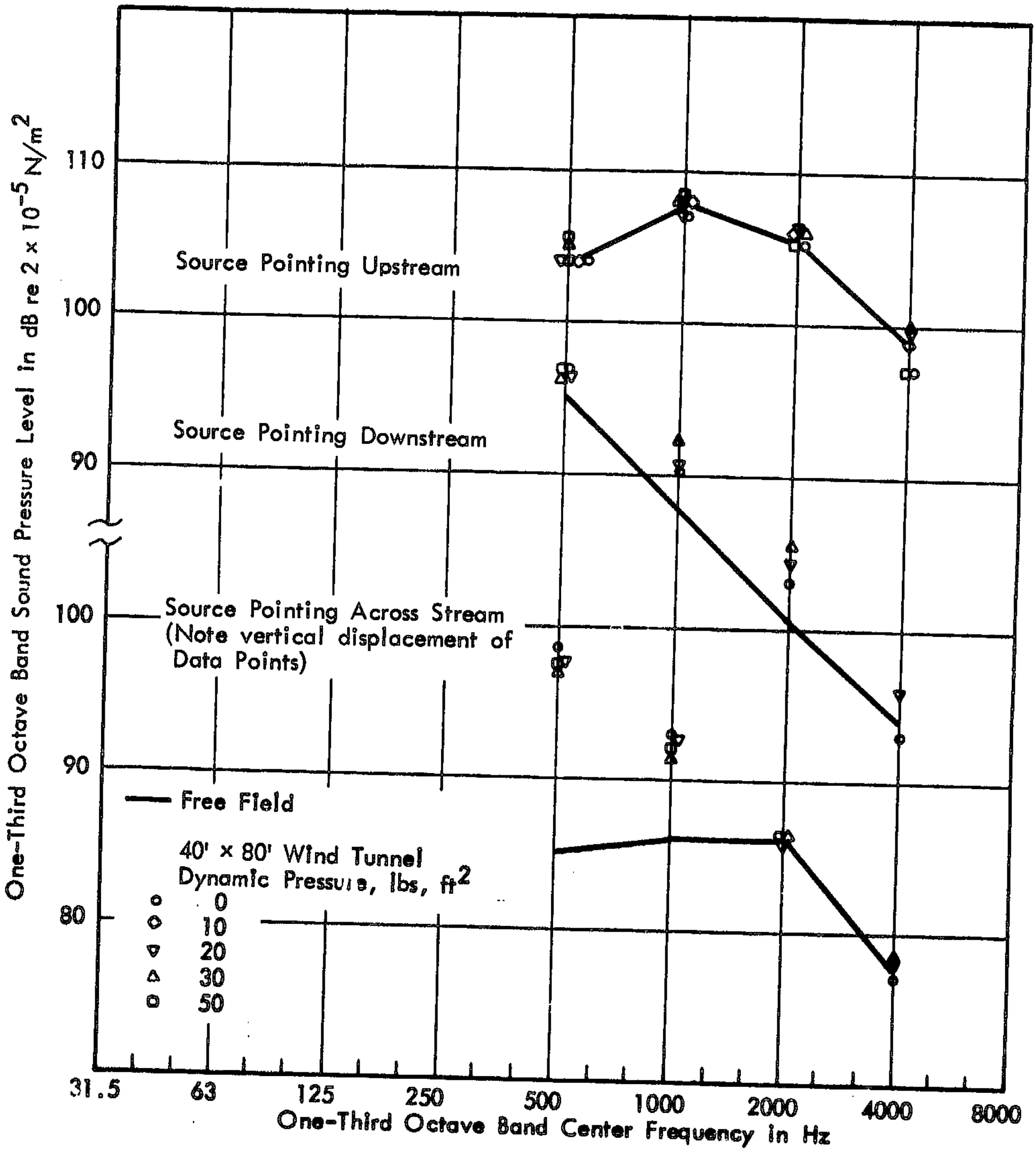

FIGURE 29. POROUS PIPE MICROPHONE MEASUREMENTS OF SOUND RADIATED BY A DIRECTIONAL SOURCE WITH THE TUNNEL OPERATING. The source was 20 ft. downstream of the microphone which was at position b.

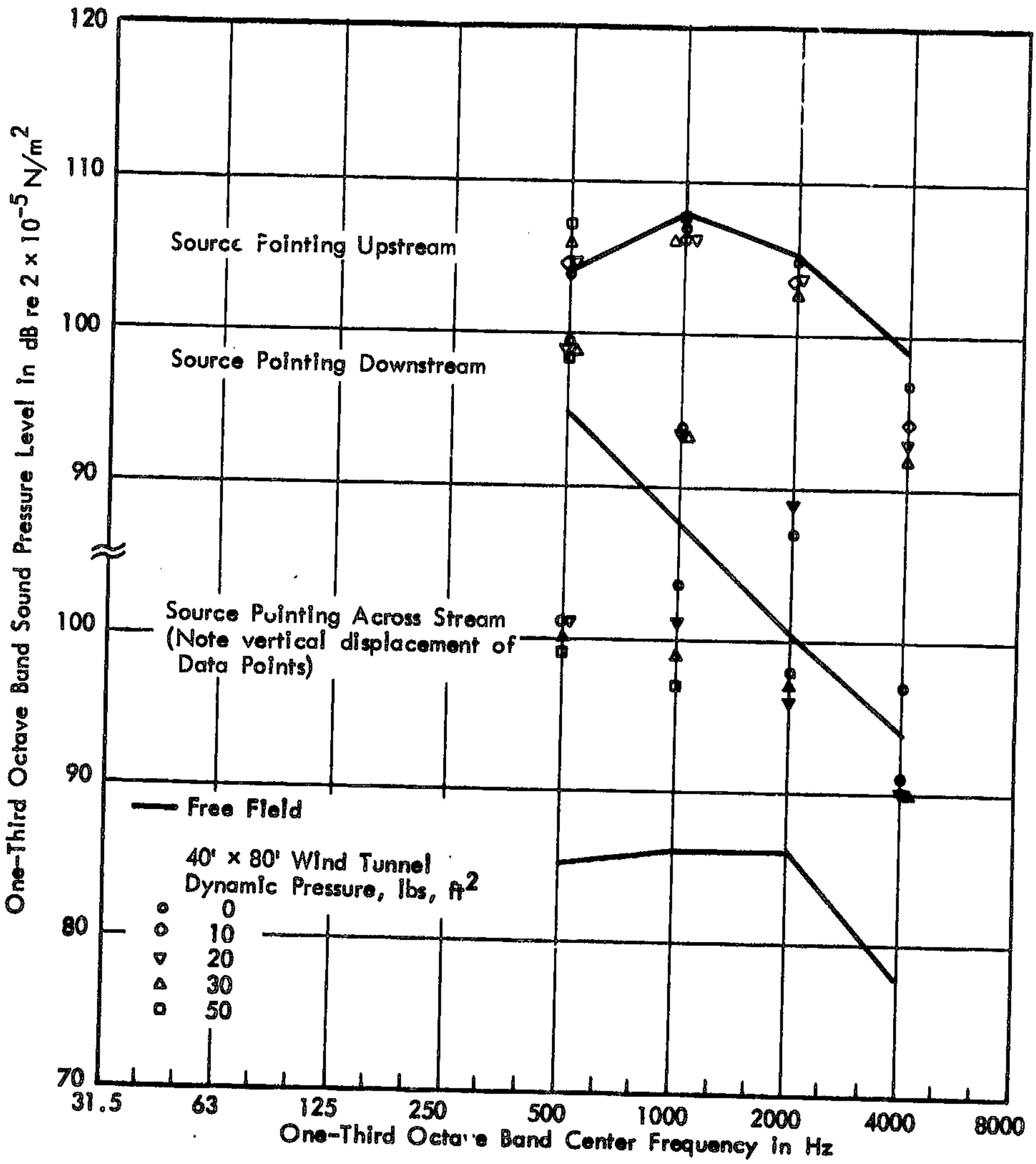

FIGURE 30. OMNIDIRECTIONAL MICROPHONE MEASUREMENTS OF SOUND RADIATED BY A DIRECTIONAL SOURCE WITH THE TUNNEL OPERATING. The source was 20 ft. downstream of the microphone which was at position b.

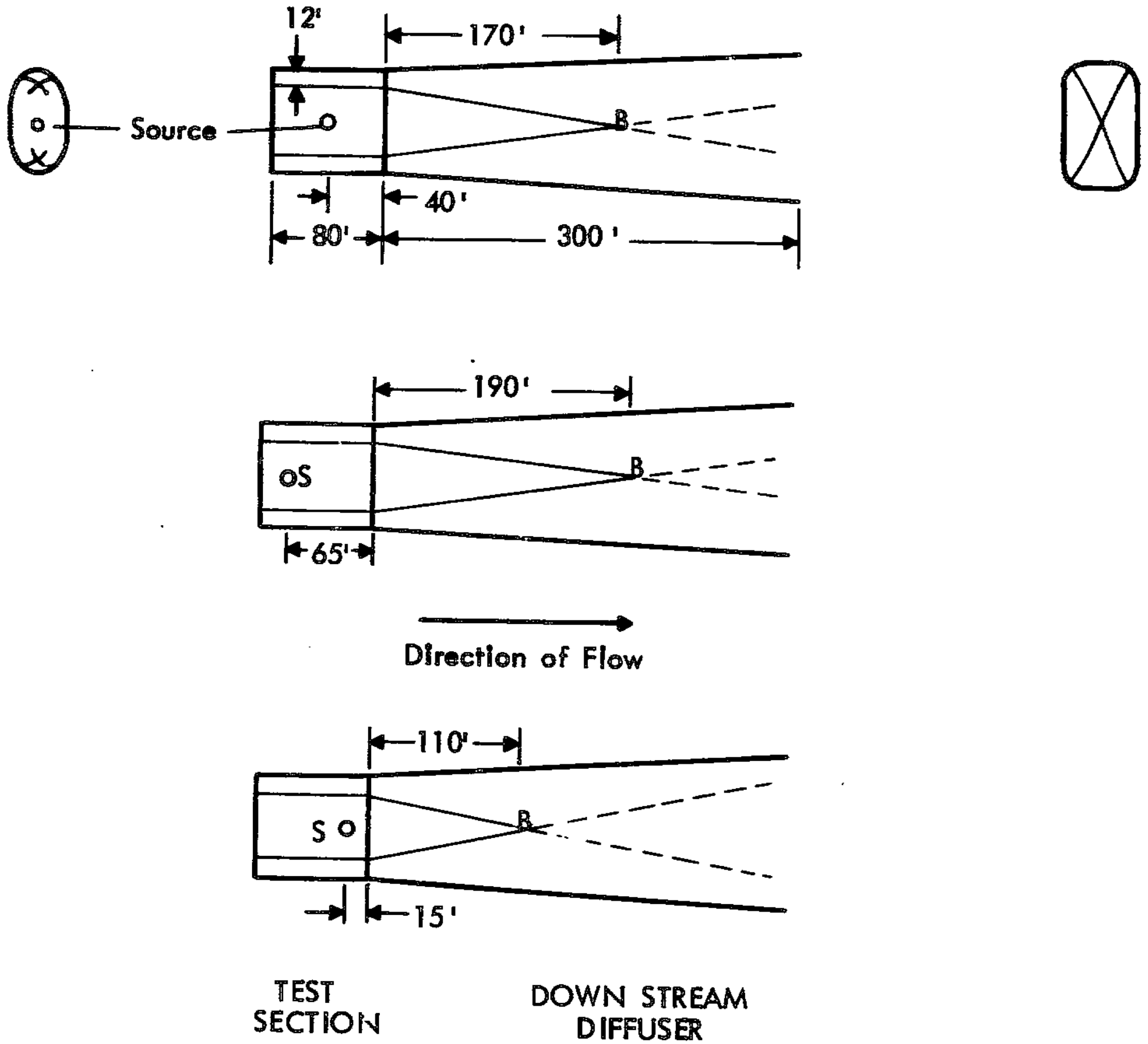

FIGURE 31. OPTICAL MODEL MAP OF SURFACES OF INTENSE FOCUSING FOR A SOURCE 20 FEET ABOVE THE FLOOR IN THE TEST SECTION ON THE CENTER LINE. B DENOTES A BRIGHT SPOT WHILE S DENOTES THE SOURCE LOCATION.

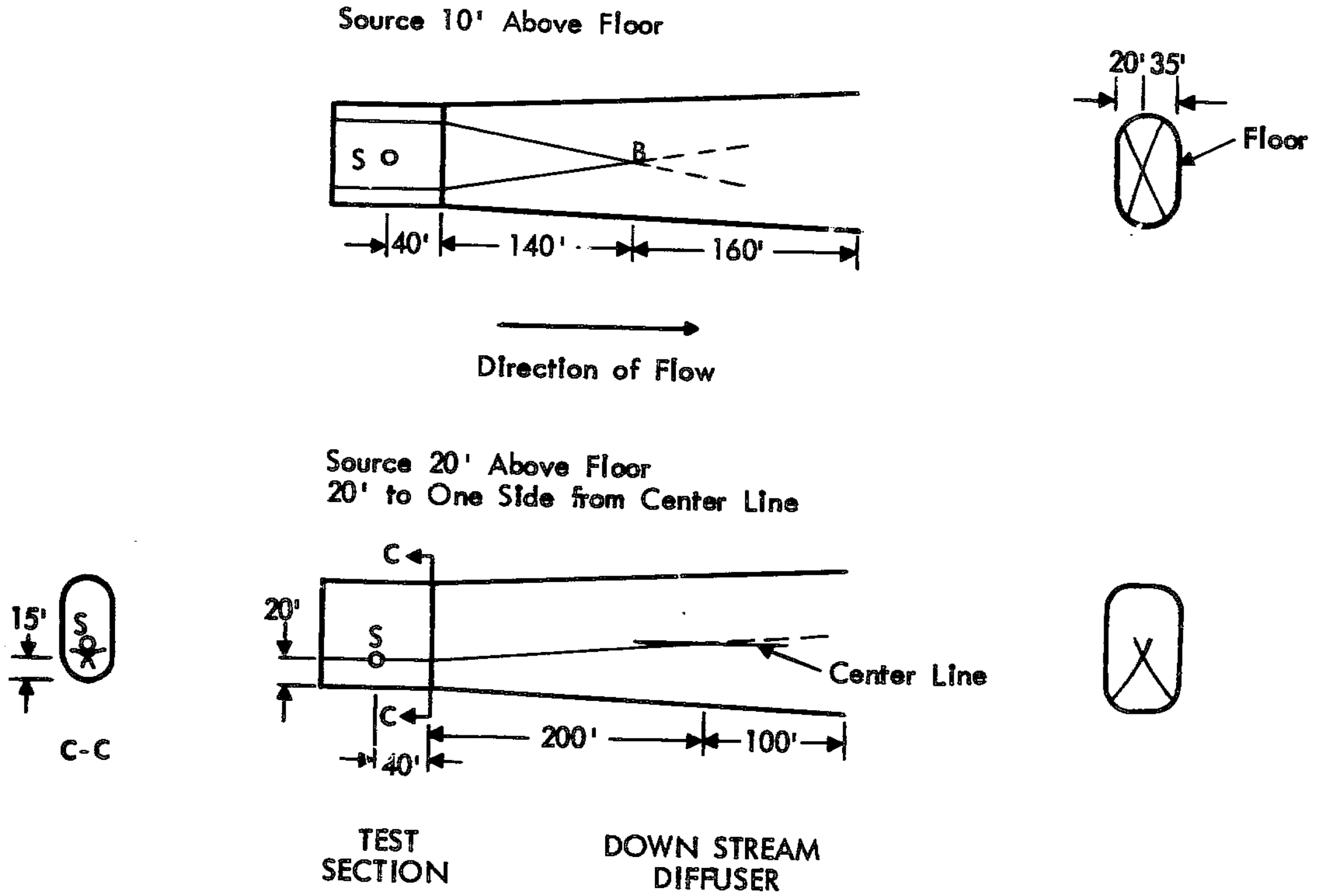

FIGURE 32. OPTICAL MODEL MAP OF SURFACES OF INTENSE FOCUSING FOR A SOURCE IN THE TEST SECTION BUT OFF THE CENTER LINE. B DENOTES A BRIGHT SPOT WHILE S DENOTES THE SOURCE LOCATION.

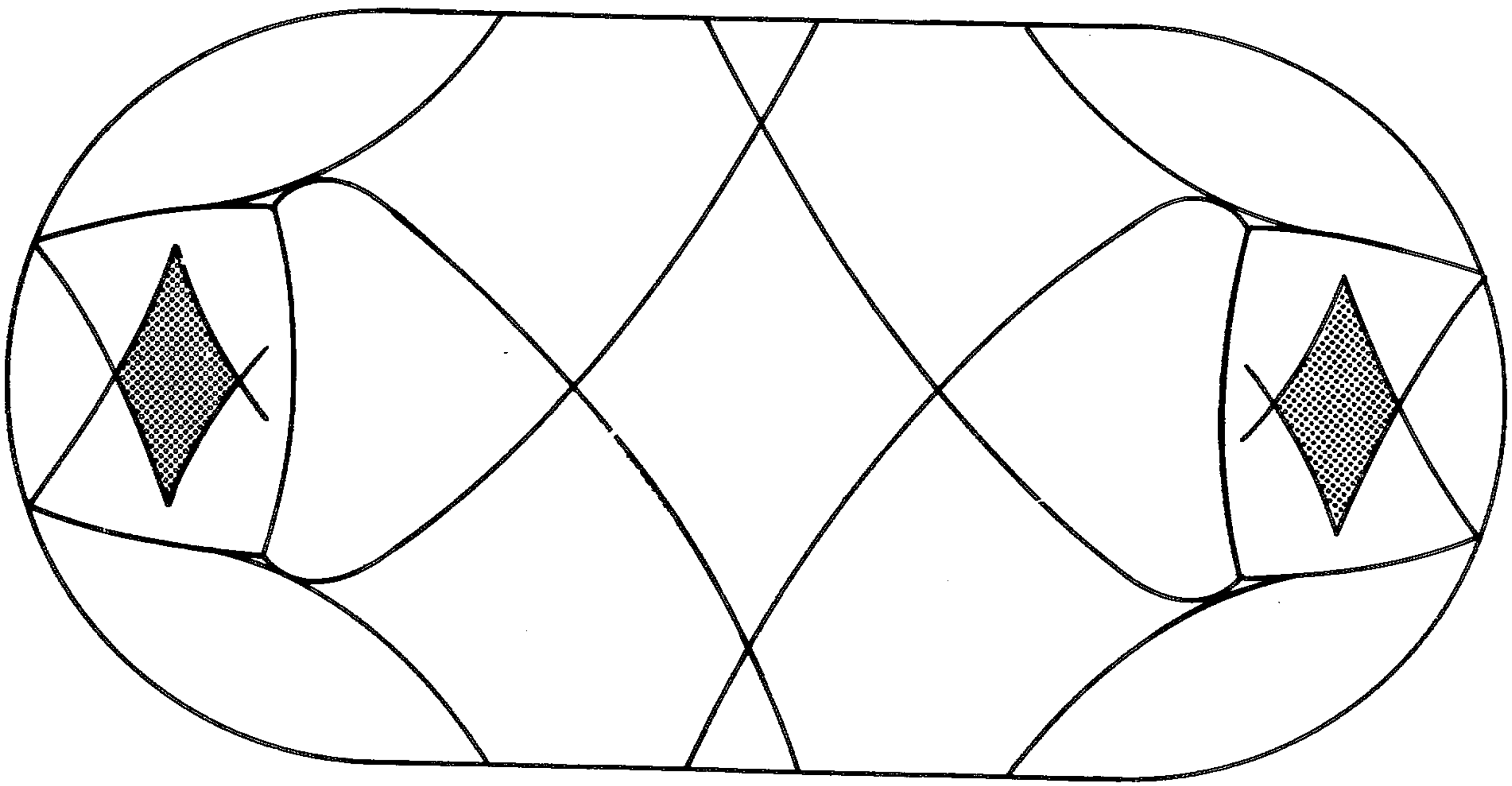

FIGURE 33. OPTICAL MODEL MAP OF REGIONS OF INTENSE FOCUSING FOR A SOURCE AT THE CENTER OF THE TEST SECTION SHOWING THE RESULTING PATTERN AT THE END OF THE TEST SECTION 40 FEET AWAY FROM THE SOURCE.

APPENDIX A

MODEL ACOUSTIC POWER MEASUREMENT FEASIBILITY CRITERION

Measurement techniques are described in the text for determining the acoustic power radiated by a model in the 40- by 80-foot wind tunnel. These techniques require, for success, that the model noise at a measurement location be distinguishable from the tunnel background noise during operation. The question will now be considered as to what the sound power of a model must be in order that it may be measured in the 40- by 80-foot wind tunnel.

During operation, background noise in the wind tunnel is primarily due to the fans. At low frequencies sound propagation losses are small and at high frequencies losses are approximately compensated by wind noise. Thus the data in Fig. 3 of the text used in conjunction with Eq. 1 of Part III of the text provides a means for conservatively estimating the background noise anywhere in the wind tunnel.

In order to be measurable in the absence of special signal processing techniques sound from a model must be at least as loud at a measurement location in the wind tunnel as the background noise. The required sound power to produce sound as loud at a measurement location as predicted using the estimation procedure described above may be determined from the relationships between sound pressure level and sound power level described in Part IV of the text. These relationships given in the last columns of Tables I, IV and VII have been used to construct Fig. A-1.

Figure A-1 shows that the model sound power required to make measurements in the area of the fans is very much greater than that required to make measurements at the edge of the test section. The figure gives model acoustic power levels required to be just detectable at low fan speed of 100 rpm. The data must be scaled according to the rule given by Eq. 1 of the text to give minimum acoustic power level requirements at higher fan speeds.

The power levels shown in Fig. A-1 are minimum levels. They would result in an increase of only 3 dB in sound pressure levels above the background levels at measurement locations. On the other hand, if the model sound power is at least 10 dB higher than the required minimum, an increase in sound pressure level at measurement locations of 10.5 dB above the background level will be observed. Such a signal would be readily detectable. The observed levels could be reduced by 0.5 dB to account for the presence of background noise. Reference to Appendix G is recommended in connection with this discussion.

The above considerations apply to measurements made in one-third octave bands. If octave band analysis is used the levels in Fig. A-1 should be raised 5 dB. On the other hand, if one-tenth octave band analysis is used they should be lowered 5 dB. If tones are considered even narrower band analysis may be used with proportionate advantage though in this case some special averaging may be required, i.e., measurements may be required at several positions in the tunnel cross section at the measurement location.

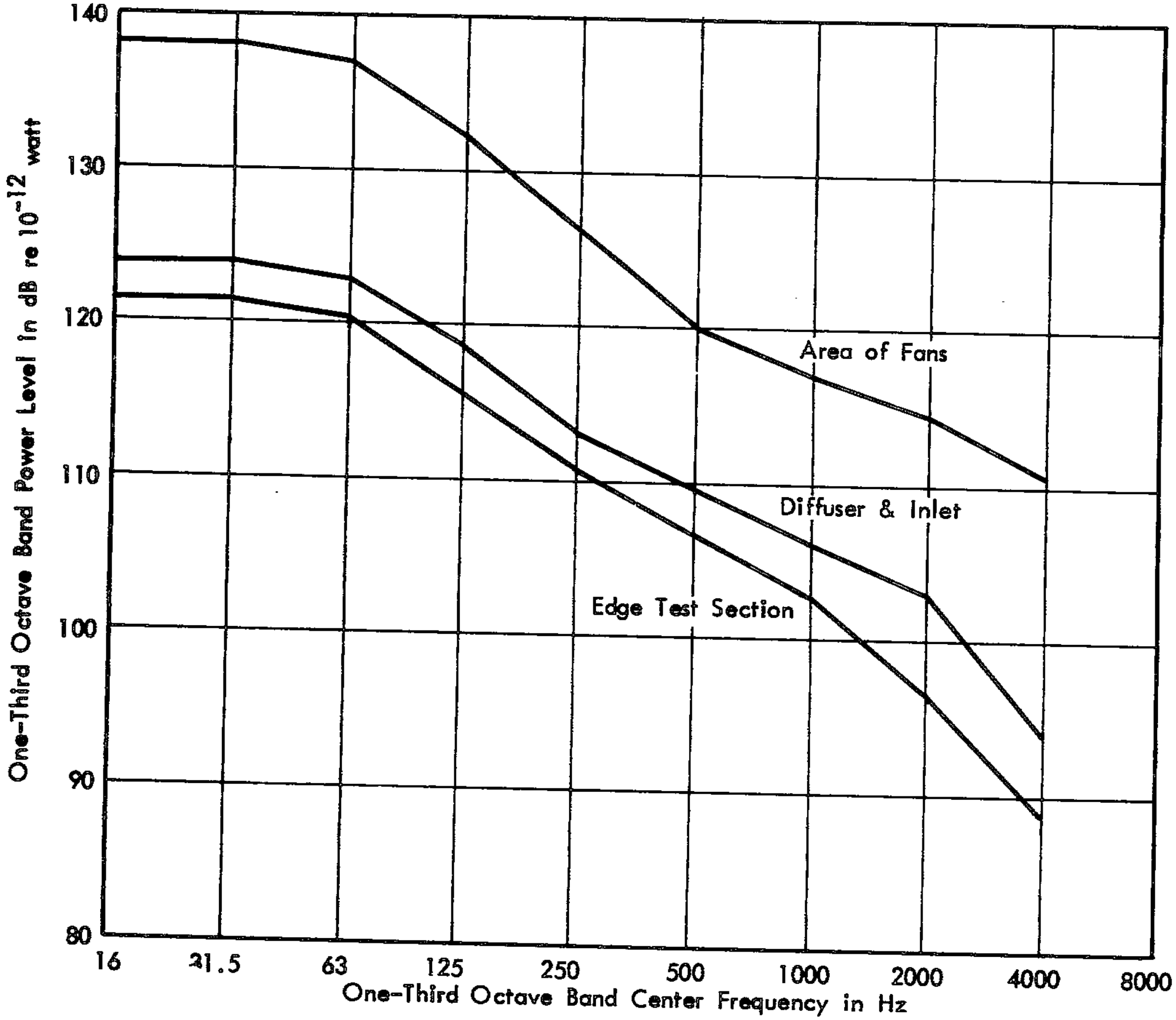

FIGURE A-1. MODEL POWER LEVEL REQUIRED TO PRODUCE SOUND PRESSURE LEVEL EQUAL TO WIND TUNNEL BACKGROUND NOISE LEVEL AT POSITIONS SHOWN AT 100 RPM FAN SPEED

APPENDIX B

POROUS PIPE MICROPHONE

The porous pipe microphone consists of a porous pipe* with a tapered cone placed internally along the tube center line and a microphone placed at the apex of the cone as shown in Fig. B-1. The cone taper and the tube wall flow resistance are chosen so that the tube is anechoic to sound waves reflected from the surface of the microphone; resonances within the tube are avoided by proper design.

If the flow resistance is properly chosen, the pressure sensitivity of the system is equal to the pressure sensitivity of the microphone alone. Due to a slightly greater flow resistance than that which is required, the pressure sensitivity of the model described here is 2.2 dB below the pressure sensitivity of the condenser microphone.

The forward on axis pressure sensitivity S_p (ratio of the pressure p_m at the surface of the condenser microphone to the pressure p_o of the plane wave incident along the axis of the pipe) is shown in Fig. B-2. This is the response relative to that of the microphone alone when the porous pipe is pointed toward a distant source.

To investigate the porous pipe directivity, the porous pipe was mounted on a rotating table in an anechoic chamber and its response to a source placed approximately 6 ft away was measured. From the polar plots which were obtained, Fig. B-3 was constructed. The figure describes the forward major lobe in the response pattern.

The angle θ relative to forward on axis at which the sensitivity is down from the sensitivity on axis by the amount indicated parametrically is shown in the figure. For example, at 1000 Hz the figure shows that the sensitivity has dropped by 1 dB at 28 degrees, by 3 dB at 45 degrees, and by 10 dB at 68 degrees. The caption makes the further point that no minor lobe had a sensitivity greater than -13 dB relative to the forward on axis sensitivity.

---

* Report 1962, Acoustic Homing Feasibility Study Interim Report by Systems Application Division Advanced Systems Concepts Laboratory, September 1969, U.S. Army MERDC, Fort Belvoir, Virginia.

For the microphone pointing away from the source the sensitivity is shown in Fig. B-4. A first null at 500 Hz and an attenuation at the maximum of the first secondary lobe of 13 dB are observed.

The theoretical description of the directivity of the porous pipe, given in the reference, predicts appreciable sensitivity even at low Mach numbers to relative flow past the pipe at high frequencies. However the predicted resulting decrease in microphone sensitivity seems not to have been observed although at a dynamic pressure of 50 lbs/ft^2 corresponding to Mach 0.18 and 4000 Hz the decrease should have been 10 dB. No explanation is available at the present time. The roll-off in sensitivity shown in Fig. B-2 also has not been explained.

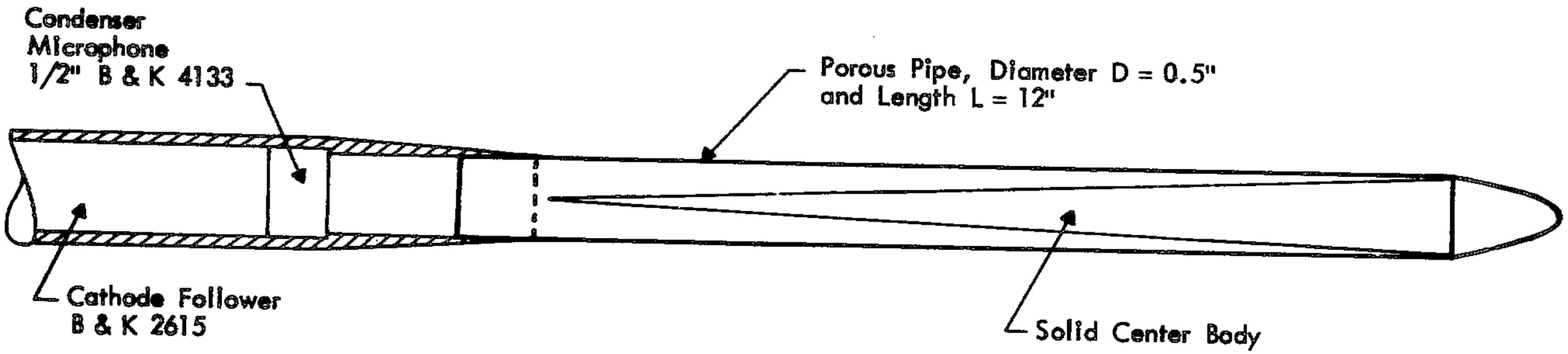

FIGURE B-1. SECTIONAL VIEW OF THE POROUS PIPE MICROPHONE

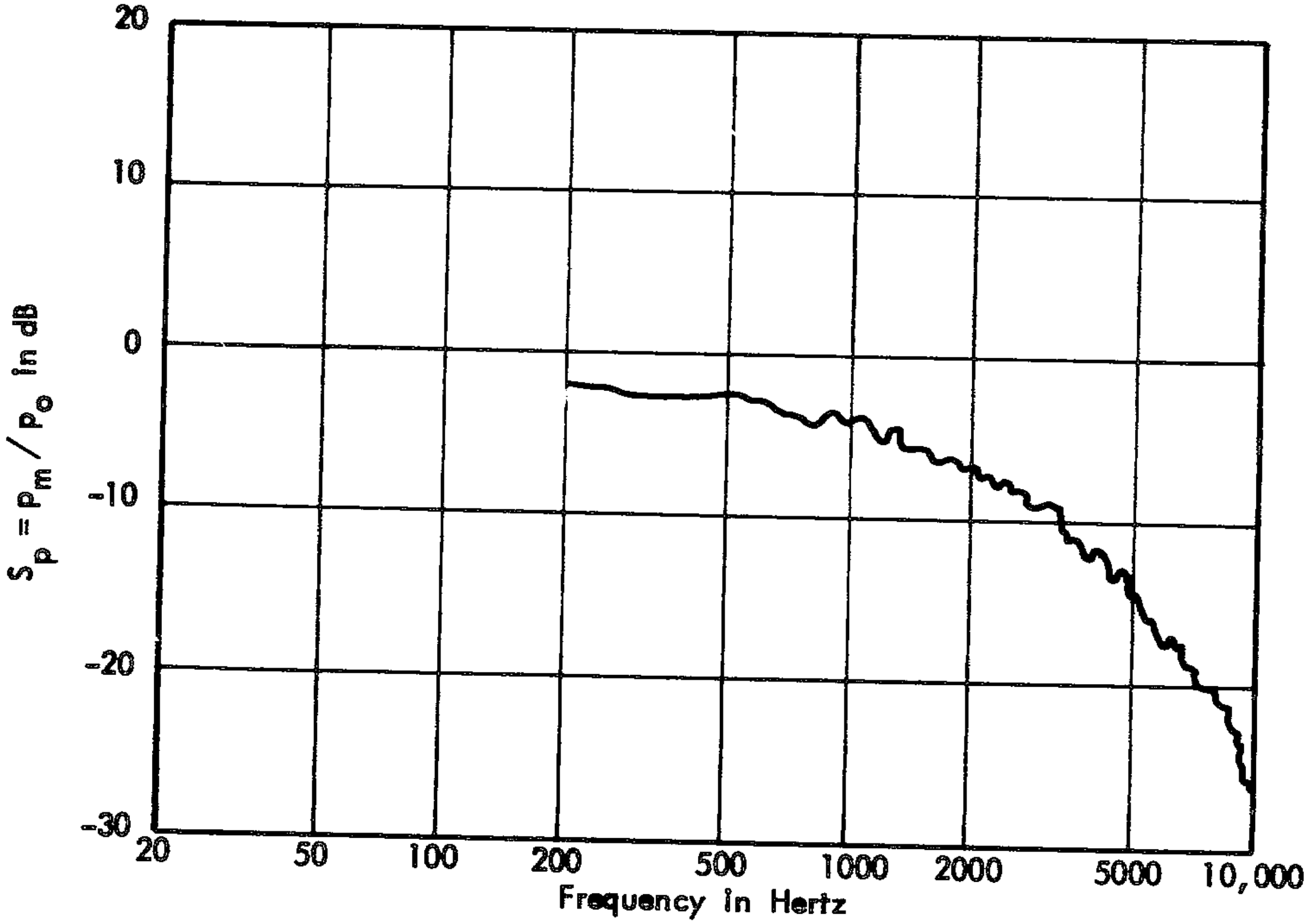

FIGURE B-2. FORWARD PRESSURE SENSITIVITY OF POROUS PIPE MICROPHONE; D = 0.5 IN., L = 12 IN., B & K MICROPHONE TYPE 4133

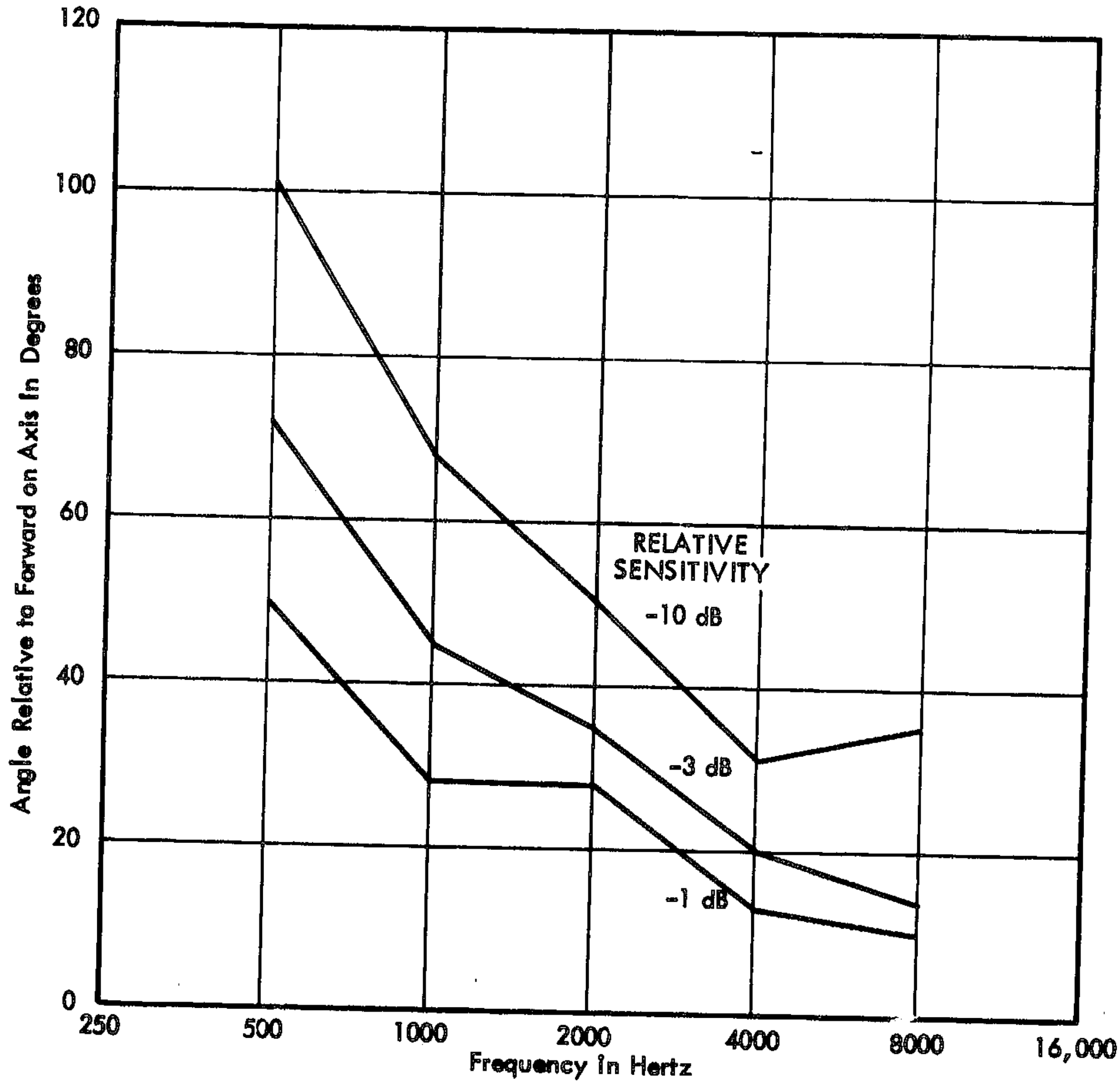

FIGURE B-3. POROUS PIPE SENSITIVITY. THE DATA DESCRIBE THE MAJOR LOBE. SENSITIVITY RELATIVE TO FORWARD ON AXIS SENSITIVITY IS SHOWN AS THE PARAMETER. NO MINOR LOBE HAS A RELATIVE SENSITIVITY GREATER THAN -13 dB.

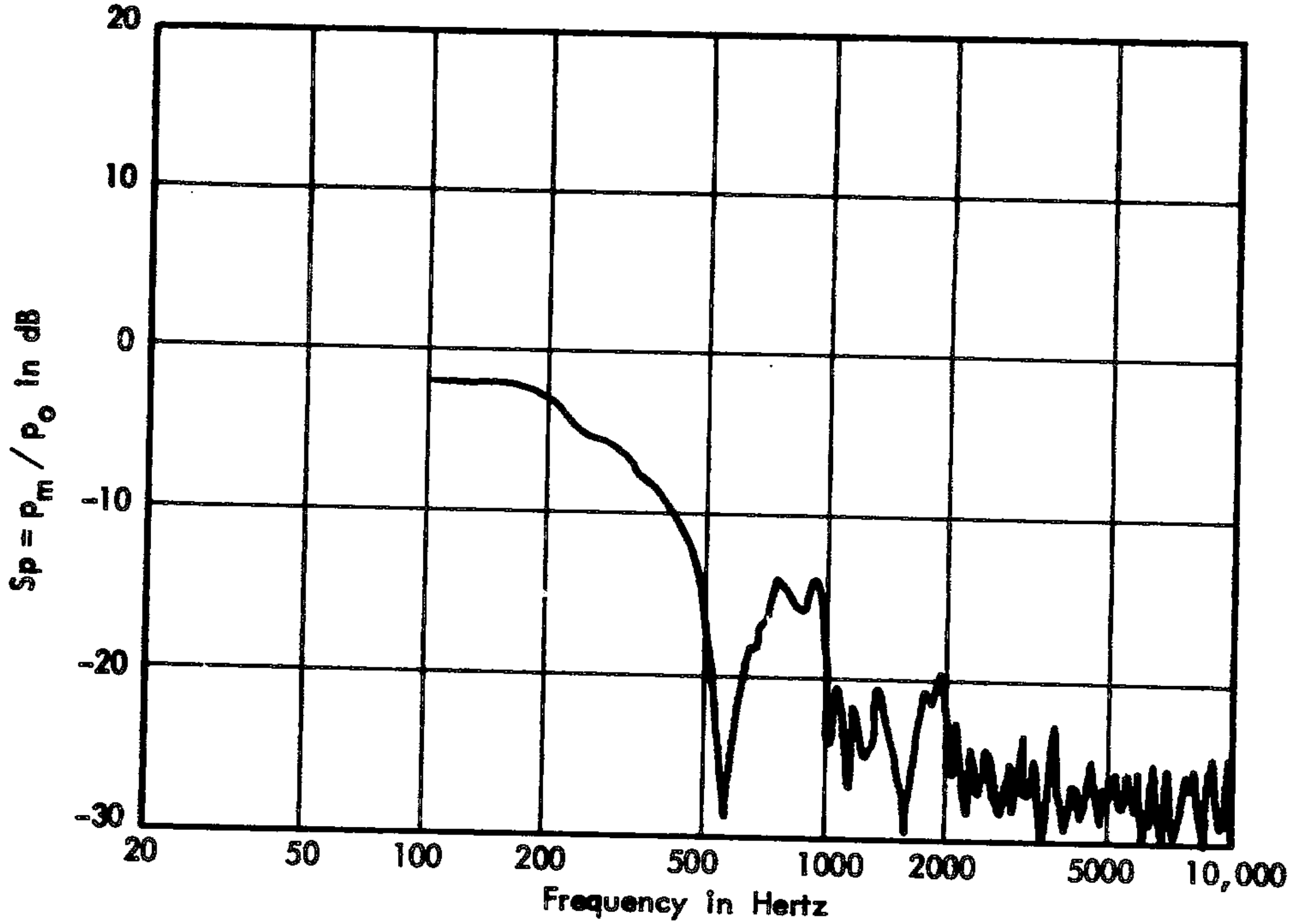

FIGURE B-4. BACKWARD PRESSURE SENSITIVITY OF POROUS PIPE MICROPHONE; D = 0.5 IN., L = 12 IN. B & K MICROPHONE TYPE 4133

APPENDIX C

DODECAHEDRON SOUND SOURCE

The National Aeronautics and Space Administration Ames Research Center has constructed a dodecahedron sound source consisting of a regular 12-sided polyhedron with an 8-in. Altec 409B speaker mounted in each face. The dodecahedron has a mean diameter of approximately 24 in. and is constructed of heavy plywood.

All speakers are connected by means of a 150 ft multi-conductor cable to an external junction box where all electrical connections to the speakers are made. When the dodecahedron was to be used as a point source, all of the speakers were driven in phase with the same amplifier and noise source. In this case the speakers were connected in four groups of three in series as shown in Fig. C-1.

For calibration purposes the dodecahedron was suspended in an anechoic chamber of dimensions 7 ft by 8 ft by 10 ft. The anechoic chamber allowed free field measurements down to about 160 Hz. Below this frequency the reflections from the wall gradually limited the usefulness of the anechoic chamber for the purpose of calibrating the source. With the dodecahedron driven as a point source the sound pressure levels in various directions at 6 ft were investigated with the results shown in Fig. C-2.

The data in the figure show that the dodecahedron behaves essentially as a point source in the frequency range up to and including the 1000 Hz 1/3 octave band and also in the 8000 Hz 1/3 octave band; but in the frequency range in between, the scatter of the data indicates that the dodecahedron does not behave as a point source. The wide variation in this range may be attributed in part to the response of the individual speakers and in part to narrow beaming of the speakers which does not allow good coalescence at angles intermediate between speaker axes.

A second way to investigate the dodecahedron as a point source is to determine whether the field increases 6 dB per doubling of distance from the source center. This was done for two orientations of the source with the results shown in

Figs. C-3 and C-4. The spread in the data in the 100 and 125 Hz 1/3-octave bands is due to failure of the anechoic chamber at these low frequencies. However for distances up to 72 in. the data for these frequencies are thought to be valid, since even in a reverberant field the source field will dominate over some range sufficiently close to the source. The results shown in Figs. C-3 and C-4 confirm the point source behavior of the dodecahedron in the frequency range below the 1000 Hz third octave band and seem to indicate that even in this band the behavior of the source is quite reasonable.

Free field radiation properties of a single speaker mounted in the dodecahedron are shown in Fig. C-5. In the frequency range below the 160 Hz 1/3 octave band the validity of the data is limited by the failure of the anechoic chamber. However theory indicates and the data in the 160 Hz band confirm that the speaker mounted in the dodecahedron acts like a point source in the low frequency range up to and including the 160 Hz band. Above the 160 Hz 1/3-octave band the dodecahedron single speaker source becomes progressively more directional.

Although only one speaker, No. 3, was investigated, it is quite reasonable to assume that all other speakers will behave quite similarly. With this assumption the data contained in Fig. C-5 were used to determine the power radiated forward and backward by a single speaker mounted in the side of the dodecahedron. The estimate was carried out by integrating pressure levels interpolated from the data in the figure.

Acoustic power output of the source may be estimated from the free field measurements conducted in the anechoic chamber. Sound power level PWL in dB re 10^{-12} watt is related to the sound pressure level SPL in dB re 2×10^{-5} N/m^2 measured over some surface of area A in square feet by the equation

$$PWL = SPL + 10 \log_{10} A - 10.5 \qquad (C-1)$$

For a point source enclosed by a sphere of radius 6 ft, the area A equals 452 ft^2. Thus the data in Figs. C-3 and C-4 may be converted to sound power level data by the following

$$PWL = SPL + 16 \qquad (C-2)$$

The computation has been carried out with the results shown in the last column of Table C-1.

The sound power of a source may also be determined by comparison of resulting sound pressure levels measured in a reverberant room with those of a known reference source. The dodecahedron source was calibrated in a reverberant room using an ILG* source as a reference source by this method with the results shown in Table C-1. As indicated in the referenced ASTM the power levels for the ILG are uncertain in the frequency range below 200 Hz and depend upon the room acoustics. However in this frequency range the anechoic chamber measurements are satisfactory. The agreement between the two methods is considered excellent.

* ASTM document designation E336-67T.

TABLE C-1

OMNIDIRECTIONAL SOUND SOURCE POWER LEVELS IN ONE-THIRD OCTAVE BANDS FOR ONE VOLT RMS INPUT

NASA Ames Research Center
Dodecahedron Sound Source

One-third octave band center frequency in Hz	Sound power level in dB re 10^{-12} watt	
	Reverberant room measurements	Anechoic room measurements
100	(86)*	87
125	(92)	94
160	(98)	101
200	(102)	103
250	100	100
315	97	96
400	95	93
500	93	91
630	90	89
800	88	88
1000	88	88
1250	84	
1600	87	
2000	87	
2500	87	
3150	85	
4000	84	
5000	85	
6300	79	
8000	76	
10000	(79)	

* Numbers in parentheses () are based on uncertain data.

SOURCE SYSTEM

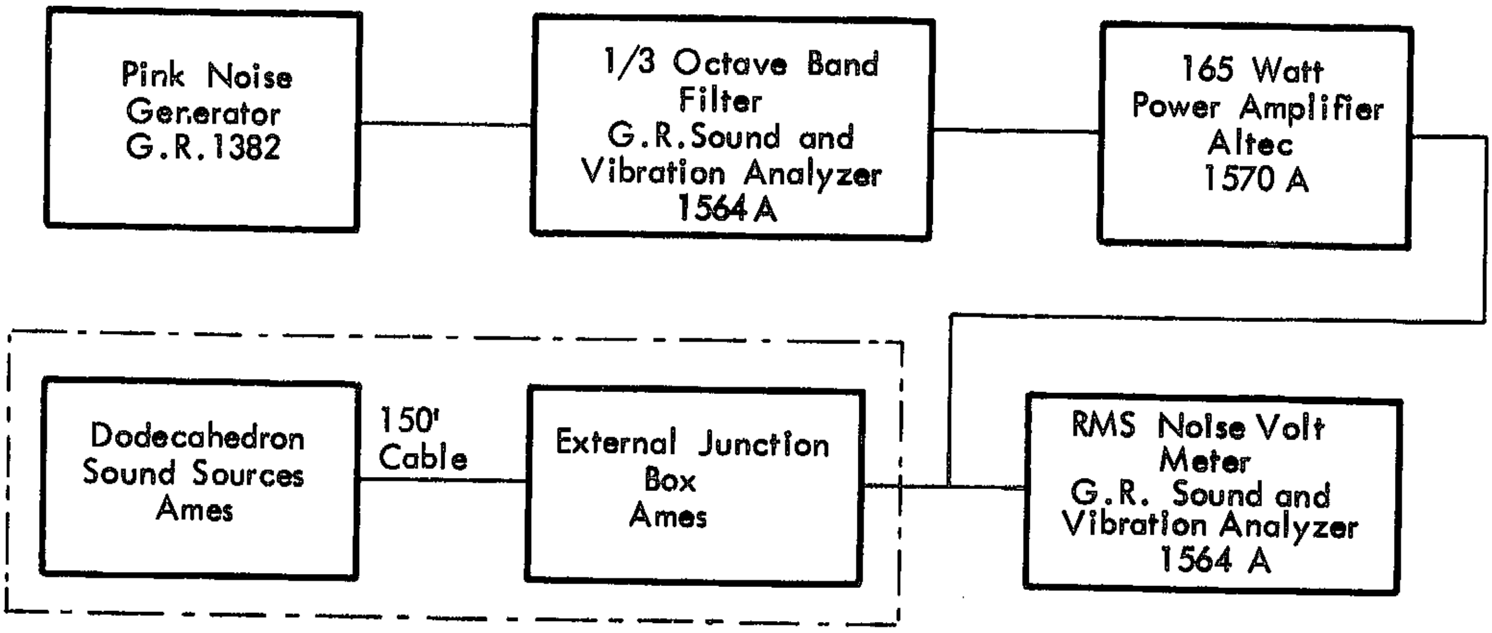

DODECAHEDRON WIRING DIAGRAM

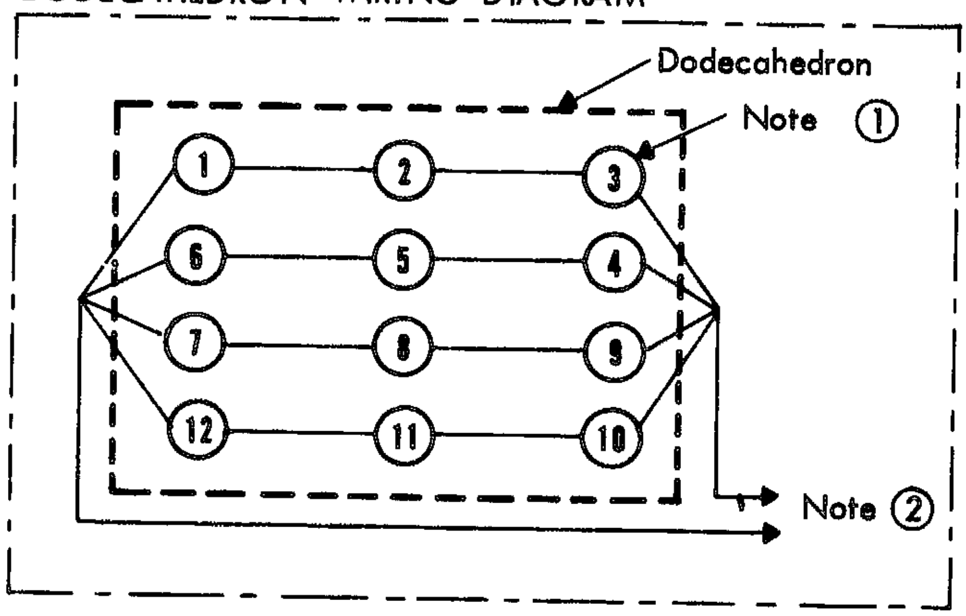

Notes:

① Altec 409B, 8 ohm input, 16 watt speakers

② All speaker input leads connect directly by means of a 150 ft, multiconductor cable to an external junction box. The cable resistance was approximately 0.5 ohm. All speaker connections (ie. those shown) were made and all input voltages were measured at the input to the external junction box.

FIGURE C-1. DODECAHEDRON SYSTEM USED FOR TUNNEL SOUND PROPAGATION MEASUREMENTS

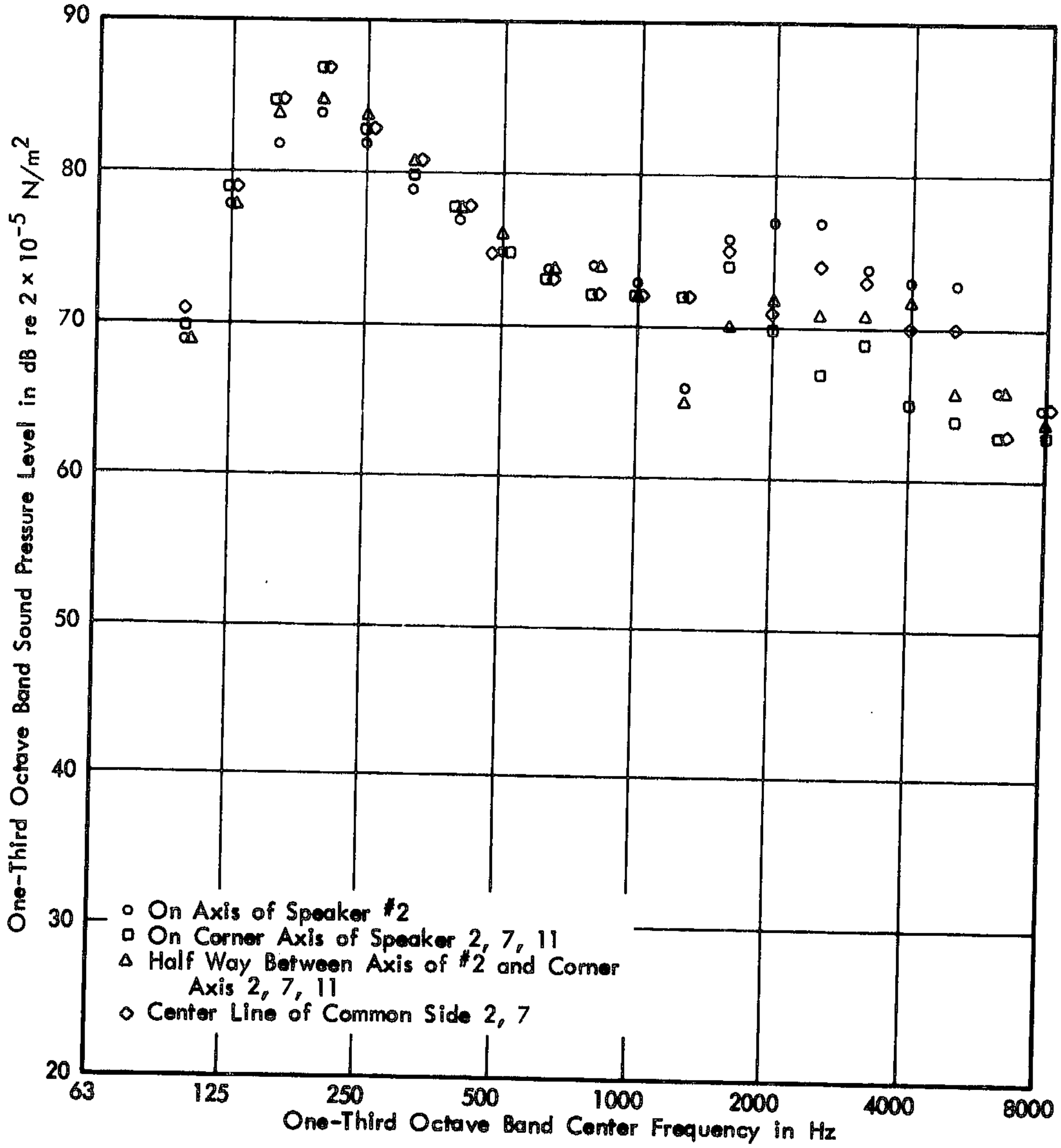

FIGURE C-2. SOUND PRESSURE LEVEL IN VARIOUS DIRECTIONS AT 6' FROM CENTER OF DODECAHEDRON WITH ALL SPEAKERS IN PLACE FOR 1 VOLT INPUT IN EACH ONE-THIRD OCTAVE BAND INTO ENTIRE SYSTEM

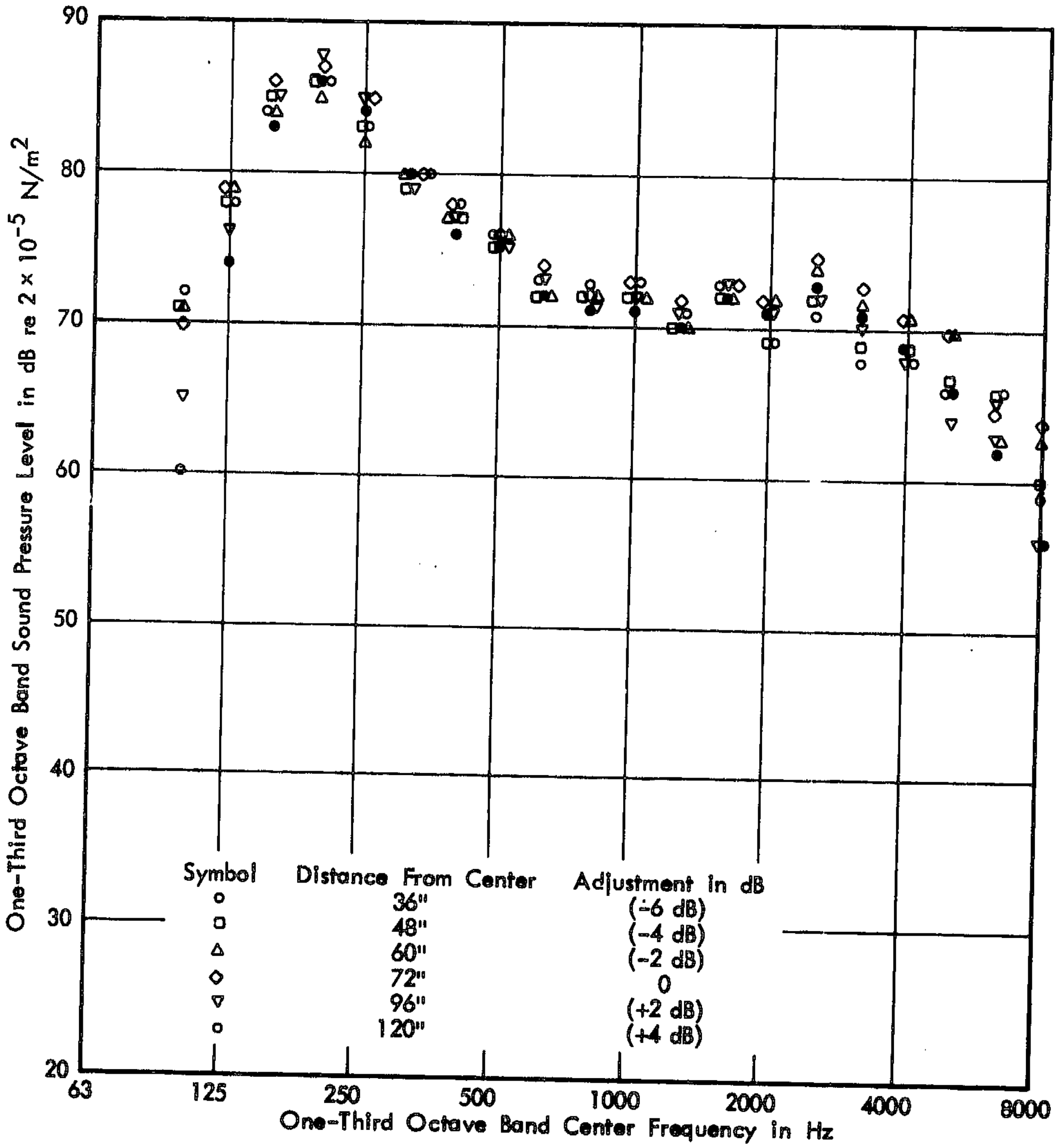

FIGURE C-3. SOUND PRESSURE LEVEL AT VARIOUS DISTANCES FROM CENTER OF DODECAHEDRON ALONG AXIS OF CORNER 3, 4, 8. All data normalized to 6' distance for 1 volt RMS in each one-third octave band into system

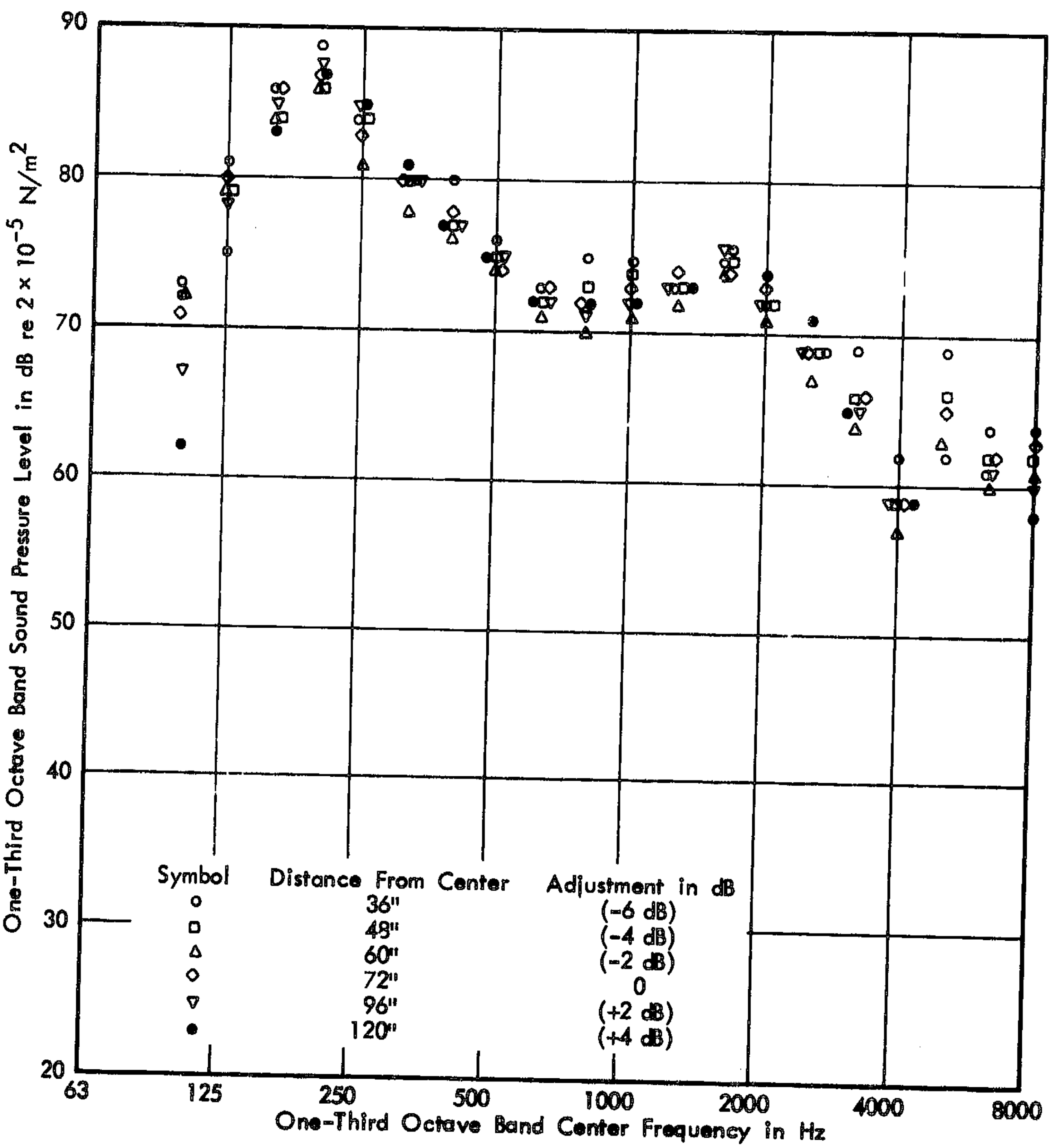

FIGURE C-4. SOUND PRESSURE LEVEL AT VARIOUS DISTANCES FROM CENTER OF DODECAHEDRON ALONG AXIS OF CORNER 2, 7, 11. All data normalized to 6' distance for 1 volt RMS in each one-third octave band into system

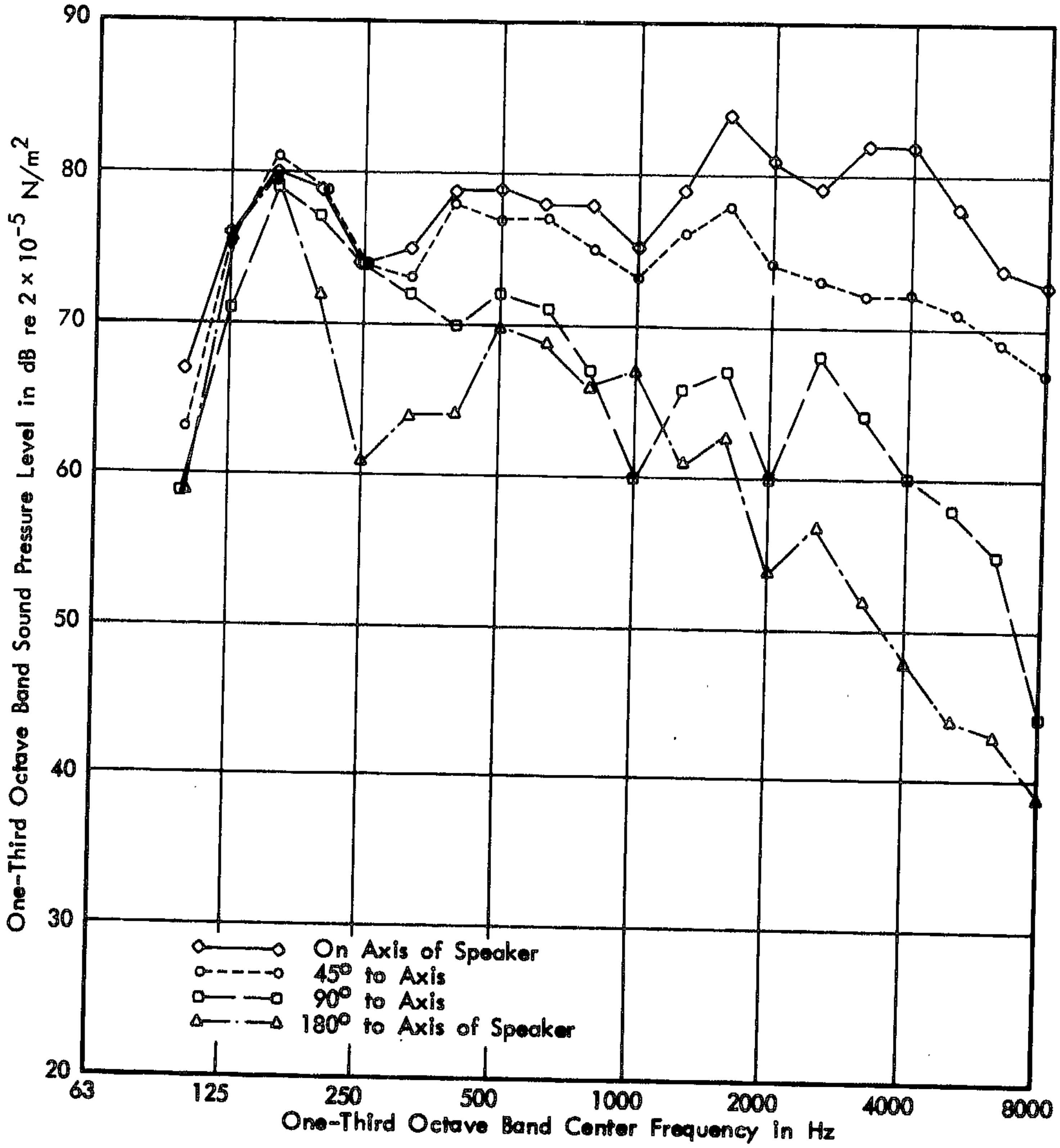

FIGURE C-5. POLAR RESPONSE OF SPEAKER 3 MOUNTED IN DODECAHEDRON. Sound pressure level at six feet for 1 volt RMS in each one-third octave band

APPENDIX D

HORN SOUND SOURCE

The directional sound source consists of a JBL 2480 high power horn driver and an RCA MI 9594 A horn. The horn driver is capable of accepting continuously 10 volts rms input over the frequency range from approximately 300 Hz to 10,000 Hz. The acoustic power output of the source for a 1 volt rms input in 1/3 octave bands is shown in Table D-1. The source power output was determined using the standard reverberation room technique and an ILG reference sound source.* The electrical system used for all tests with the horn sound source is shown in Fig. D-1.

To investigate the directivity of the horn source, it was mounted in a large acechoic chamber on a turntable and slowly rotated. Due to a slight balancing problem the axis of rotation was at the center of gravity approximately 6 in. forward of the throat of the horn. The horn was tested with its broad dimension either horizontal or vertical. The microphone was mounted at either 6 ft or 20 ft from the center of rotation. The horn and the orientations are illustrated in Fig. D-2.

The source was driven with 1/3-octave bands of noise centered at the preferred octave band frequencies 500, 1000, 2000, and 4000 Hz. Polar plots were obtained from these measurements and are shown in Figs. D-3 through D-10. Free field levels shown in Figs. 29 and 30 of the text were obtained from the data shown in these figures by interpolation. It is to be remembered that in the tunnel configuration the microphone was slightly below the plane of the source; thus some interpolation of the data was necessary.

The data of Figs. D-3 through D-6 were used to estimate the sound power radiated forward and backward from the source by integration. For this purpose the sound pressure levels were estimated over a sphere 20 ft in radius with its surface divided equally into 128 parts. Using the measurements shown on the two axes the levels at the various intermediate points were interpolated assuming a uniform change in level from one axis to the other; the sound power was determined as a summation of contributions from the various parts. The results of

---

* ASTM document designation E336-67T.

the integration are shown in the calibration columns in Table VI of the text for forward and backward radiation. At 2000 Hz and 4000 Hz the integration was not carried out but an upper bound for backward radiation was determined by inspection of Figs. D-7 through D-10.

TABLE D-1

DIRECTIONAL SOUND SOURCE POWER LEVELS IN ONE-THIRD OCTAVE BANDS FOR ONE VOLT RMS INPUT

JBL 2480 driver and RCA MI 9594 A horn

One-third octave band center frequency in Hz	Sound power level in dB re 10^{-12} watt Reverberant room measurements	
	Trial 1	Trial 2
400	99.0	98.0
500	98.5	99.5
630	99.0	99.0
800	99.5	99.0
1000	99.5	99.5
1250	100.0	100.5
1600	98.0	99.0
2000	98.0	97.0
2500	97.5	97.0
3150	95.0	95.0
4000	93.0	93.5
5000	90.0	90.0
6300	75.0	75.0
8000	66.0	--

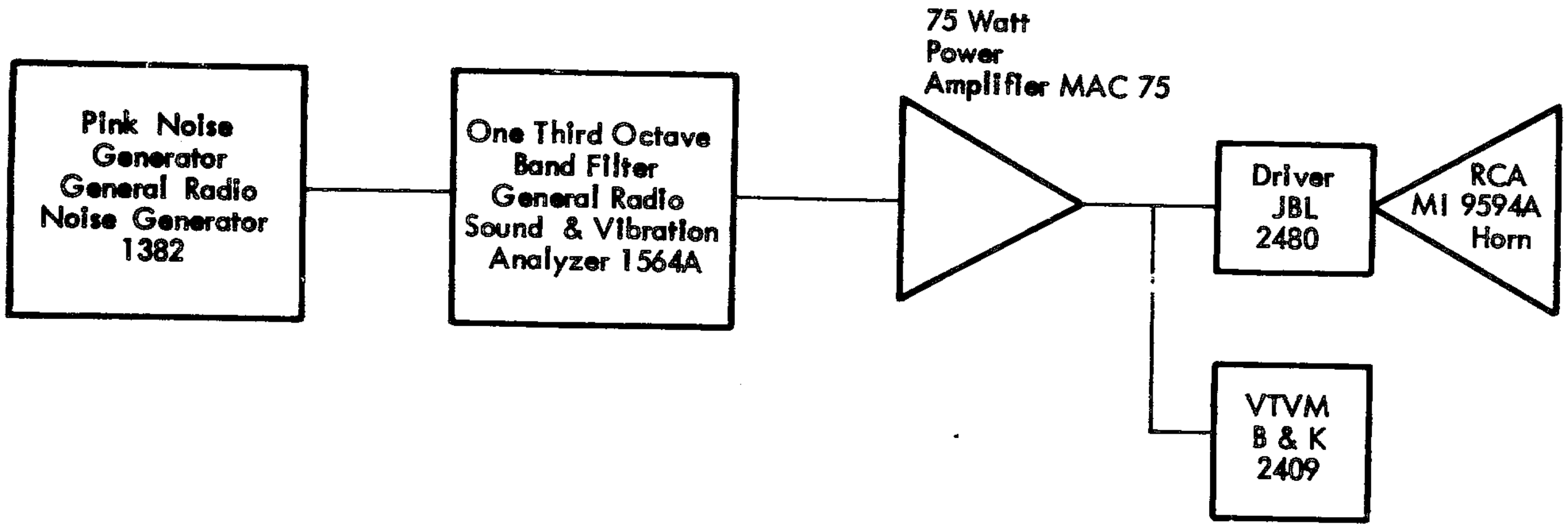

FIGURE D-1. HORN SYSTEM USED FOR TUNNEL SOUND PROPAGATION MEASUREMENTS

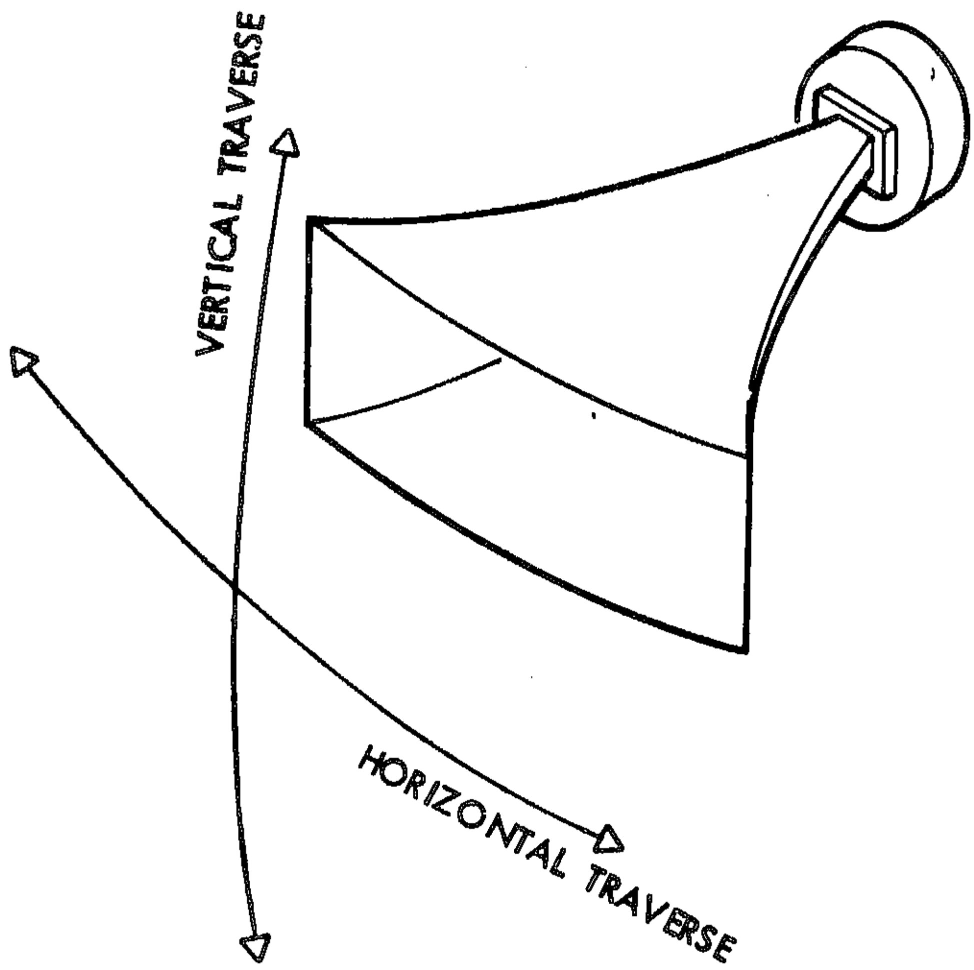

FIGURE D-2. RCA HORN MI 9594A
HORIZONTAL AND VERTICAL ORIENTATIONS ARE SHOWN AS AN AID TO INTERPRETATION OF THE HORN DIRECTIVITY POLAR PLOTS

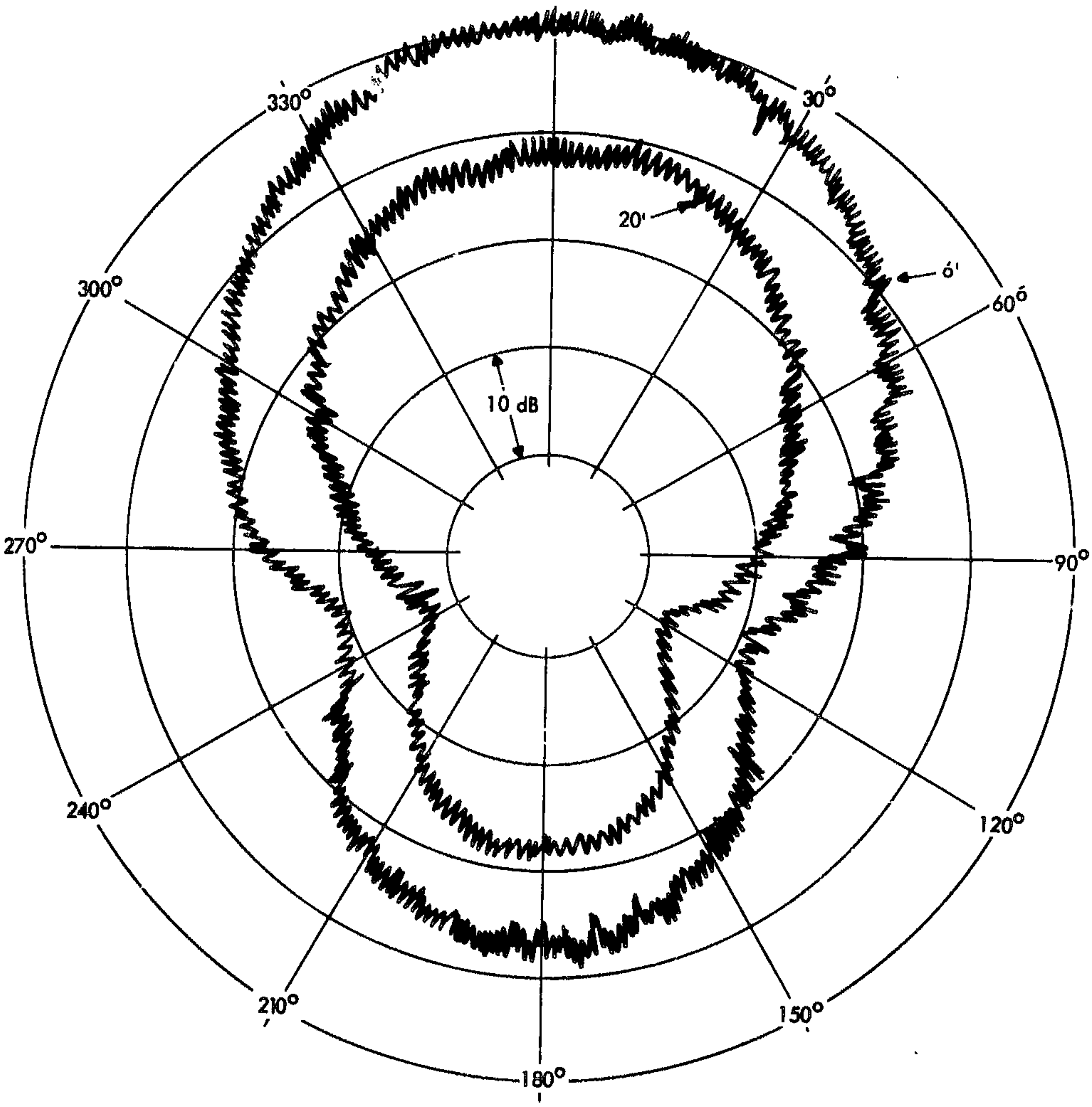

FIGURE D-3. RCA HORN RADIATION PATTERN IN THE HORIZONTAL PLANE (SEE FIG.D-2) FOR 0.5 KHZ ONE-THIRD OCTAVE BAND OF NOISE. MEASUREMENT DISTANCES SHOWN ARE RELATIVE TO A POINT 6 INCHES DOWN STREAM FROM THE HORN THROAT.

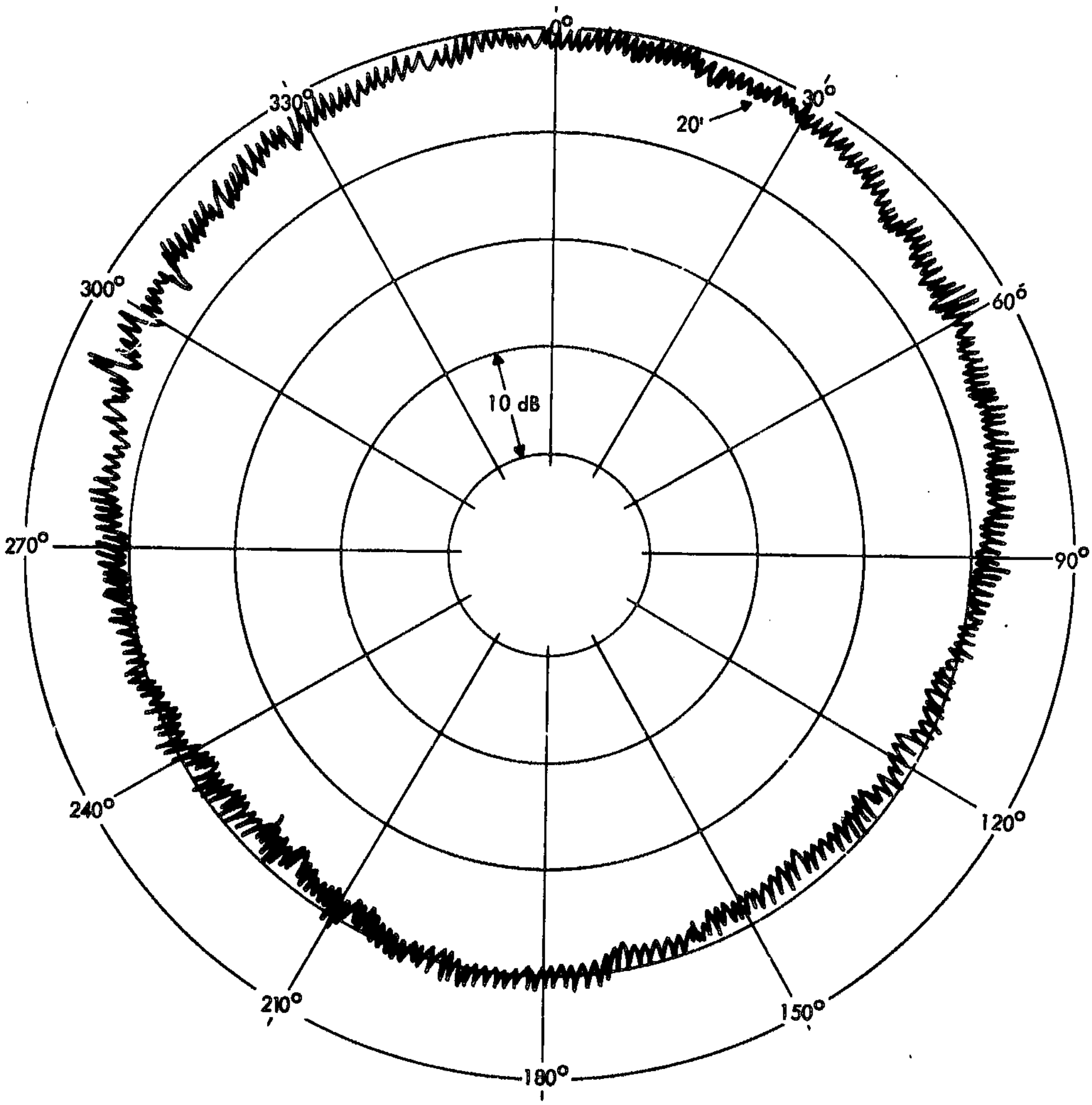

FIGURE D-4. RCA HORN RADIATION PATTERN IN THE VERTICAL PLANE (SEE FIG.D-2) FOR 0.5 KHZ ONE-THIRD OCTAVE BAND OF NOISE. MEASUREMENT DISTANCES SHOWN ARE RELATIVE TO A POINT 6 INCHES DOWN STREAM FROM THE HORN THROAT.

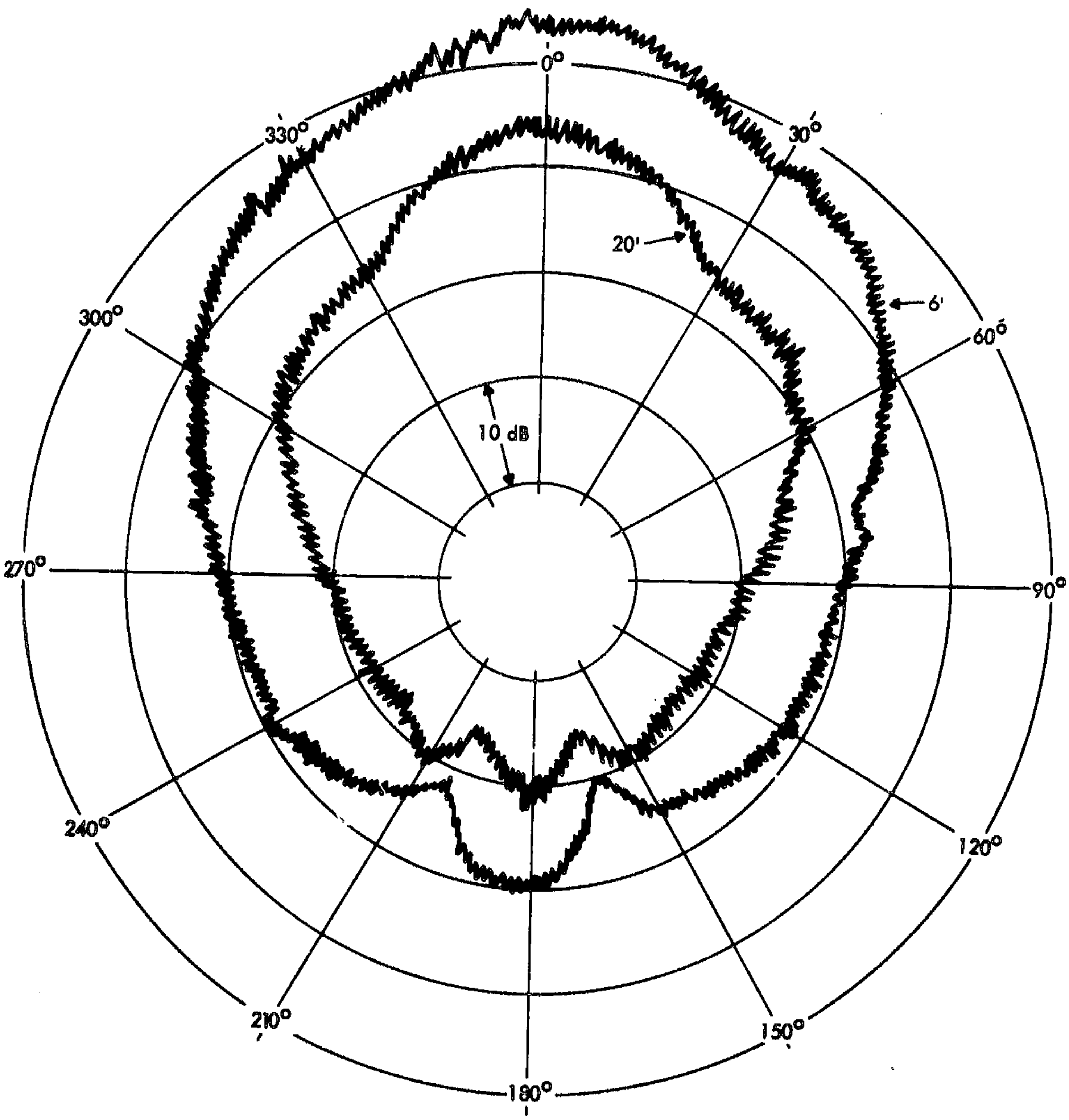

FIGURE D-5. RCA HORN RADIATION PATTERN IN THE HORIZONTAL PLANE (SEE FIG. D-2) FOR 1.0 KHZ ONE-THIRD OCTAVE BAND OF NOISE. MEASUREMENT DISTANCES SHOWN ARE RELATIVE TO A POINT 6 INCHES DOWN STREAM FROM THE HORN THROAT.

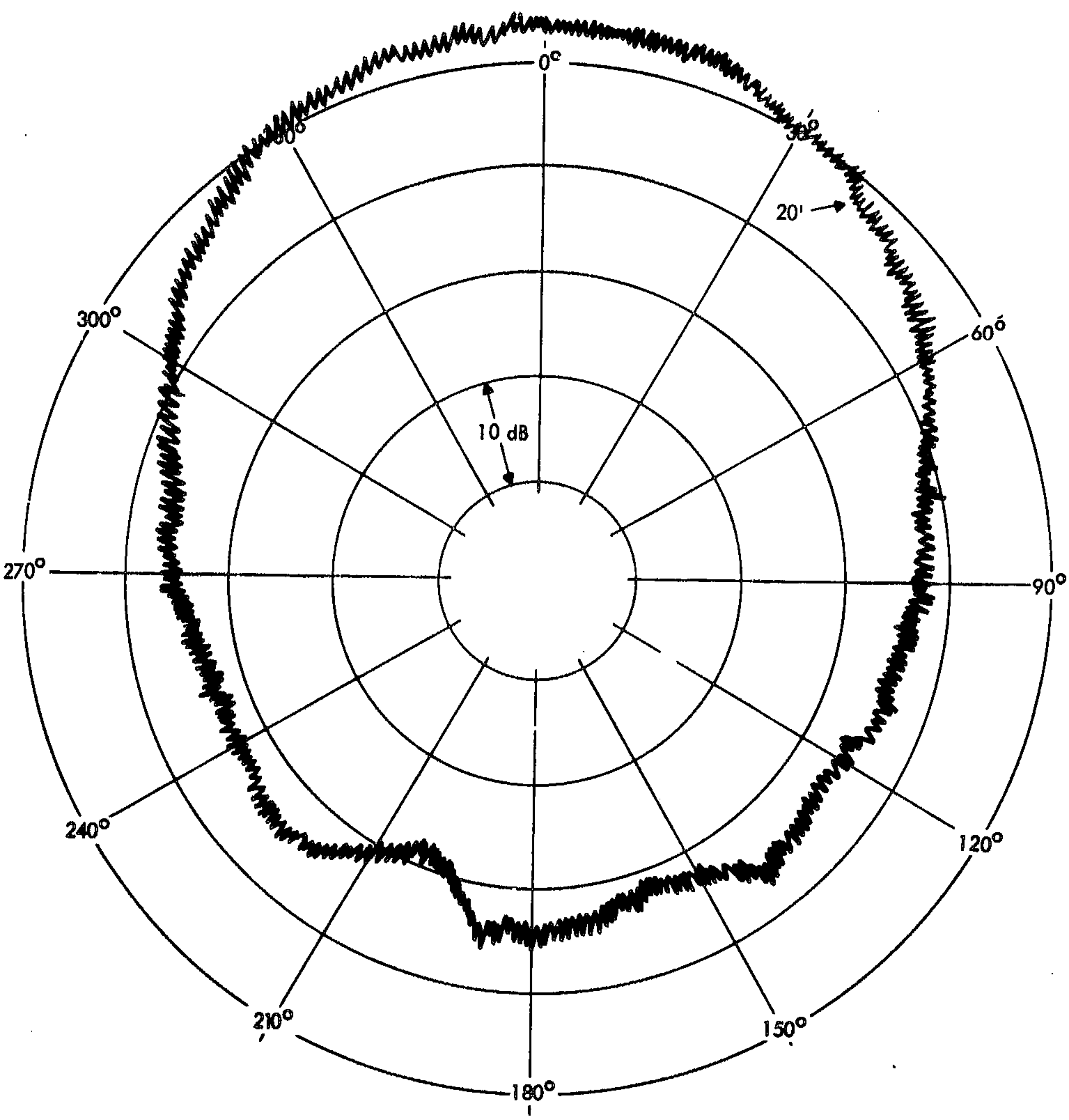

FIGURE D-6. RCA HORN RADIATION PATTERN IN THE VERTICAL PLANE (SEE FIG. D-2) FOR 1.0 KHZ ONE-THIRD OCTAVE BAND OF NOISE. MEASUREMENT DISTANCES SHOWN ARE RELATIVE TO A POINT 6 INCHES DOWN STREAM FROM THE HORN THROAT.

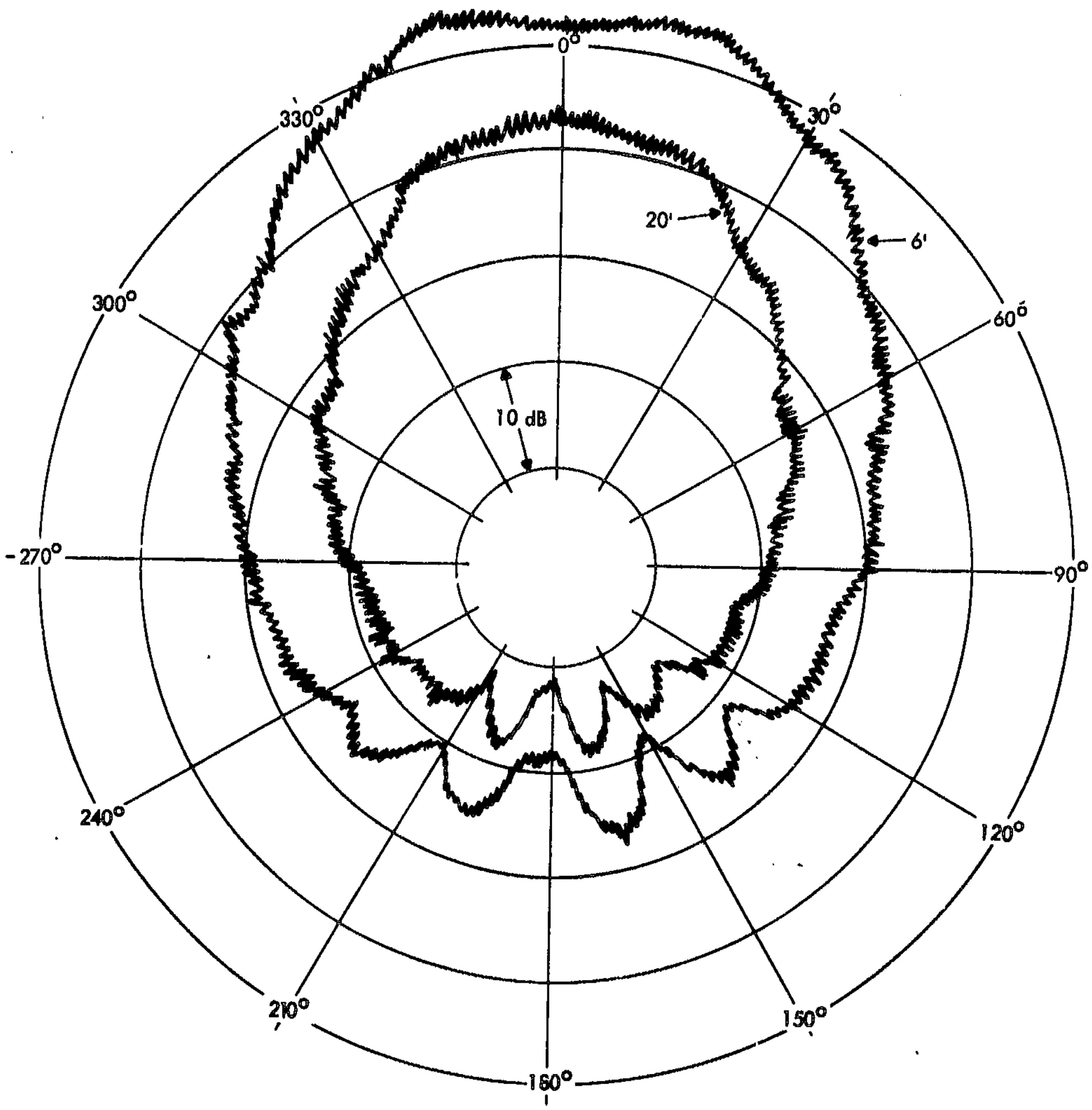

FIGURE D-7. RCA HORN RADIATION PATTERN IN THE HORIZONTAL PLANE (SEE FIG. D-2) FOR 2.0 KHZ ONE-THIRD OCTAVE BAND OF NOISE. MEASUREMENT DISTANCES SHOWN ARE RELATIVE TO A POINT 6 INCHES DOWN STREAM FROM THE HORN THROAT.

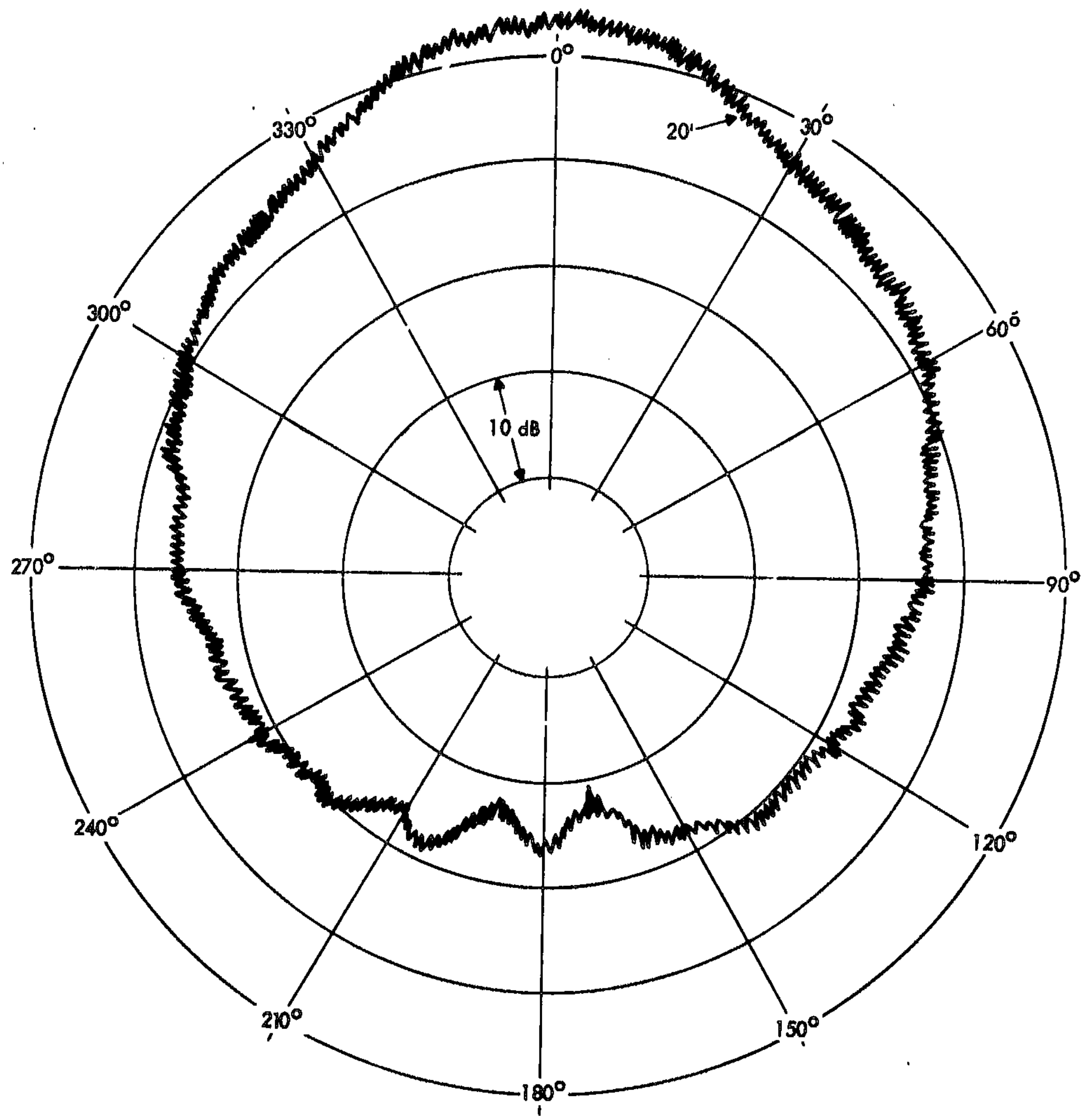

FIGURE D-8. RCA HORN RADIATION PATTERN IN THE VERTICAL PLANE (SEE FIG. D-2) FOR 2.0 KHZ ONE-THIRD OCTAVE BAND OF NOISE. MEASUREMENT DISTANCES SHOWN ARE RELATIVE TO A POINT 6 INCHES DOWN STREAM FROM THE HORN THROAT.

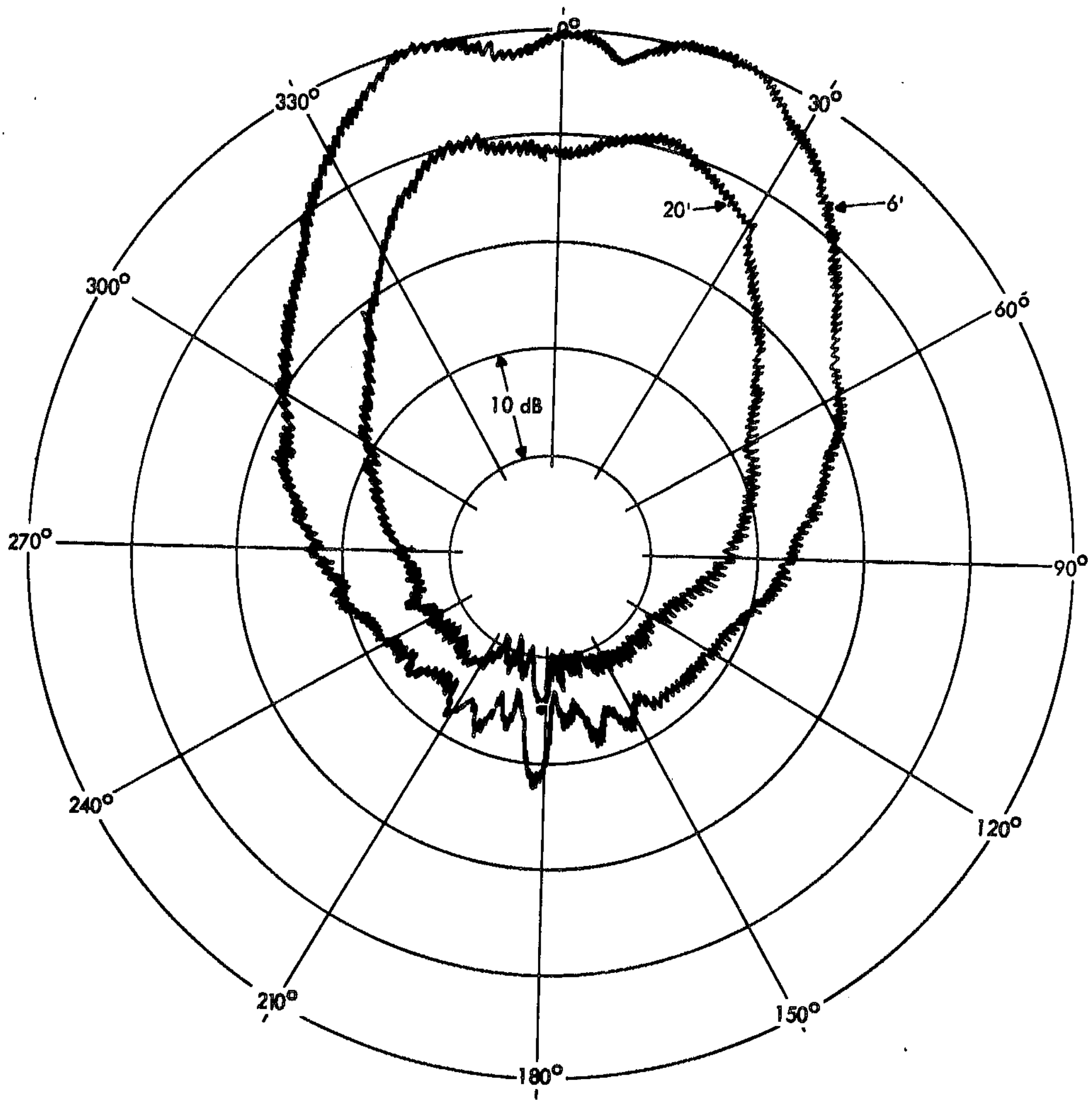

FIGURE D-9. RCA HORN RADIATION PATTERN IN THE HORIZONTAL PLANE (SEE FIG.D-2) FOR 4.0 KHZ ONE-THIRD OCTAVE BAND OF NOISE. MEASUREMENT DISTANCES SHOWN ARE RELATIVE TO A POINT 6 INCHES DOWN STREAM FROM THE HORN THROAT.

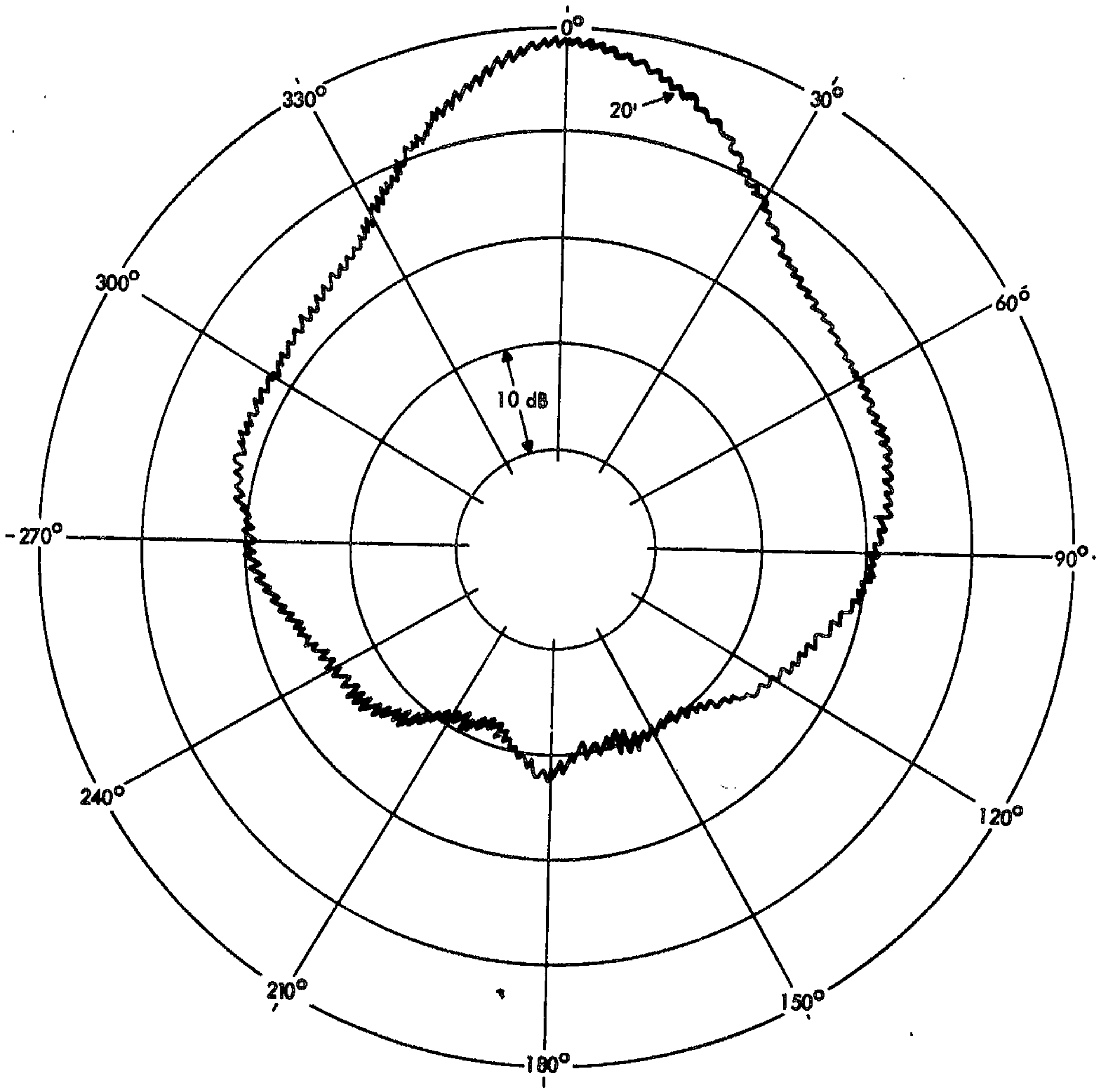

FIGURE D-10. RCA HORN RADIATION PATTERN IN THE VERTICAL PLANE (SEE FIG. D-2) FOR 4.0 KHZ ONE-THIRD OCTAVE BAND OF NOISE. MEASUREMENT DISTANCES SHOWN ARE RELATIVE TO A POINT 6 INCHES DOWN STREAM FROM THE HORN THROAT.

APPENDIX E

MEASUREMENT SYSTEMS

Measurements without flow were made with the systems shown in Fig. E-1. The omnidirectional portable system was used to measure sound pressure levels at various locations around the wind tunnel. The omnidirectional and directional mounted systems were used to make measurements in the test section at elevations well above the floor.

Measurements with flow were made with the system shown in Fig. E-2. The data were recorded during wind tunnel operation and subsequently played back for analysis.

MEASUREMENT SYSTEMS

1) Portable System

2) Omnidirectional Mounted System

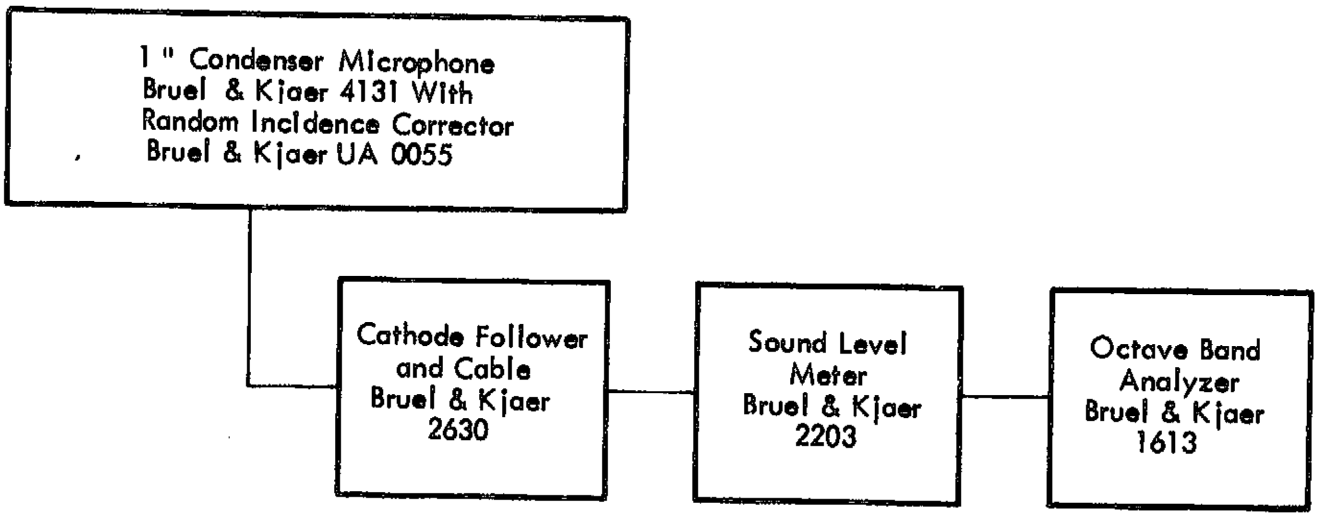

3) Directional Porous Pipe Mounted System

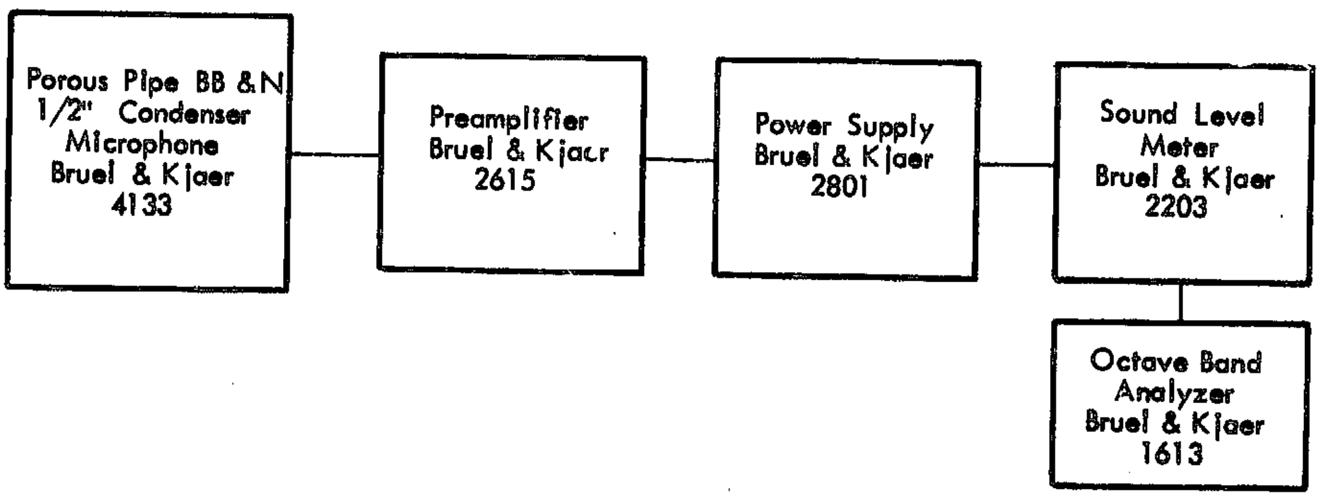

FIGURE E-1. DETECTION SYSTEMS USED FOR TUNNEL SOUND PROPAGATION MEASUREMENTS

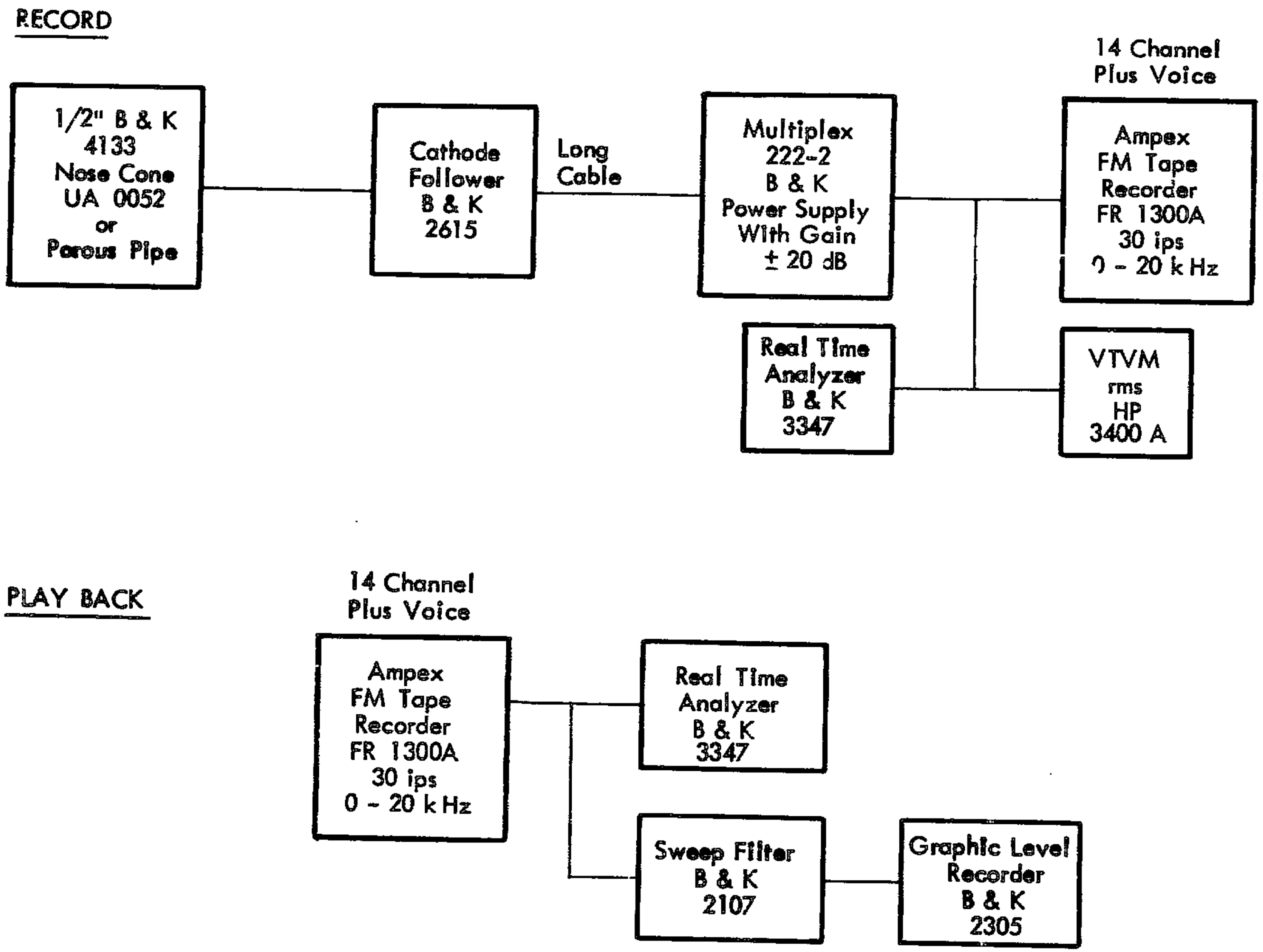

FIGURE E-2. NASA AMES RECORD AND PLAYBACK SYSTEMS USED FOR TUNNEL SOUND PROPAGATION MEASUREMENTS

APPENDIX F

ACOUSTIC POWER FLOW INVESTIGATION

The wind tunnel will be considered to be two large reverberent volumes V_1 upstream and V_2 downstream connected by the fan ducts and possibly the test section. The connecting duct in the model will provide acoustic properties equivalent to an appropriate combination of the properties of these two parts of the tunnel.

The energy densities in the two volumes will be E_1 and E_2. The loss factors are η_1 and η_2 while the coupling coefficients are η_{12} and η_{21}. Power balance equations may be written for the two volumes as follows.

$$P_1(\omega) = \omega\eta_1 E_1 V_1 + \omega\eta_{12} E_1 V_1 + \omega\eta_D E_1 V_1 - \omega\eta_{21} E_2 V_2 \qquad \text{F-1}$$

and

$$P_2(\omega) = \omega\eta_2 E_2 V_2 + \omega\eta_{21} E_2 V_2 + \omega\eta_D E_2 V_2 - \omega\eta_{12} E_1 V_1 \quad . \qquad \text{F-2}$$

Either equation says that the power introduced into a volume V_i equals the power dissipated in the volume V_i, plus the power transmitted from volume V_i to V_j, plus the power from volume V_i dissipated in the connecting duct, minus the power transmitted from volume V_j to volume V_i. The equations hold for a narrow band of frequencies centered about the angular frequency ω.

The coupling coefficients are related by the modal densities of the volumes. The modal densities are in turn approximately proportional to the respective volumes. Thus

$$V_1\eta_{12} = V_2\eta_{21} = 0 \qquad \text{F-3}$$

Two experiments were performed to aid in the evaluation of the various constants in the equations. In one experiment an omnidirectional source was placed in the test section. Equal acoustic power was delivered to each volume. Thus

$$P_1 = P_2 = P_a \qquad \text{F-4}$$

In this case the energy densities will be represented by E_1 and E_2 respectively.

In the second experiment a source was placed upstream of the fans in volume V_1. In this case

$$P_1 = P_b \text{ and } P_2 = 0 \qquad \text{F-5}$$

The resulting energy densities will be represented by E_3 and E_4 in volumes V_1 and V_2 respectively.

Equations F-4 and F-5 when introduced into Eqs. F-1 and F-2 result in four equations which taken together with Eq. F-3 provide five equations in five unknowns. However, the determinant is identically zero; loss in the connecting duct can not be distinguished by the proposed experiments from loss in the volumes. We express this formally by setting η_D equal to zero. The four power balance equations are

$$\left.\begin{aligned} P_a/\omega E_1V_1 &= \eta_1 + 0 + \eta_{12} - \eta_{21}E_2V_2/E_1V_1 \\ P_a/\omega E_2V_2 &= 0 + \eta_2 - \eta_{12}E_1V_1/E_2V_2 + \eta_{21} \\ P_b/\omega E_3V_1 &= \eta_1 + 0 + \eta_{12} - \eta_{21}E_4V_2/E_3V_1 \\ 0 &= 0 + \eta_2 - \eta_{12}E_3V_1/E_4V_2 + \eta_{21} \end{aligned}\right\} \qquad \text{F-6}$$

Equations F-6 and F-3 are five equations in four unknowns which can only hold provided that

$$P_a/P_b = E_1/(E_3 + E_4) \qquad \text{F-7}$$

If Eq. F-7 holds then the equations are not linearly independent. They may be reduced to four equations in four unknowns and solved.

The energy density is proportional to the sound pressure level. Thus the data presented in Table F-1 may be used to check the validity of Eq. F-7. For acoustical purposes the data shown in the last two columns are in reasonable agreement except in the 8000 Hz one-third octave band.*

The volumes are estimated to be, respectively

$$V_1 = 3.7 \times 10^6 \text{ ft}^3$$

and

$$V_2 = 17.1 \times 10^6 \text{ ft}^3.$$

Using these values, the data contained in columns 2 through 7, and the following equations which result from Eqs. F-6 and F-3, the values given in Table F-2 have been computed.

$$\eta_{12} = \frac{P_a}{\omega E_2 V_1}\left(\frac{E_3}{E_4} - \frac{E_1}{E_2}\right)^{-1} \qquad \text{F-8}$$

$$\eta_{21} = \frac{P_a}{\omega E_2 V_2}\left(\frac{E_3}{E_4} - \frac{E_1}{E_2}\right)^{-1} \qquad \text{F-9}$$

*Atmospheric propagation loss may be responsible for a breakdown in the proposed model at 8000 Hz. It may also be influential at 4000 Hz as well.

$$\eta_1 = \frac{P_a}{\omega E_1 V_1} - \frac{P_a}{\omega E_2 V_1}\left(1 - \frac{E_2}{E_1}\right)\left(\frac{E_3}{E_4} - \frac{E_1}{E_2}\right)^{-1} \qquad \text{F-10}$$

$$\eta_2 = \frac{P_a}{\omega E_2 V_2}\left(\frac{E_3}{E_4} - 1\right)\left(\frac{E_3}{E_4} - \frac{E_1}{E_2}\right)^{-1} \qquad \text{F-11}$$

The data in Table F-2 show that the loss factors for the upstream and downstream portions of the tunnel (relative to the fans) are approximately equal. This is expected since the loss factor is the ratio of energy dissipated per cycle to energy stored. The former is proportional to the surface area while the latter is proportional to the total volume. The implication is that the surface area to volume ratio must be constant which is true for a tunnel.

The loss factor for a reverberant space may also be determined from reverberation measurements. The loss factor determined by reverberation measurements conducted in the area of the tunnel downstream of the fans is shown for comparison in Table F-3. The latter loss factor is very much less than the loss factors η_1 and η_2 determined from power balance considerations. It is suggested that the reverberation times are controlled by energy propagating along the length of the tunnel while the loss factors η_1 and η_2 are probably controlled by reverberation between the walls, floor and ceiling of the tunnel.

The energy density distribution between volumes one and two resulting from the introduction of a directional source in the test section will now be investigated. Solving Eqs. F-1 and F-2 for the energy densities results in the following expressions

$$E_1 = \frac{P_1(\eta_2 + \eta_{21}) + P_2\eta_{21}}{V_1\omega[\eta_1\eta_2 + \eta_1\eta_{21} + \eta_2\eta_{12}]} \qquad \text{F-12}$$

and

$$E_2 = \frac{P_2(\eta_1 + \eta_{12}) + P_1\eta_{12}}{V_2\omega[\eta_1\eta_2 + \eta_1\eta_{21} + \eta_2\eta_{12}]} \qquad \text{F-13}$$

From Eqs. F-12 and F-13 we obtain the expression

$$E_1/E_2 = \frac{V_2[P_1(\eta_2 + \eta_{21}) + P_2\eta_{21}]}{V_1[P_2(\eta_1 + \eta_{12}) + P_1\eta_{12}} \qquad \text{F-14}$$

The data contained in Table F-2 have been used in conjunction with Eq. F-14 to compute the curves shown in Fig. F-1. In the figure source radiation downstream corresponds to the case where $P_1 > P_2$ while source radiation upstream corresponds to the opposite case, $P_1 < P_2$. For comparison with the theoretical curves the observed differences in sound pressure levels in the volumes upstream and downstream of the fans taken from Figs. 15 and 20 have been entered in the figure. Experiment and theory are in qualitative agreement.

It should be pointed out that it is very difficult to make acoustic measurements with an accuracy of one decibel in the environment of the wind tunnel. This would be especially true if the tunnel were in operation. The figure shows that the determination of forward and backward directivity of a source would require much greater precision in measurement than is possible. Thus, at best one could expect qualitative information about directivity from measurements in the area of the fans but not quantitative information.

TABLE F-1

RELATION BETWEEN ACOUSTIC POWER LEVEL AND SOUND PRESSURE LEVEL IN THE AREA OF THE FANS

Center Band Frequency (Hz)	One Third Octave Band Sound Power Levels in dB re 10^{-12} watt (P_a)	(P_b)	One Third Octave Band Sound Pressure Levels in dB re $2 \times 10^{-5} N/m^2$ (E_1)	(E_2)	(E_3)	(E_4)	P_a/P_b in dB	$E_1/(E_3+E_4)$ in dB
125	118.5	109	82	81	74	72	9.5	6
250	119.5	107	84	82	72	65	12.5	11
500	113.5	104.5	80	78	71	65	9.0	8
1000	109.5	105	76	73.5	71	60	4.5	4.5
2000	108.5	105.5	72	69	68	55	3.0	4
4000	105.5	103	62	58	64	46	2.5	-2
8000	97.5	102	33	29	58	30	-4.5	-25

TABLE F-2

COMPUTED VALUES OF LOSS AND COUPLING FACTORS

Center Band Frequency (Hz)	η_{12}	η_{21}	η_1	η_2
	(all values must be multiplied by 10^{-3})			
125	33	7.10	3.40	4.30
250	1.70	0.27	3.40	1.10
500	0.77	0.17	0.97	0.51
1000	0.27	0.059	0.51	0.68
2000	0.16	0.035	0.55	0.67
4000	0.12	0.026	1.50	1.60

TABLE F-3

TUNNEL LOSS FACTOR DETERMINED FROM

REVERBERATION MEASUREMENTS

Center Band Frequency f (Hz)	Average Reverberation Time T (sec)	Loss Factor $\eta = 2.2/fT$ (all values must be multiplied by 10^{-4})
125	20.7	8.50
250	18.8	4.68
500	21.6	2.04
1000	15.7	1.40
2000	11.2	0.982
4000	5.0	1.100
8000	1.4	1.570

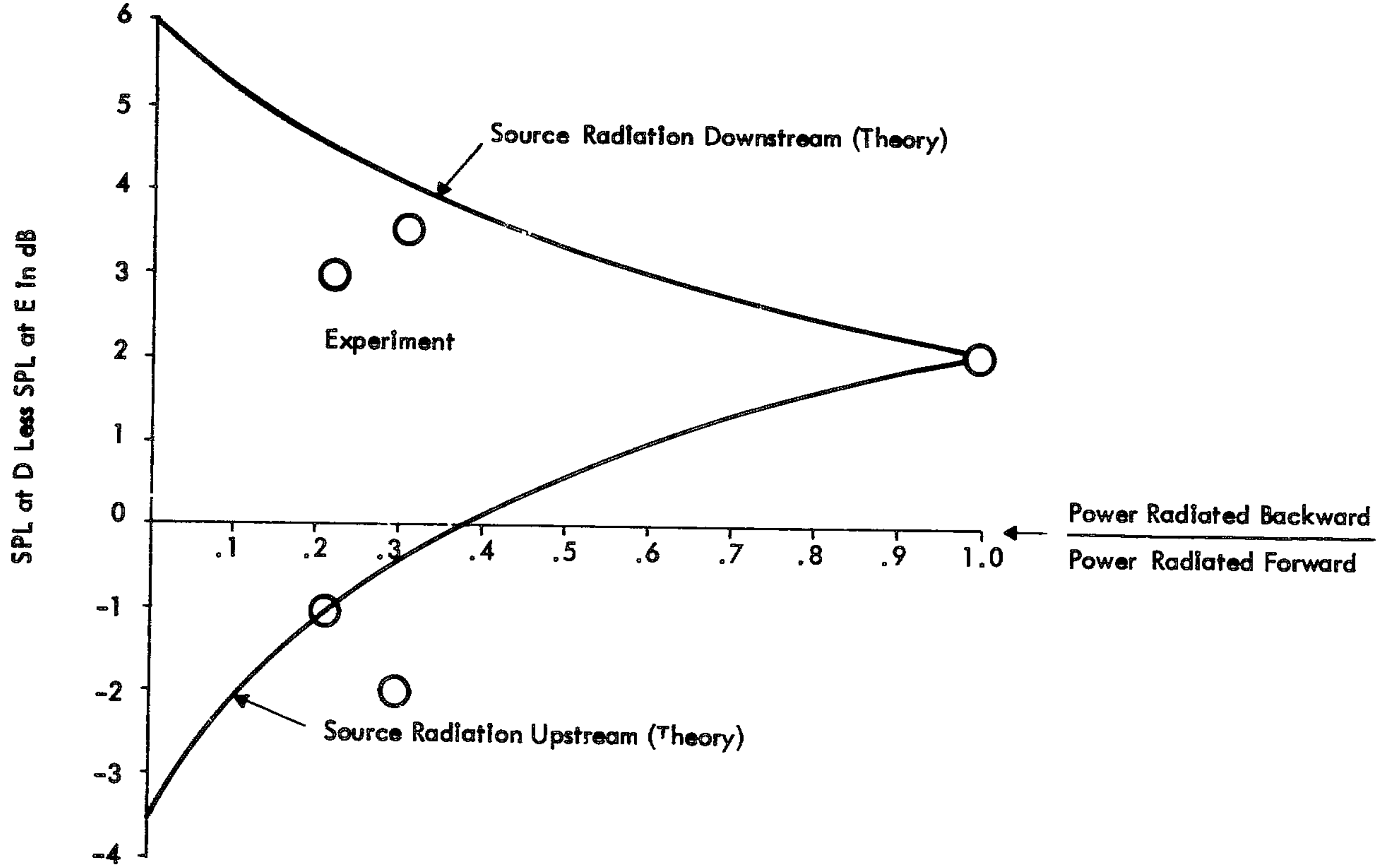

FIGURE F-1. DIFFERENCE IN SOUND PRESSURE LEVELS UPSTREAM AND DOWNSTREAM OF FANS AT 500 Hz AS AFFECTED BY SOURCE DIRECTIVITY, SOUND SOURCE IN TEST SECTION.

APPENDIX G

LOGARITHMIC ADDITION

If two narrow frequency bands of noise are characterized by root mean square sound pressures p_1 and p_2 then the resulting acoustic energy density is

$$\frac{p_1^2}{\rho c^2} + \frac{p_2^2}{\rho c^2} = \frac{p_T^2}{\rho c^2}$$

and the resulting root mean square sound pressure is p_T.

If the sound pressure levels associated with the acoustic pressures of p_1 and p_2 are measured and the sound pressure level associated with the total acoustic pressure is desired then one can either use the definition of sound pressure level,

$$SPL = 20 \log_{10} p - 20 \log_{10} (2 \times 10^{-5} N/m^2) \quad ,$$

to calculate the pressures, and finally the total sound pressure level or one can use the short-cut of logarithmic addition. With logarithmic addition the computation has been carried out and put in convenient tabular form.

As an example, suppose that sound pressure level $(SPL)_2$ is 3 dB less than sound pressure level $(SPL)_1$ then the resulting sound pressure level $(SPL)_T$ is obtained by adding 1.77 dB to $(SPL)_1$ as shown by the following computation.

$$10 \log (p_2^2/p_1^2) = -3$$

$$\log 10 (p_2^2/p_1^2) = 0.7$$

$$p_2^2/p_1^2 = 0.501$$

$$p_T^2/p_1^2 = (p_1^2 + p_2^2)/p_1^2 = 1.501$$

$$10 \log (p_T^2/p_1^2) = 1.77$$

$$(SPL)_T = (SPL)_1 + 1.77$$

For practical purposes the corrections may be rounded off to the nearest 0.5 dB. Under these circumstances the following table is useful.*

$(SPL)_1 - (SPL)_2$ in dB	Correction in dB to be added to $(SPL)_1$
0	3
1	2.5
2,3	2
4	1.5
5, 6, 7	1
8, 9, 10, 11	0.5
greater than 11	0

*For alternative presentation see *Handbook of Noise Measurement* (Sixth Edition), General Radio Company, West Concord, Mass., 1967, pp. 208, 209.

APPENDIX H

SOUND INTENSITY IN AN INFINITELY LONG RECTANGULAR DUCT OF LARGE CROSS DIMENSIONS

It will be assumed that sound originating in the test section is quickly distributed between all of the various cross modes and that it propagates out of the test section either upstream through the inlet or downstream through the diffuser. Under these assumptions it may be considered to be like an infinitely long duct. To further simplify the analysis it will be assumed that the details of the cross section geometry are not important to the distribution of energy among modes. Under this assumption, the duct may be assumed to be rectangular in cross section.

Let the coordinate system be Cartesian with the x axis along the duct length, the y axis vertical and the z axis across the duct width. An appropriate potential function is*

$$\phi = -\frac{p_o}{\omega\rho}\cos(\omega t - k_1 x)\cos k_2 y \cos k_3 z \qquad (1)$$

The particle velocity in the x direction is

$$v_x = -\frac{\partial\phi}{\partial x} = \frac{p_o k_1}{\omega\rho}\sin(\omega t - k_1 x)\cos k_2 y \cos k_3 z \qquad (2)$$

and the acoustic pressure is

$$p = \rho\frac{\partial\phi}{\partial t} = p_o \sin(\omega t - k_1 x)\cos k_2 y \cos k_3 z \qquad (3)$$

---

*Kinsler, L. E.; and Frey, A. R.: Fundamentals of Acoustics. John Wiley & Sons, Inc., 1950, Chp. 5.

In Eqs. 2 and 3, p_o is the amplitude of the acoustic pressure. The quantities ρ and ω are the air density and the angular frequency in radians per second. The time is represented by t and the wavenumbers by k_1, k_2, and k_3.

The acoustic energy intensity is

$$I = \frac{1}{T}\int_0^T p v_x dt \qquad (4)$$

where T is one period or $2\pi/\omega$. Substituting Eqs. 2 and 3 into Eq. 4 gives

$$I = \frac{p_o^2 k_1}{\rho\omega 2} \cos^2 k_2 y \cos^2 k_3 z \qquad (5)$$

Boundary conditions require that

$$k_2 = \frac{n\pi}{H}, \; n = 0, \pm 1, \pm 2, \ldots \qquad (6)$$

and

$$k_2 = \frac{m\pi}{W}, \; m = 0, \pm 1, \pm 2, \ldots \qquad (7)$$

where H is the duct height and W is the duct width. The wave equation requires that

$$\left(\frac{\omega}{c}\right)^2 = k^2 = k_1^2 + k_2^2 + k_3^2 \qquad (8)$$

From Eq. 3 the mean square pressure is

$$p_{rms}^2 = \frac{p_o^2}{2} \cos^2 k_2 y \cos^2 k_3 z \tag{9}$$

Substitution of Eq. 9 in Eq. 5 gives for the intensity

$$I = \frac{p_{rms}^2}{\rho\omega} k_1 \tag{10}$$

The expression for intensity given by Eq. 10 holds for a single value of the propagation constant k_1. It will be assumed that all propagating modes are excited and that each contributes to the root mean square pressure and intensity. Under these conditions, the intensity across the duct is given by

$$I_{av} = \frac{p_{rms}^2}{\rho\omega} k_{av} \tag{11}$$

where k_{av} is the average value of the wavenumber k_1.

The average value of the wavenumber k_1 may be determined as follows. Equations 6, 7, and 8 define a hemisphere in k space where k_2 and k_3 may be positive or negative and k_1 is positive. Note that Eq. 8 limits the number of allowed values of n and m.

For a given frequency ω and each allowed value of k_2 and k_3 given by Eqs. 6 and 7, there is one value of k_1. The number N of allowed values of k_1 for a given ω is the same as the total number of allowed combinations of k_2 and k_3. Thus

$$N = \pi k^2 \left(\frac{WH}{4\pi^2}\right) \tag{12}$$

The volume of the hemisphere in k space may be written in terms of k and in terms of a summation over all values of k_1 as follows

$$\frac{2}{3} \pi k^3 = \sum_{i=1}^{N} \overline{k_i} \left(\frac{4\pi^2}{WH}\right) \quad (13)$$

Equation 13 may be rewritten in terms of the average value of k_1 as

$$\frac{2}{3} \pi k^3 = N k_{av} \left(\frac{4\pi^2}{WH}\right) \quad (14)$$

Combining Eqs. 12 and 14 and solving for k_{av} gives

$$k_{av} = \frac{2}{3} k = \frac{2\omega}{3c} \quad (15)$$

Substitution of Eq. 15 in Eq. 11 results in the desired expression for the average intensity.

$$I_{av} = \frac{2}{3} \frac{p_{rms}^2}{\rho c} \quad (16)$$